3.2 Results in RF-EMF research

3.2.1 Genotoxic effects

3.2.1.1 Human HL-60 cell line (Participant 2)

Genotoxic effects of EMF may occur directly either by damage to chromosomes and/or by damage to DNA repair mechanisms. Indirect genotoxic effects may arise by various processes such as generation of oxygen radicals or impairment of radical-scavenging mechanisms. Direct and indirect genotoxic effects of defined RF-EMF were investigated in the human cell line HL-60.

A. Direct genotoxicity

RF-EMF increased the micronucleus frequency and the number in DNA strand breaks in HL-60 cells dependent on the energy of radiation as determined by the cytokinesis-block in vitro micronucleus assay and the Comet assay.

The effect of RF-EMF on the formation of micronuclei (MN) and DNA strand breaks was examined by use of the cytokinesis-block in vitro micronucleus assay and the alkaline Comet assay. To validate the MN assay and to prove the susceptibility of HL-60 cells to physical noxes, cells were exposed to ionising-irradiation. As shown in Figure 70, a dose-dependent induction of micronuclei in HL-60 cells was found for doses of exposure increasing from 0.5 to 3.0 Gy. Cell division was effected by ionising-irradiation at doses ≥1.0 Gy as shown in Figure 71, inferred from the ratio of BNC against mono-, bi-, tri- and tetranuclear cells (in %).

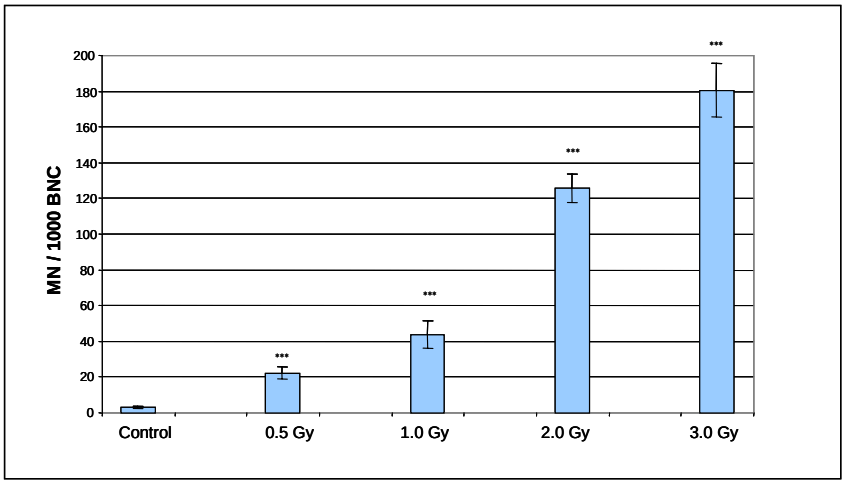

Figure 70. Effect of ionising-irradiation (6 MeV) on micronuclei formation in binucleated HL-60 cells. Each data point is based on at least three independent experiments. Each bar represents the mean ± SD of results obtained in three independent experiments. *** P<0.001 (Student's t-test, two-sided). All in all (mono-, bi-, tri-, and tetranucleated) 15000 cells were analysed.

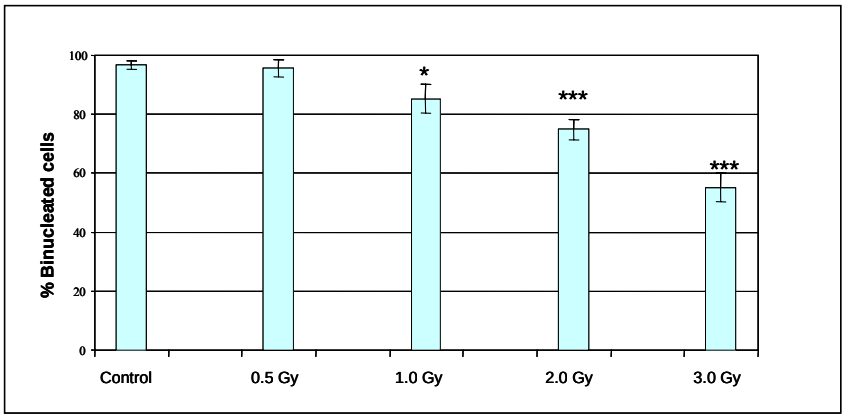

Figure 71. Effect of ionising-irradiation on HL-60 cell division. The number of binucleated cells relative to the number of mono-, bi-, tri-, and tetranuclear cells following ionising-irradiation (6 MeV) of HL-60 cells. Each bar represents the mean ± SD in % of results obtained in three independent experiments; *p<0.05, ***p<0.001 (Student's t-test, two-sided).

In a series of experiments SAR levels ranging from 0.2 W/kg to 3.0 W/kg were examined in order to clarify whether the effects of RF-EMF exposure (1800 MHz, continuous wave, 24 h) on MN frequencies in HL-60 cells are energy dependent (Figure 72). Whereas at SAR of 0.2 W/kg, 1.0 and 3.0 W/kg MN frequencies were not changed in RF-EMF-exposed cells as compared to sham controls and incubator controls, MN frequencies were significantly increased at SAR of 1.3 W/kg and above. The maximum increase was noted at a SAR of 1.3 and 1.6 W/kg. This effect was approximately 66 % of the effect observed after 0.5 Gy ionising-irradiation (6 MeV, exposure time: 5.2 s). At a SAR of 3.0 W/kg the MN frequency was similar to that found in sham-exposed cells. While MN frequencies of incubator controls were around 3.5, the MN frequency determined after RF-exposure at a SAR of 1.3 W/kg was 13.3 (approximately 3.8 fold higher). The MN frequency determined in cells after exposure to ionising-irradiation (0.5 Gy, exposure time: 5.2s), used as a positive control, was 22.3 ± 3.5 (n=3; 6.3 fold increase compared to control).

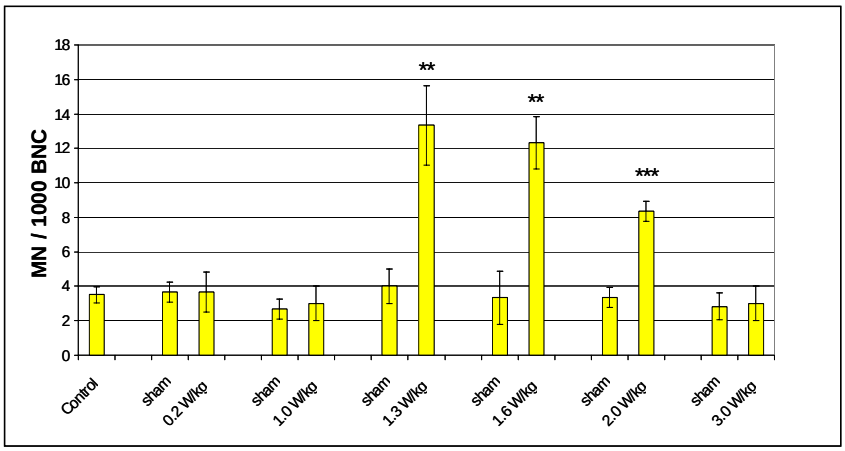

Figure 72. Micronucleus frequencies in binucleated HL-60 cells after exposure to RF-field (1800 MHz, continuous wave) for 24h ranging from SAR 0.2 to 3.0 W/kg, compared to control and sham-exposure. Each bar represents the mean ± SD of results obtained in three independent experiments (except of control: n = 11). Each data point is based on at least three independent experiments except of the control with 11 independent experiments and on a total number of 11000 (control), 18000 (sham-exposed) and 18000 (RF-exposed) bi-nucleated HL-60 cells. All in all (mono-, bi-, tri-, and tetra-nucleated) 47000 cells were analysed. The micronuclei frequency of BNC after exposure to ionising-irradiation (0.5 Gy, exposure time: 5.2s), which was used as a positive control, were on average 22.3 ± 3.5 (n=3). ** P<0.01; *** P<0.001 (Student's t-test, two-sided).

In order to compare micronuclei induction in cells exposed to RF-fields at different ranges of SAR, the average micronuclei frequencies (MN/1000 BNC) were calculated for the following groups: experiments performed at all SAR tested (range 0.2 W/kg to 3.0 W/kg, number of independent experiments n=18), experiments performed at SAR ranging from 1.0 W/kg to 2.0 W/kg (number of independent experiments n=12), and experiments at SAR of 0.2 W/kg and 1.0 W/kg (number of independent experiments n=6). While the calculated average of MN/1000 BNC in HL-60 cells at a SAR of 0.2 W/kg to 1.0 W/kg was not significantly different from that observed in sham-exposed controls, both groups ranging from 0.2 W/kg to 3.0 W/kg ($p<0.01$) or from 1.0 W/kg to 2.0 W/kg ($p<0.001$) exhibited a significant increase in micronuclei induction after RF-exposure as compared to sham-exposed controls (Figure 74A).

Previous experiments had clearly shown that RF-EMF exposure results in an increase of DNA strand breaks in HL-60 cells. In order to achieve a better understanding of whether these effects are energy dependent, additional experiments were performed applying RF-exposure (1800 MHz, continuous wave, 24h) at SAR of 0.2 W/kg to 3.0 W/kg. As shown in Figure 73 the effect of RF-EMF on DNA strand breaks at these exposure conditions exhibited a similar energy dependency as the effect of RF-EMF on micronucleus formation (Figure 72). RF-EMF exposure at a SAR of 1.0 W/kg and below had no effect on Comet formation in HL-60 cells (expressed as Olive Tail Moment OTM) as compared to control and sham-exposed cells. On the other hand RF-EMF at SAR of 1.3 W/kg and above caused a significant increase in DNA strand breaks. The maximum of this effect was observed at SAR 1.3 W/kg (OTM = 2.20 ± 0.16) and 1.6 W/kg (2.24 ± 0.10). At a SAR of 3.0 W/kg Comet formation in RF-EMF exposed cells (OTM 1.23 ± 0.12) was similar to that observed in sham-exposed cells (OTM 1.18 ± 0.03). While the Olive Tail Moment was around 1.0 in sham-exposed and incubator controls, the OTM determined after exposure at a SAR of 1.3 W/kg was approximately 2.2 fold higher (Figure 73). The OTM determined in cells after exposure to hydrogen peroxide (100 µmol/l, 1h), used as a positive control, was 8.3 ± 1.3 (n=3; 8 fold increase compared to control).

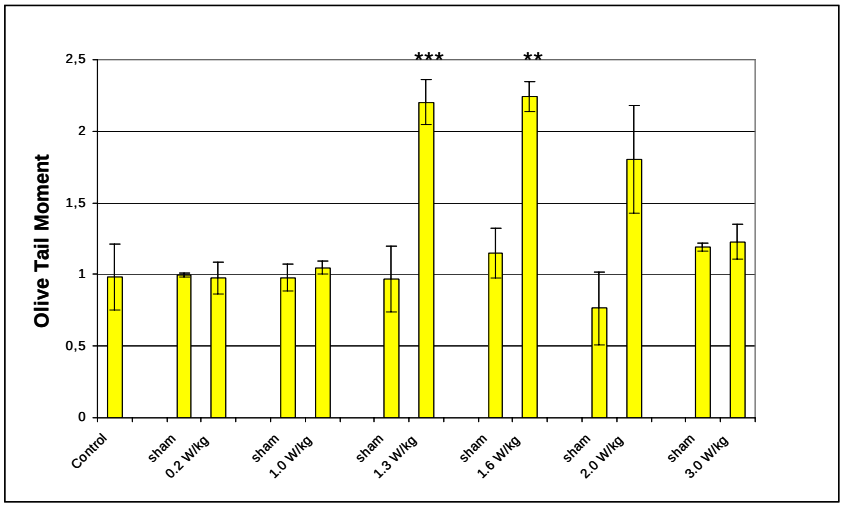

Figure 73. Comet formation in HL-60 cells after exposure to RF-field (1800 MHz, continuous wave) for 24h ranging from SAR 0.2 to 3.0 W/kg, expressed as Olive Tail Moment, compared to control and sham exposure. Each bar represents the mean ± SD of results obtained in at least three (except SAR 1.3 W/kg: n=4) independent experiments. The OTMs of the Comets after exposure to hydrogen peroxide (100 µmol/l, 1 h), which was used as a positive control, were on average 8.3 ± 1.3 (n=3). ** $P<0.01$; *** $P<0.001$ (Student's t-test, two-sided).

In order to compare Comet formation in cells exposed at different SAR ranges the average values of the Olive Tail Moments were calculated for the following groups: experiments performed at all SAR tested (range 0.2 W/kg to 3.0 W/kg, number of independent experiments n=18), experiments performed at SAR ranging from 1.0 W/kg to 2.0 W/kg (number of independent experiments n=12), and experiments at SAR of 0.2 W/kg and 1.0 W/kg (number of independent experiments n=6). While the calculated average of OTMs in HL-60 cells at SAR of 0.2 W/kg and 1.0 W/kg was not significantly different from that observed in sham-exposed controls, both groups ranging from 0.2 W/kg to 3.0 W/kg ($p<0.01$) or from 1.0

W/kg to 2.0 W/kg ($p<0.001$) exhibited a significant increase in Comet formation after RF-exposure as compared to sham-exposed controls (Figure 74B).

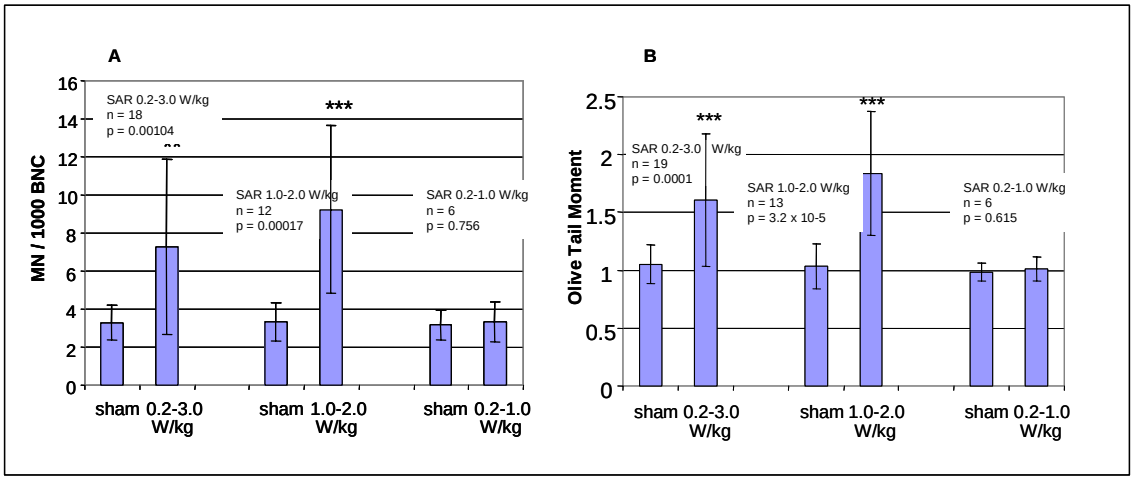

Figure 74. MN induction and Comet formation in HL-60 cells after RF-field exposure (1800 MHz, continuous wave, 24 h) over all SAR groups tested versus total sham, expressed as MN per 1000 BNC (A) and as Olive Tail Moment (B). Each bar represents the mean ± SD of results obtained in indicated number of experiments. ** $P<0.01$; *** $P<0.001$ (Student's t-test, two-sided).

RF-EMF increased the micronucleus frequency and the number of DNA strand breaks in HL-60 cells dependent on the exposure time as determined by the cytokinesis-block in vitro micronucleus assay and the Comet assay.

Using the cytokinesis-block MN assay it was also investigated, whether the duration of exposure of HL-60 cells to RF-fields has an influence on MN induction (Figure 75). Short exposure periods (6 h) caused no or less pronounced effects compared to longer exposure periods of 24 and 72h. The level of the effect on MN frequency noted after RF-EMF exposure for 72h (MN/1000 BNC: 20.22 ± 2.08) was comparable to that observed after 0.5 Gy ionising-irradiation (6 MeV, exposure time: 5.2 s) (MN/1000 BNC: 22.33 ± 2.48).

Furthermore, it was investigated, whether the duration of exposure of HL-60 cells to RF-EMF has an influence on Comet formation (Figure 76). Short exposure periods (2 and 6h) caused less pronounced effects compared to the longer exposure period of 24h. After 72h of exposure Comet formation was similar to that observed after short exposure times (2 and 6h).

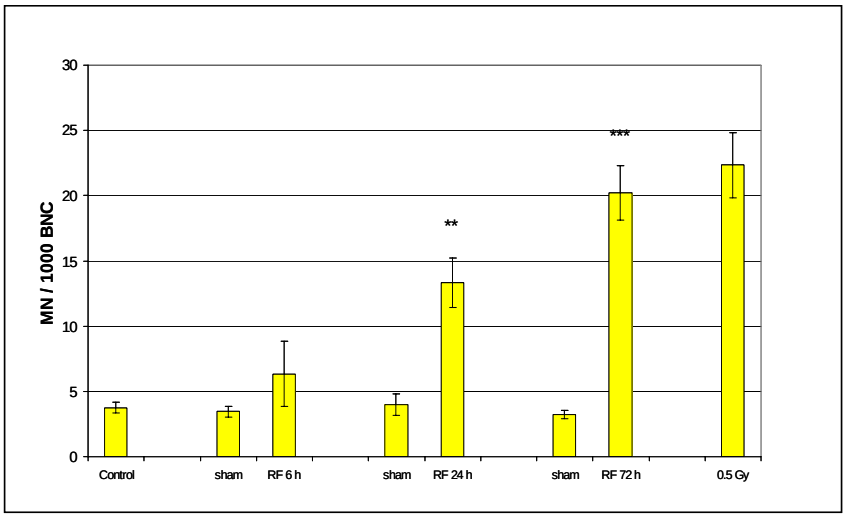

Figure 75. Micronucleus frequencies in binucleated HL-60 cells after exposure to RF-fields (1800 MHz, continuous wave, SAR = 1.3 W/kg) for 6, 24 and 72h, compared to control and sham-exposure. Positive control: 0.5 Gy ionising-irradiation (6 MeV). Each bar represents the mean ± SD of results obtained in three independent experiments (except control: n = 4). Data points are based on a total cell number of 4000 (control), 9000 (sham-exposed), 9000 (RF-exposed) and 3000 (0.5 Gy-exposed, exposure time: 5.2s) binucleated HL-60 cells. All in all (mono-, bi-, tri-, and tetranucleated) 25000 cells were analysed. ** P<0.01; *** P<0.001 (Student's t-test, two-sided).

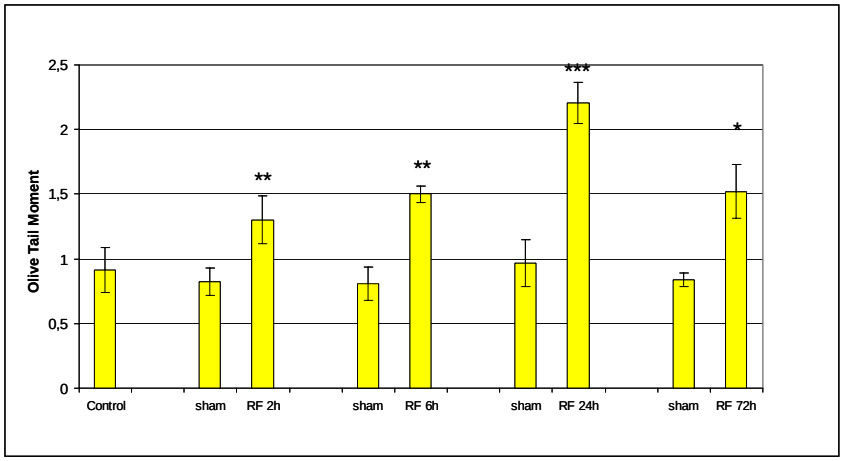

Figure 76. Comet formation in HL-60 cells after exposure to RF-fields (1800 MHz, continuous wave, SAR 1.3 W/kg) for 2, 6, 24 and 72h, expressed as Olive Tail Moment, compared to control and sham-exposure. Each bar represents the mean ± SD of results obtained in at least three (except RF-field exposure, 24h with n=4) independent experiments. * P<0.05; ** P<0.01; *** P<0.001 (Student's t-test, two-sided).

The effects of RF-EMF on genomic integrity of HL-60 cells were exposure-signal-dependent as determined by the cytokinesis-block in vitro micronucleus assay and the Comet assay.

In a further series of experiments it was studied, whether different RF-signals (1800 MHz, SAR 1.3 W/kg: continuous wave, C.W., 5 min on/10 min off; GSM-217Hz, GSM-Talk) for 24h are capable to cause MN induction in HL-60 cells (Figure 77) The number of independent experiments was extended to at least three independent experiments for each of the different types of RF-signals at that SAR with the most pronounced effect (SAR 1.3 W/kg). Using the cytokinesis-block MN assay the different RF-signals had similar effects on MN induction as observed following continuous wave exposure. While the MN frequency of continuous wave-exposed cells was 13.33 ± 1.89, the MN frequencies determined after different other RF-exposure signals were 16.11 ± 3.10 (C.W., 5 min on/10 min off), 13.22 ± 2.88 (GSM-

217Hz) and 17.66 ± 1.70 (GSM-Talk). The MN frequency determined in cells after exposure to ionizing-irradiation (0.5 Gy, 6 MeV, exposure time. 5.2 s), used as a positive control, was 22.3 ± 3.5 (n=3; 6.3 fold increase compared to control).

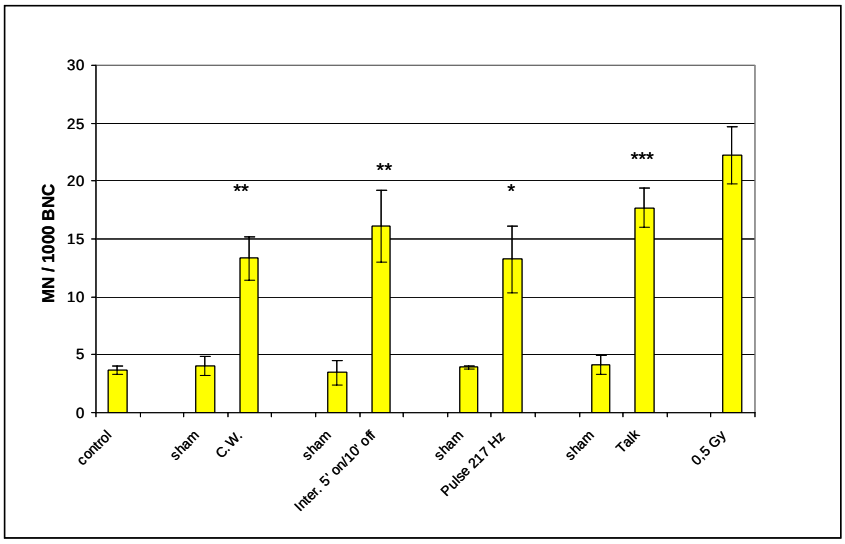

Figure 77. Micronucleus frequencies in binucleated HL-60 cells after exposure to RF-field (1800 MHz, SAR 1.3 W/kg, 24h) compared to control and sham-exposure for different signal modulations. Positive control: 0.5 Gy ionising-irradiation (6 MeV, exposure time: 5.2s). Bars represent means ± SD of three independent experiments (except control = 5). * P<0.01; ** P<0.01; *** P<0.001 (Student's t-test, two-sided). Each data point is based on at least three independent experiments except the control with five and the positive control with three independent experiments and on a total of 5000 (control), 12000 (sham-exposed), 12000 (RF-exposed) and 4000 (0.5 Gy-exposed) binucleated HL-60 cells. All in all (mono-, bi-, tri-, and tetranucleated) 32000 cells were analysed.

Calculation of the average numbers of micronuclei per 1000 BNC determined after exposure (SAR of 1.3 W/kg, 24h) to all RF-signals tested (continuous wave, C.W., 5 min on/10 min off; GSM-217Hz, GSM-Talk) showed an increase in micronuclei induction as compared to sham-exposure at a significant level (number of independent experiments n=12, P<0.001) (Figure 79A).

Using the Comet assay the different RF-signals had similar effects on Comet formation as observed after continuous wave exposure (Figure 78). While the OTM of continuous wave-exposed cells was 2.20 ± 0.16, the OTMs determined after different other RF-exposure signals were 2.11 ± 0.05 (C.W., 5 min on/10 min off), 1.77 ± 0.01 (GSM-217Hz) and 2.26 ± 0.24 (GSM-Talk).

Calculation of the average value of Olive Tail Moments determined after exposure to all RF-signals tested (continuous wave, C.W., 5 min on/10 min off; GSM-217Hz, GSM-Talk) showed a significant increase in Comet formation compared to sham-exposed controls (n=14, P<0.001 (Figure 79B).

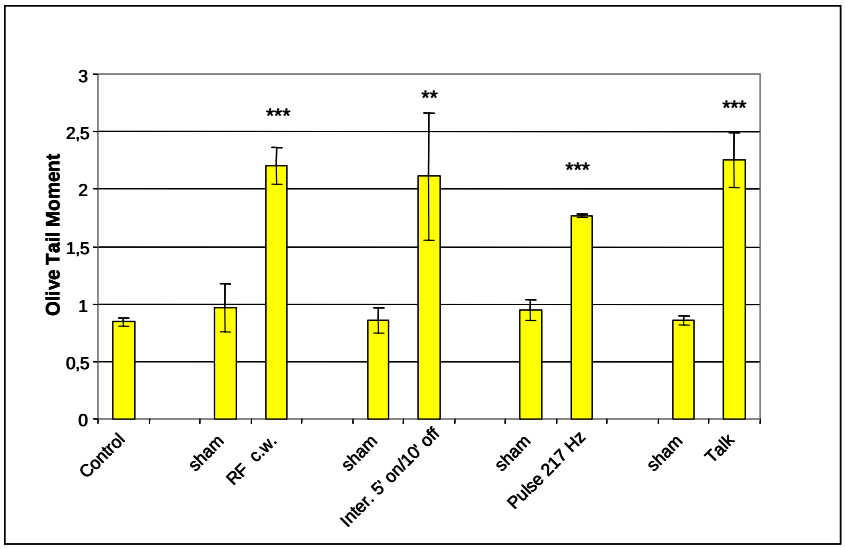

Figure 78. Comet formation in HL-60 cells after exposure to RF-fields (1800 MHz, SAR 1.3 W/kg) for different signal modulations, expressed as Olive Tail Moment, compared to control and sham exposure. Each bar represents the mean ± SD of results obtained in at least three (except continuous wave and C.W., 5 min on/10 min off: n=4) independent experiments. ** P<0.01; *** P<0.001 (Student's t-test, two-sided).

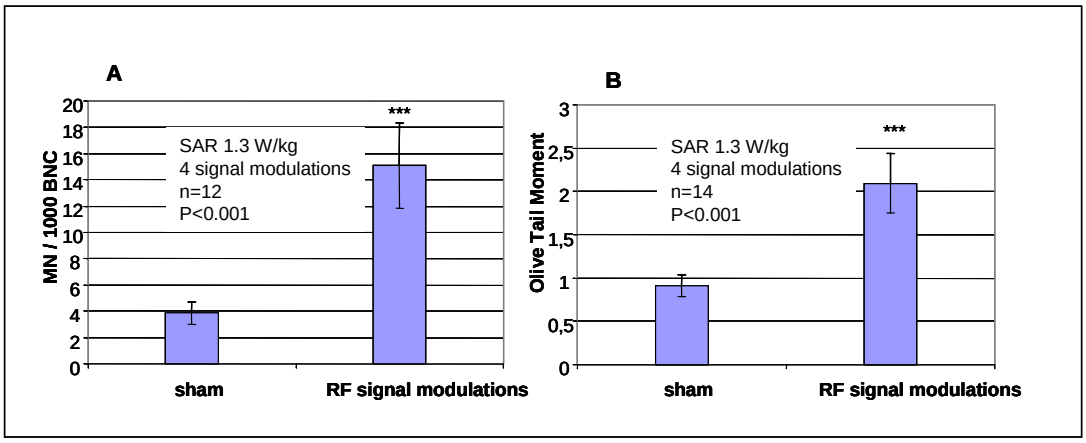

Figure 79. MN induction and Comet formation in HL-60 cells over all RF-field signal modulations at 1800 MHz, 24h, versus total sham, expressed as MN per 1000 BNC (A) and as Olive Tail Moment (B). Each bar represents the mean ± SD of results obtained in indicated number of experiments. *** P<0.001 (Student's t-test, two-sided).

As shown by flow cytometric analysis RF-EMF increased the micronuclei frequency, but did not affect cell cycle.

The results of the flow cytometric analysis of MN induction in HL-60 cells following RF-EMF exposure at the SAR level of 1.3 W/kg tested above using the continuous wave signal, according to the method of Nüsse et al. 1984, 1997, parallel the results obtained using the cytokinesis-block MN assay. Figure 80 shows a representative flow cytometric analysis of MN induction for sham-exposed (A) and RF-exposed (B) HL-60 cells after exposure to RF (1800 MHz, continuous wave, SAR 1.3 W/kg) for 24h. The DNA distribution of micronuclei (marker M1) and nuclei (marker M2) is obtained by projection of the particles defined by their side scatter intensities as micronuclei and nuclei. The percentage of MN is higher in the RF-exposed sample than in the sham-exposed sample (4.1% MN versus 2.7% MN).

The quantitative results of MN content analysis in four independent experiments are presented in Table 13. In all HL-60 cell experiments the MN content of the RF-exposed samples is higher than in sham-exposed samples. Normalisation of MN content in sham-exposed cells to 100% revealed a significant induction of MN after exposure to RF-field by 138.2 ± 18.4% ($P<0.01$; Student's t-test, two-sided). This result parallels those obtained using the microscopic analysis of MN frequencies.

Moreover, by means of flow cytometry the DNA-content of G1/G0, S and G2/M phase can be quantified by determining the fraction of each sub-population. The DNA-content distribution (ethidium bromide fluorescence) showed no differences between RF-field exposed and sham-exposed cells, indicating no influence of RF-EMF on cell cycle (Figure 80). Furthermore, cell cycle analysis demonstrated no accumulation of cells arrested in S and G2/M phase following exposure to RF fields. Additionally, for 24h RF-field exposure (1800 MHz, continuous wave, SAR 1.3 W/kg) no increase of the cell population in he sub G1 peak, which can be considered a marker of apoptotic cell death, was observed by flow cytometry.

Table 14 shows the data of DNA content distribution as percentage of gated cells for G1/G0, G2/M and S phase for RF-field exposed cells (continuous wave, SAR 1.3 W/kg, 24h), as compared to incubator control, sham-exposure and positive control hydrogen peroxide (100 µmol/l for 1 hour). The distribution of G1/G0, G2/M and S phase in the incubator control was 51.9 ± 4.2%, 18.3% ± 3.7 and 19.4 ± 1.7%; that of the positive control hydrogen peroxide: 28.4 ± 12.1%, 9.1 ± 5.2% and 9,0 ± 3.6%. Overall, the percentage of gated cells for the positive control was clearly lower than in all other conditions due to the fact, that here out of the gate analysed a high content of cellular debris was detected. This serves as a measure of cytotoxicity exerted by hydrogen peroxide. Sham-exposed and RF-exposed cells showed a similar DNA distribution as in the incubator control. No significant differences in DNA distribution of RF-exposed cells compared to sham-exposed cells were observed.

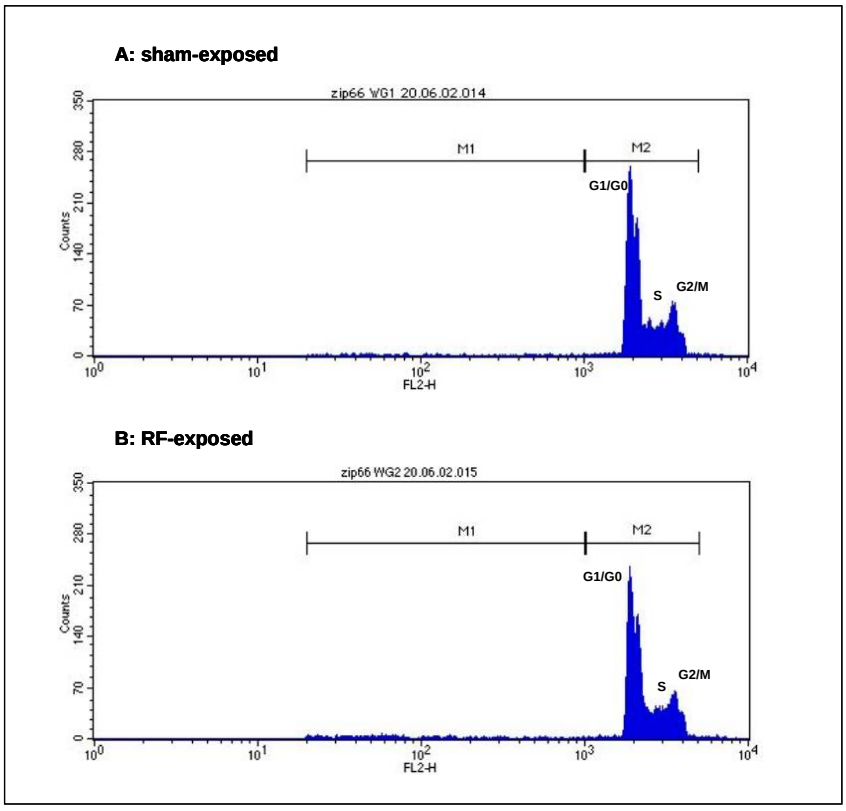

Figure 80. Flow cytometric analysis of micronuclei induction and determination of the proportions of cells in G1/G0, S and G2/M phases of the cell cycle after exposure of HL-60 cells to sham (A) or RF field (B, 1800 MHz, continuous wave, SAR 1.3 W/kg) for 24h.

The diagrams show representative ethidium bromide fluorescence histograms of micronucleated cells/nuclei suspension after treatment with FACS solution I and II. The method was performed according to Nüsse and Kramer (1984), Nüsse and Marx (1997) and Wessel and Nüsse (1995). G1/G0, S and G2/M peaks are indicated. For measurement of MN the G1/G0 peak was adjusted to approximately 2000 relative fluorescence units (FL2-H). The sort window for counting the MN comprised the relative DNA fluorescence units from 20 to 1000 (M1). For quantitative determination of MN the ratio of events in M1 (micronuclei) was compared to the events in M2 (nuclei) and expressed as % MN. For this representative experiment out of four the results for sham-exposure is 2.7% MN (A) and for RF-exposure is 4.1 % MN (B).

Table 13. Quantitative flow cytometric analysis of micronuclei frequencies after RF-field exposure (1800 MHz, continuous wave, SAR 1.3 W/kg, 24 h), compared to sham-exposure.

No. of experiment	Content of MN [%]		
	Sham-exposed	RF-field exposed	Content of MN in RF-exposed cells rel. to sham-exposed cells (100%)
1	2.69	4.08	151.67
2	5.49	6.37	116.03
3	4.24	6.57	154.95
4	1.85	2.41	130.70
mean	3.57 ± 1.62	4.86 ± 1.98	138.23 ± 18.41 **

Data of column 4 are values of RF-exposed cells in percentage relative to the corresponding sham-exposed value.
** Significant difference between the content of MN of RF-exposed cells to sham-exposed cells at P<0.01 (Student's t-test, two-sided).

Table 14. DNA distribution and cell cycle analysis of HL-60 cells after exposure to RF-field (1800 MHz, continuous wave, SAR 1.3 W/kg) for 24 h, compared to control, sham-exposure and positive control hydrogen peroxide (100 µmol/l for 1 h). Data represent DNA content distribution as percentage of gated cells in G1/G0, G2/M and S phase.

Group	n	G1/G0 [%]	S [%]	G2/M [%]
control	3	51.90 ± 4.17	18.25 ± 3.65	19.37± 1.71
sham	4	54.98 ± 6.69	19.45 ± 3.50	18.43 ± 4.07
RF-field	4	52.94 ± 6.19	19.01 ± 3.54	20.06 ± 2.73
positive control H_2O_2 (100 µmol/l for 1h)	3	28.37 ± 12.11	9.11 ± 5.17	8.96 ± 3.59

RF-EMF did not affect apoptosis as demonstrated by the Annexin V and TUNEL assay.

As the findings of structural alterations on the genomic level correlated with an external cellular stimulus do per se not prove a genotoxic effect, it has to be ruled out, that such changes are due to induction of apoptosis. Apoptotic cells typically undergo a series of structural changes: blebbing of the plasma membrane, condensation of the cytoplasm and intact organelles, and nuclear fragmentation. The most common biochemical property of apoptosis is the endonucleolytic cleavage of chromatin, initially to large fragments of 50-300 kilobase pairs and subsequently to monomers and multimers of 180-200 base pairs.

By establishing two flow cytometry methods for detection of apoptosis, Annexin V assay and TUNEL assay, a differentiation approach was included in the experimental strategy. By means of these two tests the detection of apoptotic changes at different stages in the apoptotic process became feasible. As a positive control for apoptosis induction by camptothecin, a topoisomerase I inhibitor, was used in the flow cytometry assays.

After initiation of apoptosis most cell types translocate phosphatidylserine (PS) from the inner plasma membrane leaflet to the cell surface. Once on the cell surface, PS can easily be detected by staining with a FITC conjugate of Annexin V, a protein that has strong natural affinity for phosphatidylserine. As

externalisation of phosphatidylserine occurs before nuclear changes, associated with apoptosis, take place, the Annexin V test detects apoptotic cells significantly earlier than do DNA-based assays.

Figure 81 shows a representative flow cytometric analysis of Annexin V staining following RF- (1800 MHz, 1.3 W/kg, continuous wave, 24h) and sham-exposure of HL-60 cells. As a positive control the apoptosis inducer camptothecin, a topoisomerase I inhibitor, was used to prove inducibility of apoptosis in the HL-60 cell system. The histograms show apoptosis associated Annexin V-FITC-signals (FL-1) versus DNA content propidium iodide (PI) signals. In order to prove that the gating of the corresponding cell populations for scoring the content of apoptotic cells did not select sub-populations, the histograms for "gated" and "not gated" cells are presented.

The TUNEL method (Terminal Deoxynucleotidyl Transferase Biotin-dUTP Nick End Labeling) identifies apoptotic cells *in situ* by using terminal deoxynucleotidyl transferase (TdT) to transfer FITC-dUTP to the free 3´-OH of cleaved DNA. These labelled cleavage sites can then be detected by flow cytometry.

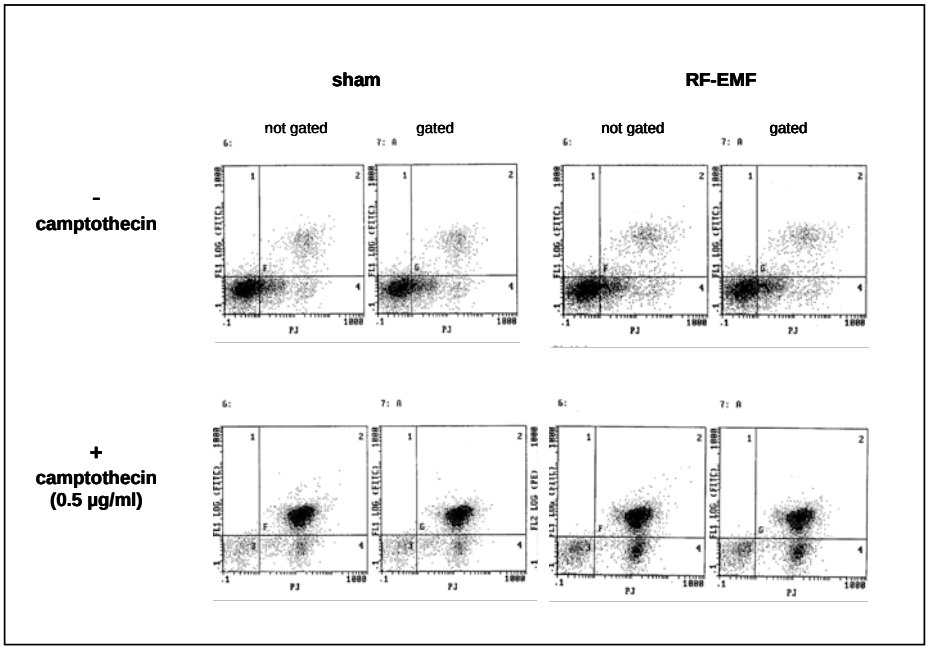

Figure 81. Flow cytometric analysis of RF- (1800 MHz, continuous wave, 1.3 W/kg, 24h) and sham-exposed HL-60 cells after staining with Annexin V-FITC (FL-1) and propidium iodide (PI, DNA content). The apoptosis inducer camptothecin is included as a positive control.

The histograms show apoptosis associated Annexin V-FITC (FL-1) versus DNA content propidium iodide (PI) signals. In order to prove that the gating of the corresponding cell populations for scoring the content of apoptotic cells did not select certain sub-populations, the histograms for "gated" and "not gated" cells are presented.

Figure 82 shows a representative flow cytometric analysis of TUNEL staining following RF-exposure (1800 MHz, , continuous wave, SAR 1.3 W/kg, 24h) and sham exposure of HL-60 cells. As a positive control the apoptosis inducer camptothecin, a topoisomerase I inhibitor, was used to prove inducibility of apoptosis in the HL-60 cell system. The histograms show apoptosis associated TUNEL-FITC-signals (FL-1) versus DNA content propidium iodide (PI) signals. In order to prove that within the quantification procedure no differences in cell population analysed occurs, histograms for "gated" and "not gated" cells are presented (Figure 82).

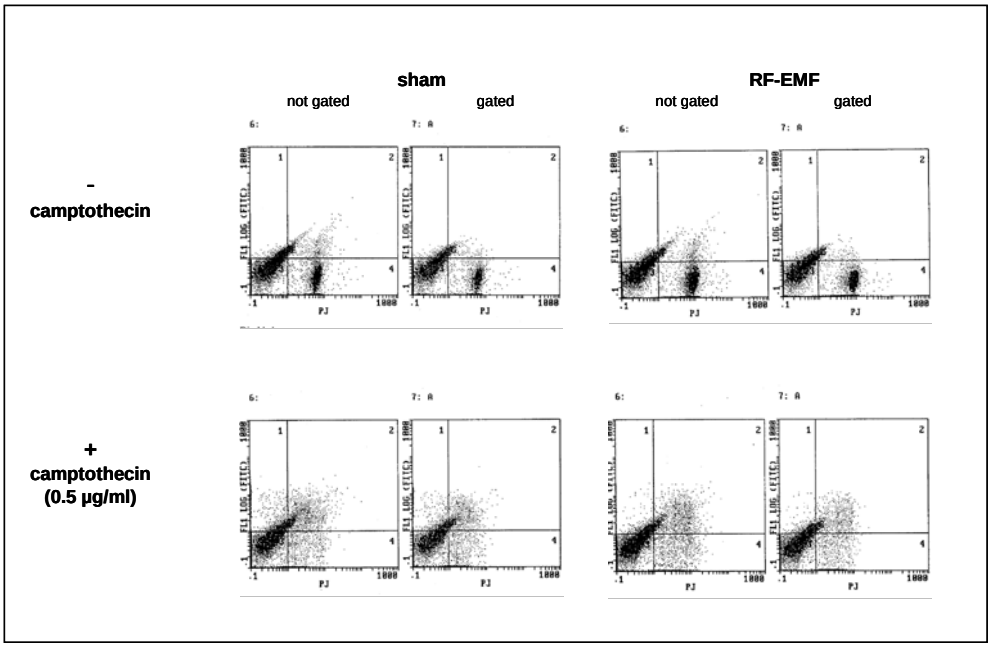

Figure 82. Flow cytometric analysis of RF- (1800 MHz, continuous wave, 1.3 W/kg, 24h) and sham-exposed HL-60 cells after labelling with TUNEL reaction mixture (Roche, Mannheim) for 1 hour at 37°C. The cells then underwent flow cytometric analysis in order to determine the number of green stains (representing apoptotic DNA fragmentation). DNA content analysis was performed on a Becton Dickinson FACScan by using the manufacturer's protocol. The apoptosis inducer camptothecin is included as a positive control.

The histograms show apoptosis associated TUNEL-FITC-signals (FL-1) versus DNA content propidium iodide (PI) signals. In order to prove that the gating of the corresponding cell populations for scoring the content of apoptotic cells did not select certain sub-populations, the histograms for "gated" and "not gated" cells are presented.

Neither by the Annexin V assay nor by the TUNEL assay, apoptosis induced by RF-electromagnetic fields (1800 MHz, continuous wave, SAR 1.3 W/kg, 24h) could be detected in HL-60 cells. Moreover, HL-60 cells exposed to RF-field at SAR 1.3 W/kg and continuous wave signal for 24h show no induction of the cell population in the sub G1 peak, which can be considered a marker of cell death by apoptosis (Figure 80).

RF-EMF did not exert a cytotoxic effect on HL-60 cells.

The trypan blue vitality test did not reveal any cytotoxic effects on the HL-60 cells from any RF-field applied. The vitality of the exposed cells was on the same order of magnitude (≈ 90%) as the cells of the sham-exposed and the incubator control. To exclude minor effects of RF-fields on viability of HL-60 cells, cell viability was examined spectrophotometrically by the MTT assay (Figure 83). Supplementary, also by this method no cytotoxic effect was detectable: absorbance A_{570nm} (RF-exposed HL-60 cells) = 0.91 ± 0.13 ; A_{570nm} (sham-exposed HL-60 cells) = 0.98 ± 0.15.

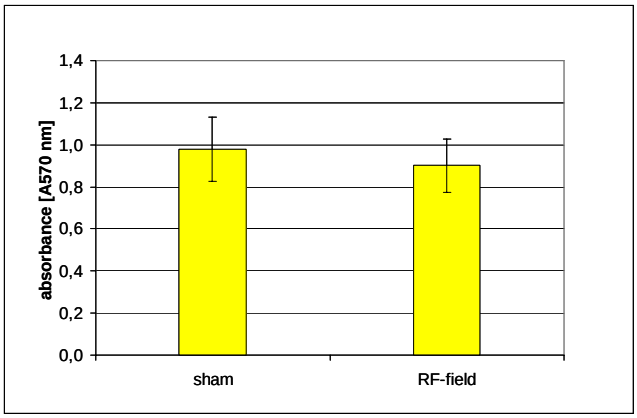

Figure 83. Viability of HL-60 cells after exposure to RF-field (1800 MHz, continuous wave, SAR 1.3 W/kg, 24h) compared to sham exposure. Cell viability was evaluated by the MTT assay and reported as absorbance at 570 nm. Bars represent means ± SD of 12 independent experiments.

In addition, the ratio of binucleated cells (BNC) against mono-, bi-, tri- and tetranucleated cells (% BNC) was determined as a measure of cell division and cell cycle progression. No effect of RF-EMF exposure on % BNC for different energies (Figure 84) or for different signal modulations (Figure 85) was found in comparison to sham-exposed or ionising-irradiated (0.5 Gy, 6 MeV, exposure time: 5.2s) HL-60 cells.

Additionally, no significant differences in DNA distribution of RF-exposed cells compared to sham-exposed cells were observed with respect to increased incidence of cellular debris as a measure of cytotoxicity (Table 14).

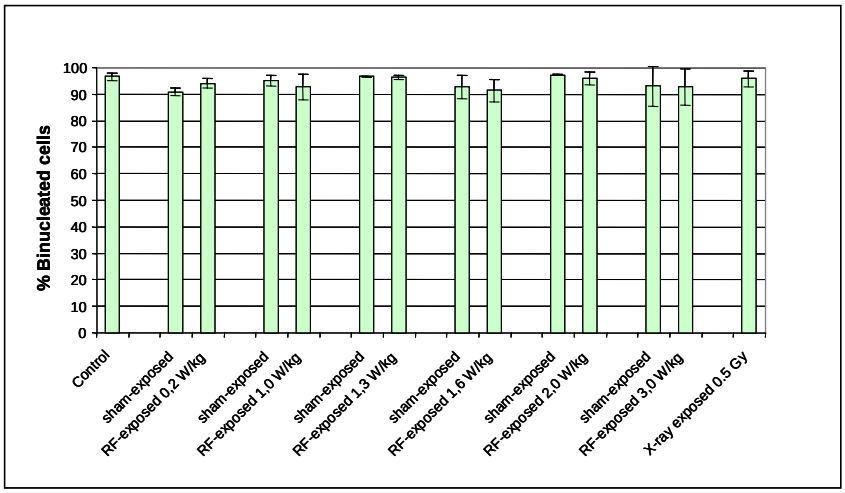

Figure 84. Effect of RF-field exposure on cell division. Shown is the number of binucleated HL-60 cells relative to the number of mono-, bi-, tri-, and tetra-nuclear cells (% BNC) following RF-field exposure (1800 MHz, continuous wave, different SAR levels, 24h). Positive control: 0.5 Gy ionising-irradiation (6 MeV, exposure time: 5.2s). Each bar represents the mean ± SD of results obtained in three independent experiments.

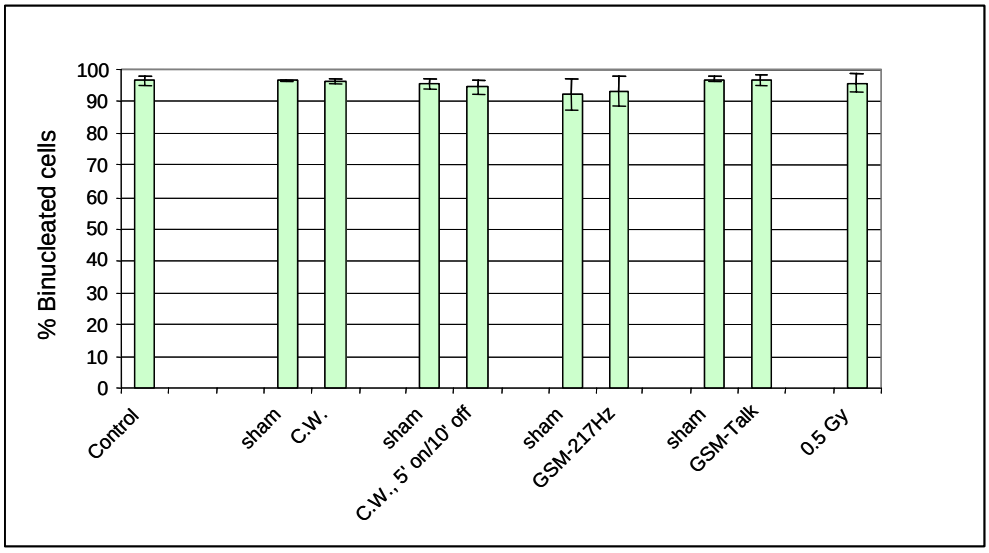

Figure 85. Effect of RF-field exposure on cell division. Shown is the number of binucleated HL-60 cells relative to the number of mono-, bi-, tri-, and tetranuclear cells (% BNC) following RF-field exposure (1800 MHz, SAR 1.3 W/kg, different signal modulations, 24h). Positive control: 0.5 Gy ionising-irradiation (6 MeV, exposure time: 5.2s). Each bar represents the mean ± SD of results obtained in three independent experiments.

Concludingly no in vitro cytotoxic effects of RF-EMF could be detected in RF-EMF-exposed and sham-exposed cells for the exposure conditions tested using either microscopic evaluation (trypan blue exclusion, % BNC), colorimetric MTT assay or flow cytometric analysis (nuclear ethidium bromide staining).

B. Indirect genotoxicity (by reactive oxygen species)

RF-EMF induced formation of reactive oxygen species as shown by flow cytometric detection of oxyDNA and rhodamine fluorescence.

It was the aim of these series of experiments to examine whether RF-EMF (1800 MHz at SAR 1.3 W/kg, 24h exposure) is capable to induce indirect genotoxic effects by affecting the generation and elimination of reactive oxygen species (ROS). For monitoring these ROS-formation and elimination steps, different assays, measuring nitric oxide, oxyDNA, oxidative DNA-damage via Dihydrorhodamine 123 (DHR123), lipid peroxidation, glutathione peroxidase activity, superoxide dismutase activity, have been established and were applied following RF-field exposure of HL-60 cells at that exposure condition with the most significant effect on DNA integrity (1800 MHz, continuous wave, 1.3 W/kg, 24h).

Nitric oxide (NOx)

Nitric oxide (NOx), was measured using the colorimetric Nitric Oxide Assay Kit, Calbiochem, Bad Soden, Germany. The data in Table 15 show the NOx production from HL-60 cells after exposure to RF-field (1800 MHz, continuous wave, SAR 1.3 W/kg, 24h), compared to control and sham-exposed cells. For an amount of 0.25 x 10^5 cells, in neither treatment group the detection limit of 1 µmol NOx/l was exceeded. The results presented are the means of three independent experiments. Concludingly, with this assay no in vitro effect of RF-field exposure on NOx formation was detected for the exposure conditions tested.

Table 15. NO_x formation in HL-60 cells after exposure to RF-field (1800 MHz, continuous wave, SAR 1.3 W/kg, 24h), compared to control and sham-exposure.

Group	NOx [µmol/l]
control	< 1
sham	< 1
RF-field	< 1

0.75×10^6 viable HL-60 cells/3 ml cell culture medium were cultivated for 24h at 37°C. After centrifugation, aliquots of culture media corresponding to 0.25×10^5 cells were collected and analysed for nitric oxide (NOx) by the colorimetric Nitric Oxide Assay Kit, Calbiochem, Bad Soden, Germany.
The results presented are representative for three independent experiments.

Flow cytometric detection of oxidative DNA damage (oxy-DNA)

The presence of oxidised DNA (by a fluorescent probe, directly binding to 8-oxoguanine as the major oxidative DNA product) was indicated by a green/yellow fluorescence that could be detected using a flow cytometry system. In Figure 86 a partial augmentation (occurring as a shoulder on the right side of the signal, see arrow Figure 86 of FL-1 fluorescence intensity), indicating the presence of oxidised DNA, was observed for the RF-exposed signal (green) in contrast to sham-exposed signal (blue). Additionally, RF-exposed cells showed a significant shift to the left as compared to sham-exposed cells. Table 16 shows the data for the quantification of ROS levels using oxyDNA-FITC conjugate to stain 8-oxoGuanosine residues on oxidatively damaged DNA of HL-60 cells. RF-field exposure of HL-60 cells induced a mean increase of oxidative DNA damage of 21.7 ± 2.0 %.

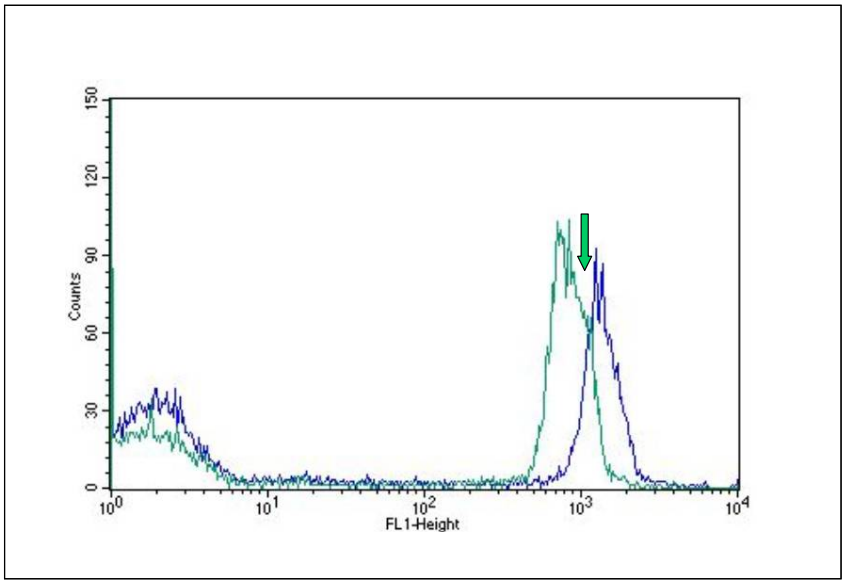

Figure 86. Flow cytometric detection of ROS levels using oxyDNA-FITC conjugate to stain 8-oxoGuo residues on oxidatively damaged DNA of HL-60 cells. The diagram shows the signal of oxidatively damaged DNA of RF-field exposed cells (green line) compared to sham-exposed cells (blue line). One representative histogram plot out of four independent experiments is shown. A partial augmentation (shoulder at the right side of the signal, indicated by arrow) of FL-1 fluorescence intensity was observed for the RF-exposed signal in contrast to sham-exposed signal.

Table 16. Quantification of ROS levels of HL-60 cells after exposure to RF-field (1800 MHz, continuous wave, SAR 1.3 W/kg) for 24h using oxyDNA-FITC conjugate to stain 8-oxoGuo residues on oxidatively damaged DNA.

No. of experiment	% augmentation of fluorescence signal of RF-field exposed cells (area under curve AUC of shoulder at the right side of the signal)
1	21.38
2	24.44
3	19.80
4	20.98
mean ± SD	21.65 ± 2.0

0.75 x 10^6 HL-60 cells/dish were sham- or RF-field exposed for 24 h. oxyDNA-FITC was used to stain 8-oxoGuo residues on oxidatively damaged DNA using the oxyDNA assay from Calbiochem-Novabiochem GmbH, Bad Soden, Germany. Oxidatively damaged DNA was quantified by determination of the area under the curve (AUC) of the shoulder at the right side of the signal fluorescence intensity (see arrow Figure 83) in RF-field exposed cells * Significant difference between the median of fluorescence intensity of RF-field exposed cells and sham-exposed cells at P<0.05 (n=4, Student's t-test, two-sided).

Oxidative DNA damage measured by DHR123 and flow cytometry

Cellular production of ROS was determined by measuring the rhodamine fluorescence of HL-60 cells, incubated in growth medium containing 5 µmol/l dihydrorhodamine 123 (DHR123) for 24h at 37°C. DHR123 is a non-fluorescent reduced Rhodamine 123 (Rh123) derivative that is freely permeable through cell membranes. Intracellular oxidation converts DHR123 to the fluorescent Rh123, which is retained intracellularly by the mitochondrial potential.

Figure 87 displays the overlay fluorescence histograms for RF-field exposed cells (1800 MHz, continuous wave, SAR 1.3 W/kg), compared to sham-exposed cells after simultaneous incubation with DHR123 for 24h. The figure shows that, in RF-field exposed cells, the fluorescence intensity signal shifts to the right in comparison to the signal of sham-exposed cells. In contrast, treating cells with 100 µmol/l H_2O_2 resulted in an even more pronounced shift of fluorescence signal. These shifts indicate enhanced fluorescence intensities and thereby increased production of intracellular ROS during RF-field exposure or H_2O_2 treatment of HL-60 cells.

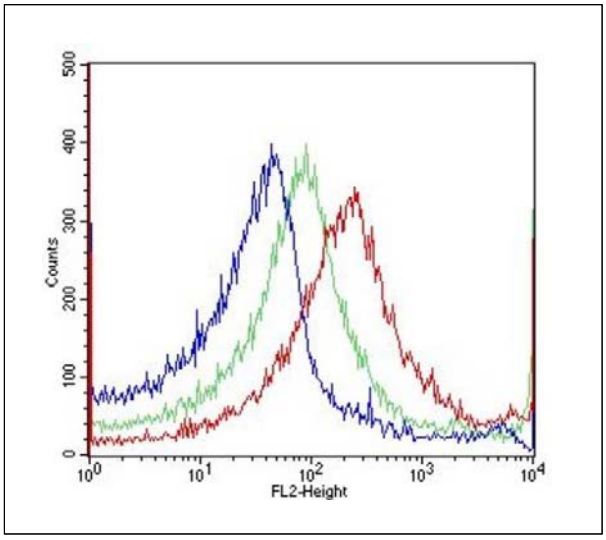

Figure 87. Fluorescence histograms for RF-field exposed (1800 MHz, continuous wave, SAR 1.3 W/kg, 24h) and sham-exposed HL-60 cells simultaneous treated with 5 µmol/l dihydrorhodamine 123 (DHR123). Blue line represents sham-exposed sample, green line represents RF-field exposed sample and red line represents H_2O_2-treated positive control (100 µmol/l for 1 hour). DHR123 reacts with intracellular ROS to form fluorescent Rh123, which is then retained by the mitochondria, enabling a flow cytometric assessment of cellular oxidant production.

By means of the DHR123 flow cytometry detection assay the shift of the signal can be quantified by determining the medians of the fluorescence intensities and the increase in rhodamine fluorescence for each population compared to sham, expressed in percent (Table 17). The data show that there is no difference in the level of oxidatively damaged DNA for control cells and sham-exposed HL-60 cells, expressed as the median of fluorescence intensity. The median values for control cells were 41.8 ± 5.8 and for sham-exposed cells 39.9 ± 8.5 (n=3). The values for the positive control (H_2O_2, 100 µmol/l, 1h) were 230.6 ± 100.3. In contrast, exposing cells to RF-fields resulted in a significant increase in median (75.5 ± 19.2; P<0.05, n=3). The percentage increase of rhodamine fluorescence for RF-field exposed cells compared to sham-exposed cells is 17.8 ± 9.7%, that of H_2O_2-treated cells 31.9 ± 12.4% (Table17).

Table 17. Detection and quantification of ROS levels with Dihydrorhodamine 123 after exposure to RF-field (1800 MHz, continuous wave, SAR 1.3 W/kg, 24 h), compared to control, sham-exposed and H_2O_2-treated HL-60 cells. For quantitative measurement the shift in median and the increase of fluorescence intensity was evaluated.

No. of exp.	Median of fluorescence intensity [units]				% increase of rhodamine 123 fluorescence relative to sham-exposure [a]	
	control	sham-exposed	RF-field exposed	H_2O_2-treated	RF-field exposed	H_2O_2-treated
1	39.95	30.51	95.60	149,89	28.98	43.12
2	37.18	42.17	57.26	199.02	12.35	18.53
3	48.26	46.98	73.65	342.89	11.97	33.91
mean	41.8 ± 5.8	39.9 ± 8.5	75.5 ± 19.2 *	230.6 ± 100.3	17.8 ± 9.7	31.9 ± 12.4

[a] differences of rhodamine 123 fluorescence (AUC, area under curve) of cells exposed to RF-field or those treated with H_2O_2 was determined and the values were plotted as percentage increase relative to sham-exposure.
* Significant difference between the median of RF-exposed cells to the median of sham-exposed cells and the median of RF-exposed cells to that of control cells at P<0.05 (Student's t-test, two-sided).

Lipid peroxidation

Lipid peroxidation was measured using the colorimetric Lipid Peroxidation Assay Kit, Calbiochem, Bad Soden, Germany. Malondialdehyde (MDA) and 4-hydroxy-2(E)-nonenal (4-HNE), products of lipid peroxidation, were estimated spectrophotometrically at 586 nm after reaction with a chromogenic reagent at 45°C. The absorbance values obtained for the samples were compared with a standard curve of known concentrations of MDA / 4-HNE (1 - 20 µmol/l). For MDA and 4-HNE the amounts of lipid peroxidation markers in all experiments and samples were below 1 µmol/l. Table 18 shows that there is no difference in the level of lipid peroxidaton for RF-field exposed HL-60 cells, compared to control and sham-exposed cells (n=3).

Table 18. Lipid peroxidation (LPO) in HL-60 cell homogenates after exposure to RF-field (1800 MHz, continuous wave, SAR 1.3 W/kg, 24h), compared to control and sham-exposed cells.

Group	amount of (MDA + HNE) [µmol/l]		
	exp. 1	exp. 2	exp. 3
control	< 1.0	< 1.0	< 1.0
sham	< 1.0	< 1.0	< 1.0
RF-field	< 1.0	< 1.0	< 1.0

Lipid peroxidation was measured using the colorimetric Lipid Peroxidation Assay Kit from Calbiochem, Bad Soden, Germany. Malondialdehyde (MDA) and 4-hydroxy-2(E)-nonenal (4-HNE), products of lipid peroxidation, were estimated spectrophotometrically at 586 nm in an aliquot corresponding to 6 x 10^5 cells after reaction with a chromogenic reagent at 45°C. The results presented are means of three independent experiments.

Antioxidant enzyme activities

RF-EMF did not affect antioxidant enzyme activities of HL-60 cells (SOD and GPx activity).

To screen the possible effect of RF-EMF on endogenous antioxidant enzyme activity, the activities of superoxide dismutase (SOD) and glutathione peroxidase (GPX) were determined in the HL-60 cells that were exposed to RF-fields (1800 MHz), continuous wave, SAR 1.3 W/kg for 24h. Positive controls as indicated in the assays by the manufacturer were included in the analysis.

Superoxide dismutase (SOD) activity

Superoxide dismutase (SOD) activity of cell homogenates was determined using the Superoxide Dismutase Assay Kit from Calbiochem, Bad Soden, Germany. The data in Table 19 show SOD activities in HL-60 cells after exposure to RF-field (1800 MHz, continuous wave, SAR 1.3 W/kg, 24h), compared to control and sham-exposed cells. For an amount of 4 x 10^5 cells, in neither treatment group the detection limit of 0.2 U/ml SOD activity was exceeded. The results presented are means of two independent experiments. Concludingly, no in vitro effect of RF-field exposure on SOD activity was detected for the exposure conditions tested.

Table 19. Superoxide dismutase (SOD) activity in HL-60 cell homogenates after exposure to RF-field (1800 MHz, continuous wave, SAR 1.3 W/kg, 24h), compared to control and sham-exposed cells.

Group	SOD_{525} activity [U/ml]	
	exp. 1	exp. 2
control	< 0.2	< 0.2
sham	< 0.2	< 0.2
RF-field	< 0.2	< 0.2

Superoxide dismutase (SOD) activity of cell homogenates was determined using the Superoxide Dismutase Assay Kit from Calbiochem, Bad Soden, Germany. The SOD-mediated increase in the rate of autooxidation of the reaction mixture was utilized to yield a chromophore with maximum absorbance at 525 nm. SOD activity was measured in an aliquot corresponding 4 x 10^5 cells (n=2). Detection limit for SOD activity is 0.2 U/ml.

Glutathione peroxidase (GPx) activity

Glutathione peroxidase (GPx) activity of cell homogenates was determined using a cellular Glutathione Peroxidase Assay Kit, Calbiochem, Bad Soden, Germany. The data in Table 20 show the GPx activity in HL-60 cells after exposure to RF-field (1800 MHz, continuous wave, SAR 1.3 W/kg, 24h), compared to control and sham-exposed cells. For an amount of 1 x 10^6 cells, in neither treatment group the detection limit of 5.6 mU/ml GPx activity was exceeded. The results presented represent two independent experiments. Concludingly, no in vitro effect of RF-field exposure on GPx activity was detected for the exposure conditions tested.

Table 20. Glutathione peroxidase (GPx) activity in HL-60 cell homogenates after exposure to RF-field (1800 MHz, continuous wave, SAR 1.3 W/kg, 24h), compared to control and sham-exposed cells.

Group	GPx activity [mU / ml]	
	exp. 1	exp. 2
control	< 5.6	< 5.6
sham	< 5.6	< 5.6
RF-field	< 5.6	< 5.6

Glutathione peroxidase (GPx) activity of cell homogenates was determined in two independent experiments using the cellular Glutathione Peroxidase Assay Kit from Calbiochem, Bad Soden, Germany.
Cell homogenisate of 1 x 10^6 cells is added to a 1050 µl of a solution containing glutathione (GSH, 1mmol/l), GSH reductase (0.4 U/ml) and NADPH. The reaction is initiated by the addition of 350 µl of the diluted organic peroxide t-butyl hydroperoxide and the absorbance at 340 nm was recorded over a period of 5 minutes. The rate of decrease in the absorbance is directly proportional to the GPx activity in the cell homogenisate. Detection limit for GPx activity is 5.6 mU/ml.

Summarising, the endogenous antioxidant enzyme activities of HL-60 cells (SOD and GPx activity) were not altered by RF-field exposure compared to sham-exposure using the conditions of the assays described above. This screening approach revealed, that the analysis of antioxidant enzyme activities does not show enough methodological sensitivity for the amounts of ROS to be generated by RF-field exposure of HL-60 cells.

Indirect genotoxicity by modulation of cellular toxifying and detoxifying capacities

The generation of genotoxic effects through RF-EMF was inhibited by ascorbic acid.

In a further series of experiments it was examined, whether ascorbic acid as a free radical scavenger and inhibitor of reactive oxygen species is capable to inhibit MN induction and DNA damage by co-administration to RF-field-exposure (continuous wave, SAR 1.3 W/kg, 24h). The inhibition of micronuclei induction and Comet formation was measured by use of the cytokinesis-block in vitro Micronucleus assay and the Comet assay. In both tests systems, ascorbic acid effectively reduced the RF-field induction of micronuclei and DNA damage (Figures 85 and 86).

Figure 88 displays the inhibition of MN induction induced by RF-fields (continuous wave, SAR 1.3 W/kg, 24h) and simultaneous treatment of cells with ascorbic acid (AA, 10 µmol/l) for 24h. MN frequencies for sham-exposed and RF-field exposed cells were 4.1 ± 0.2 and 11.6 ± 1.9 expressed as MN / 1000 BNC. After co-incubation of sham-exposed and RF-exposed HL-60 cells with ascorbic acid (AA, 10 µmol/l) for 24h the frequencies were 4.3 ± 0.4 and 4.8 ± 1.9. The MN frequency for the incubator control was 3.4 ± 0.4. Data show, that ascorbic acid inhibits RF-field associated MN induction significantly (n=3, P<0.05). The inhibition resulted in an induction by factor 1.08 compared to sham.

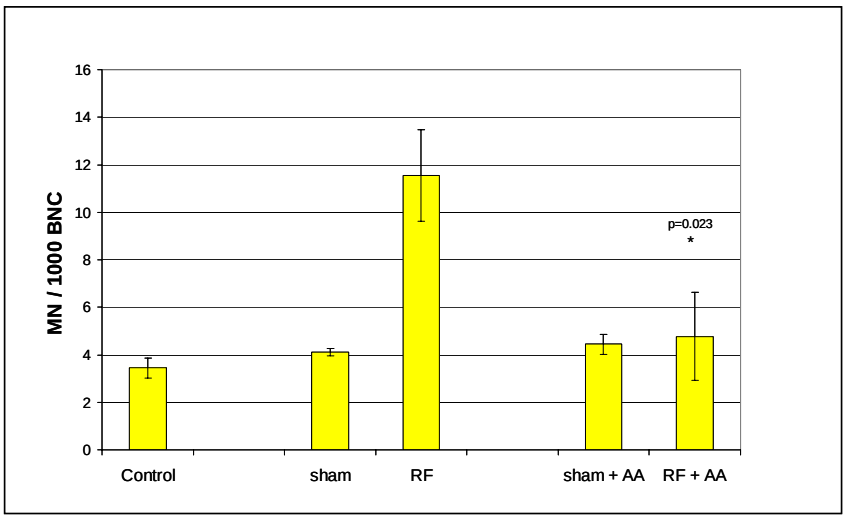

Figure 88. Effect of ascorbic acid (AA, 10 µmol/l) on RF-field (1800 MHz, continuous wave, SAR 1.3 W/kg, 24h) induced MN frequencies in HL-60 cells, compared to control and sham-exposed cells. Each bar represents the mean ± SD of results obtained in at least three independent experiments. Significant differences between RF-field exposure and sham-exposure with co-administration of AA is given by * P<0.05 (Student's t-test, two-sided).

Figure 89 displays the inhibition of DNA damage induced by RF-fields (continuous wave, SAR 1.3 W/kg, 24h) and simultaneous treatment of cells with ascorbic acid (AA, 10 µmol/l) for 24h. The values of Olive Tail Moment for sham-exposed and RF-field exposed cells were 0.9 ± 0.1 and 2.0 ± 0.2. After co-incubation of sham-exposed and RF-field exposed HL-60 cells with ascorbic acid (AA, 10 µmol/l) for 24h the values were 1.0 ± 0.1 and 1.2 ± 0.03. The OTM for the incubator control was 0.8 ± 0.05. Data show, that ascorbic acid inhibits the RF-field induced DNA damage significantly (n=3, P<0.01). The inhibition resulted in an induction by factor 1.2 compared to sham. Additionally, no induction of cytotoxicity (trypan blue test), no alteration of cell medium pH value and no influence on cell growth or cell cycle progression was observed for ascorbic acid alone and for co-administration of ascorbic acid together with RF-field exposure over 24h.

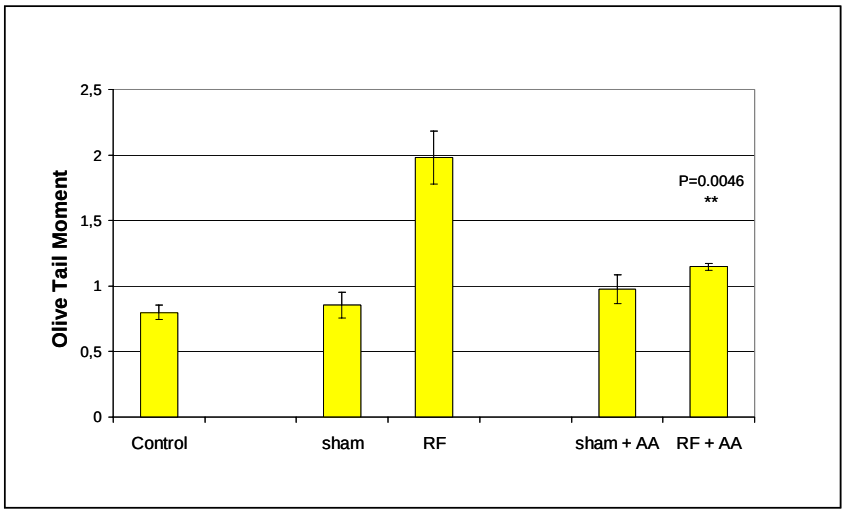

Figure 89. Effect of ascorbic acid (AA, 10 µmol/l) on RF-field induced Comet formation in HL-60 cells (1800 MHz, continuous wave, SAR 1.3 W/kg, 24 h), compared to control and sham-exposed cells. Each bar represents the mean ± SD of results obtained in at least three independent experiments. Significant differences between RF-field exposure and sham-exposure with co-administration of AA is given by ** P<0.01 (Student's t-test, two-sided).

Concludingly, this observed inhibition of genotoxicity by ascorbic acid supports the hypothesis that the effect of RF-field on genomic integrity may be explained by the generation of free oxygen radicals.

3.2.1.2 Human fibroblasts and granulosa cells of rats (Participant 3)

RF-EMF generated DNA strand breaks in human fibroblasts and in granulosa cells of rats.

The influence of RF-EMF exposure on the generation of DNA strand breaks in cells of two different tissues (human fibroblasts, rat granulosa cells) was evaluated using alkaline and neutral Comet assay. Four different sets of exposure conditions were tested: continuous (1800 MHz, 2 W/kg), intermittent (5 min on/10 min off, 1800 MHz, 2 W/kg), pulse modulation (1800 MHz, 2 W/kg, amplitude 217 Hz, 5 min on/10 min off) and talk modulation (1800 MHz, 1.2 W/kg, DTX 66%, GSM basic 34%, continuous). Different exposure duration was applied (4, 16 and 24 hours).

An elevation of Comet assay levels in exposed cells compared to sham-exposed controls could be detected in each of these experiments, even at continuous exposure (Figure 90). This elevation became significant at 16 hours of exposure, but no significant differences between 16 and 24 hours could be detected. At intermittent, pulse modulation and talk modulation Comet assay levels were significantly higher than at continuous exposure. Human fibroblasts and granulosa cells responded equally to RF-EMF, albeit the latter exhibited higher basal and higher end levels (Figure 91). The Comet factors with neutral Comet assay were similar, albeit lower (Figures 92, 93). Dose response investigations with human fibroblasts, which were exposed intermittently (5 min on/10 min off) for 24 hours, revealed a dose dependent increase of the Comet tailfactor beginning already at a SAR of 0.3 W/kg with a peak level at 1.0 W/kg (Figure 94).

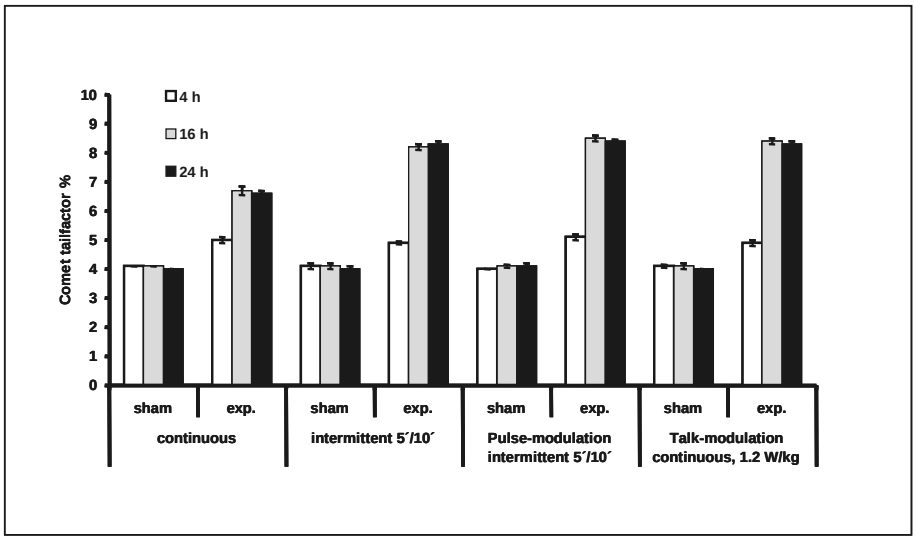

Figure 90. Influence of exposure time and of different exposure conditions on formation of DNA single and double strand breaks in human fibroblasts determined with Comet assay under alkaline conditions (cell strain ES 1, 1800 MHz, SAR 2 W/kg).

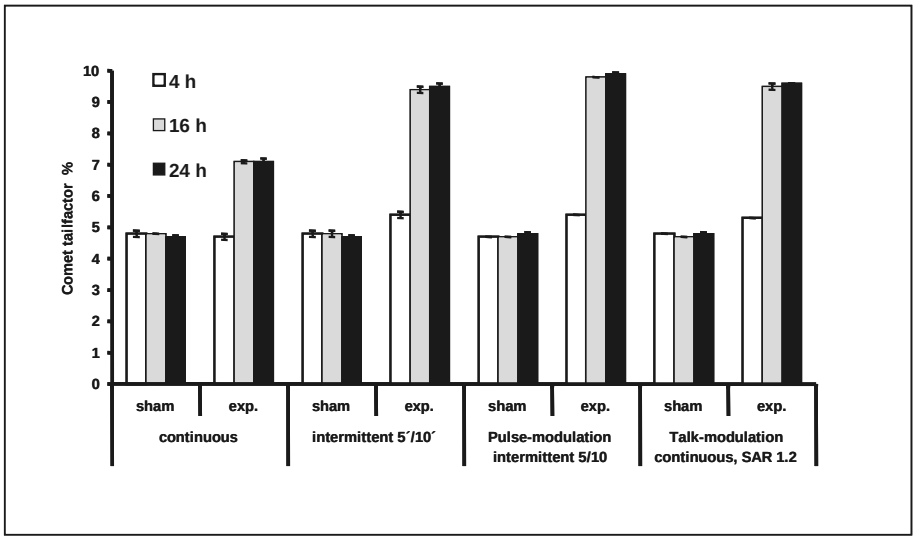

Figure 91. Influence of exposure time and of different exposure conditions on formation of DNA single and double strand breaks in granulosa cells determined with Comet assay under alkaline conditions.

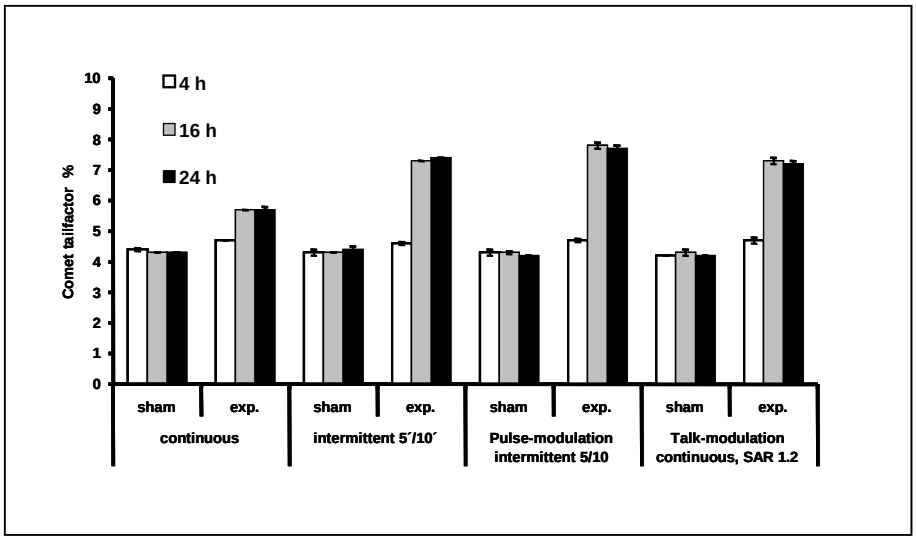

Figure 92. Influence of exposure time and of different exposure conditions on formation of DNA double strand breaks in human fibroblasts determined with Comet assay under neutral conditions (cell strain ES 1, 1800 MHz, SAR 2 W/kg).

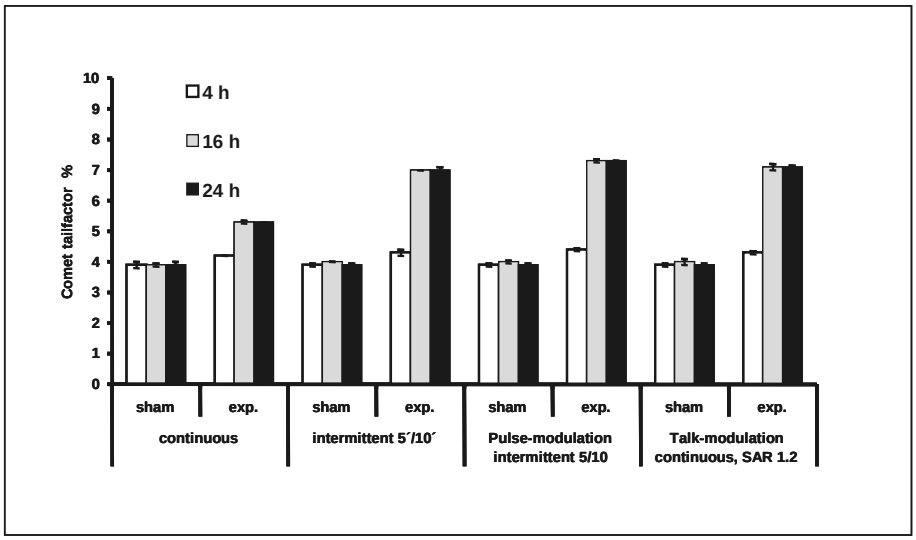

Figure 93. Influence of exposure time and of different exposure conditions on formation of DNA double strand breaks in granulosa cells determined with Comet assay under neutral conditions (1800 MHz, SAR 2 W/kg).

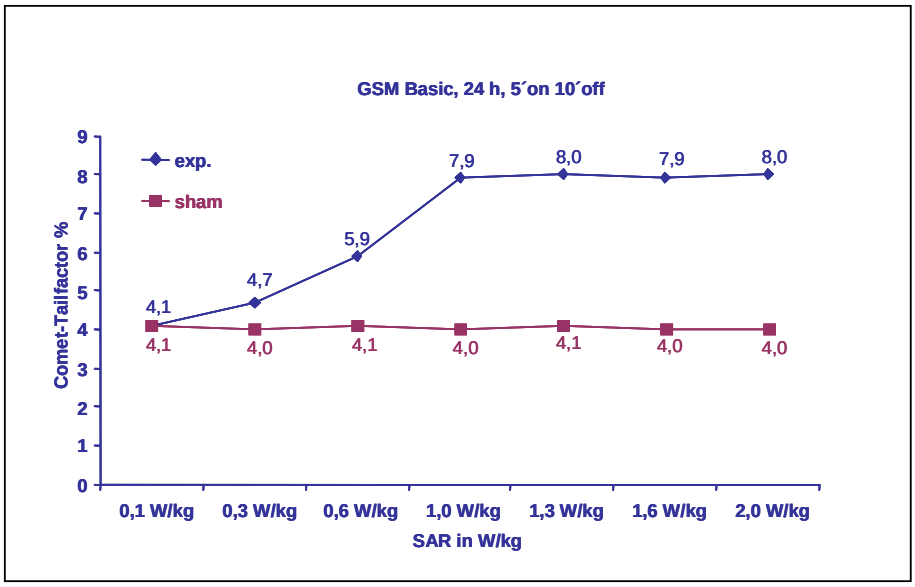

Figure 94. Dose dependent increase of DNA single and double strand breaks in human fibroblasts determined with the Comet assay under alkaline conditions

RF-EMF generated chromosomal aberrations in human fibroblasts.

Since we could demonstrate an induction of DNA strand breaks in human fibroblasts after RF-EMF exposure and due to the results of chromosome aberrations upon ELF-EMF exposure, we also evaluated the chromosome aberrations after RF-EMF exposure (GSM basic 1950 MHz, 1 W/kg, 5 min on/10 min off, 15 hours). These preliminary experiments (500 metaphases scored) revealed in RF-EMF exposed fibroblasts a 10-fold increase in chromosome gaps, a 4-fold increase in chromosome breaks and very high incidences of dicentrics and acentric fragments (Table 21).

Table 21. Percentage of chromosomal aberrations induced by RF-EMF exposure (GSM basic 1950 MHz, 1 W/kg, 5 min on/10 min off, 15h) in cultured human fibroblasts[a]

types of aberration	RF-exposed (% ± SD)	sham-exposed (% ± SD)	p-value[b]
chromosome gaps	57.5 ± 2.1 %	4.8 ± 1.6 %	< 0.001
chromosome breaks	8.1 ± 0.7 %	1.7 ± 0.1 %	< 0.001
dicentric chromosomes	4.5 ± 0.7 %	---	
acentric fragments	1.5 ± 0.7 %	---	

[a] a number of 1,000 metaphases were scored in each of five independent experiments. Results are expressed as percentage chromosomal aberrations per cell.
[b] Significant differences (p<0.05) as compared to sham-exposed controls using Student's t-test for independent samples

RF-EMF induced micronuclei in human fibroblasts.

Cultured human fibroblasts were exposed to RF-EMF (GSM basic 1950 MHz, 15h, 2 W/kg) and micronuclei frequencies were evaluated. These results showed an induction of micronuclei in RF-EMF exposed fibroblasts (Figure 95a). The observed increase in micronucleus frequencies was about 20-fold compared to sham exposed cells or non-exposed controls, but not as high as in bleomycin (10 µg/ml, 17h) treated cells, which were used as positive controls.

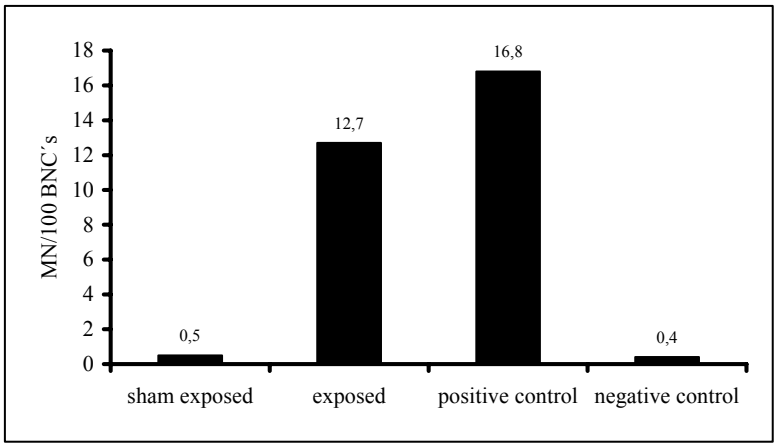

Figure 95. Micronucleus frequencies of RF-EMF exposed (GSM basic 1950 MHz, 15h, 2 W/kg) cultured human fibroblasts and control cells. Bleomycin-treated cell were used as a positive control.

Results on the influence of RF-EMF on the mitochondrial membrane potential were inconsistent.

Evaluating changes in the mitochondrial membrane potential after RF-EMF exposure (GSM basic 1950 MHz, 1 W/kg, 5 min on/10 min off, 15h) using JC-1, revealed a significant decrease in the mitochondrial membrane potential in one experiment, which could not be reproduced..

3.2.1.3 Mouse embryonic stem cells (Participant 4)

RF-EMF affected double-strand DNA break induction in ES cell derived neural progenitors immediately after exposure.

We studied the possible effects of RF-EMF on the integrity of DNA strands in differentiating ES cell from EB outgrowths. Two schemes were applied: (1) For RF-EMF exposure (GSM signal 217-Hz, 1.71 GHz, 1.5 W/kg, intermittency 5 min on/30 min off, 6h), the percentage of primary DNA damage was measured in the alkaline and neutral Comet assay immediately after the RF-EMF exposure at the stage of neural differentiation (4+4d - 4+6d) and 18 hours after the RF-EMF exposure. No differences in the induction of single-strand breaks as measured by the alkaline Comet assay were observed 0 and 18 hours after exposure. The tailfactor was slightly, but significantly increased in the neutral Comet assay immediately after exposure ($p<0.05$) (Table 26). In the second set of experiments, the same RF-EMF exposure conditions were applied for 48 hours instead of 6 hours, and the alkaline Comet assay was done immediately after exposure, while the neutral Comet assay was done 24 or 48 hours post exposure. However, no significant differences were observed in the induction of single- or-double DNA strand breaks between sham-exposed or EMF exposed neural progenitors after prolonged exposure (48h).

3.2.1.4 Summary (Participant 1)

Our data indicate a genotoxic action of RF-EMF in various cell systems. This conclusion is based on the following findings:

- RF-EMF exposure was able to induce DNA single and double strand breaks as well as an increase in micronuclei in HL-60 cells (3.2.1.1).
- The DNA damage generated by RF-EMF in HL-60 cells was dependent on the time of exposure, the field strength and the type of RF-EMF signals (3.2.1.1).
- The DNA damage in HL-60 cells probably resulted from an increase in free oxygen radicals induced during RF-EMF exposure (3.2.1.1).
- RF-EMF exposure at a SAR value between 0,3 and 2,0 W/kg produced DNA single and double strand breaks in human fibroblasts and in granulosa cells of rats dependent on the exposure time and the type of signals (3.2.1.2).

- RF-EMF exposure at a SAR value of 2 W/kg caused an increase in chromosomal aberrations in human fibroblasts demonstrating that the DNA repair was not error-free (3.2.1.2).
- RF-EMF exposure at a SAR value of 1,5 W/kg caused a slight, but significant increase in DNA double strand breaks in neural progenitor cells stemming from mouse embryonic stem cells (3.2.1.3).

3.2.2 Cell proliferation and cell differentiation

3.2.2.1 Human neuroblastoma cell line NB69 and neural stem cells (NSC) (Participant 5)

RF-EMF did not affect growth or viability of NB69 neuroblastoma cells and neural stem cells (NSC).

NB69 cells were exposed at day 3 postplating to GSM-Basic over a 24-hour period. After exposure, the cells were left to grow in the absence of field for an additional 24 hour lapse (5 days postplating). The field exposure was applied alone or in combination with bFGF. As it is shown in Figure 96, the GSM-Basic signal alone did not affect significantly cell growth or cell viability. The morphological analysis did not show significant differences between exposed and control groups, either (data not shown). The treatment with bFGF alone induces differentiation in NB69 cells, which exhibit significant increases in the number and the extension of processes per cell and in the cell size (see 3.2.4.2). An equivalent response was obtained after exposure to the combined treatment with bFGF plus GSM-Basic.

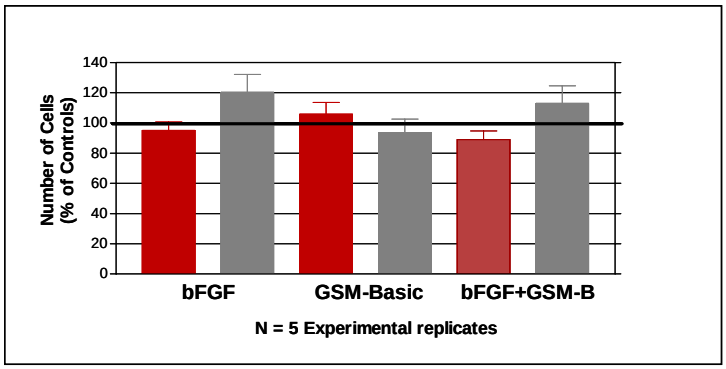

Figure 96. Number of living (red) and dead (grey) cells after a 24-h exposure to GSM-Basic signal followed by 24 additional hours of incubation in the absence of the RF-EMF. No significant changes were observed in the exposed samples when compared to the respective controls

NS cells were exposed at day 2 postplating to GSM-Basic over a 24-hour period. After exposure, the cells were left to grow in the absence of field for an additional 48-hour lapse (5 days postplating). At the end of this period, the samples were studied for cell growth and/or cell viability. The treatment did not affect cell growth (Figure 97A) and did not induce significant changes in the cells' morphology (data not shown). However, the cell size in the exposed samples was observed to be slightly, but not significantly augmented when compared to the respective controls (Figure 97B; image analysis of 60 microscope fields per condition of a total of 4 experimental replicates). The observed, slight reductions in the percent of dead cells, and in the increase of the cells' size after exposure to the GSM-Basic signal (Figure 97) could be due to an enhancement of the cell attachment to the substrate in the exposed samples. Such an attachment was microscope observed, though not image-analysis quantified (data not shown).

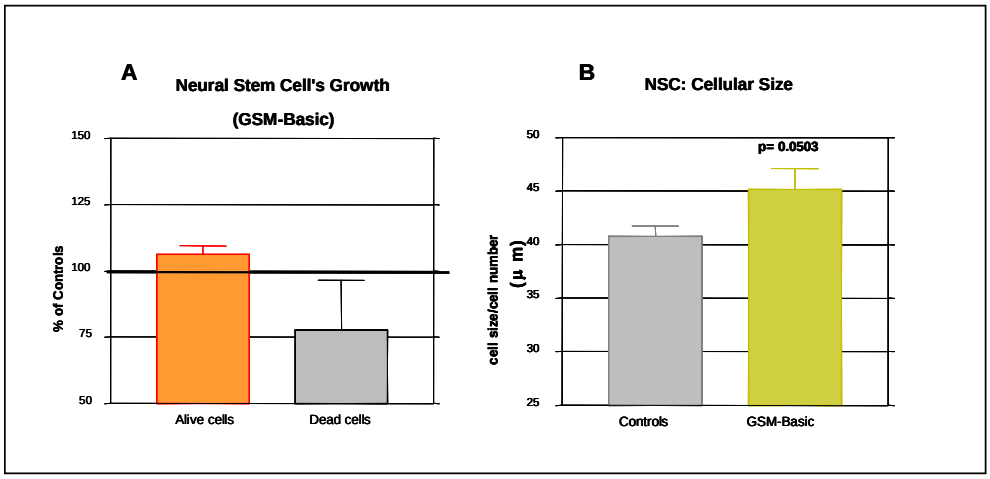

Figure 97. (A) Number of living and dead cells after a 21-h exposure to GSM-Basic signal followed by 48 additional hours of incubation in the absence of RF-EMF (5 days postplating). No significant changes were observed, even though a small reduction of dead cells occurs in the exposed samples. (B) The cell size in the exposed samples was observed to be slightly, but not significantly augmented when compared to the respective controls.

RF-EMF may affect the expression of FGF receptors in NB69 human neuroblastoma cells and in neural stem, potentially influencing cellular differentiation.

See 3.2.4.2

RF-EMF affected the differentiation of neural stem cells (NSC), but not of neuroblastoma cells (NB69).

The aim of the study was to determine whether the exposure of neural stem cells (NSC) to GSM-1800 signals (GSM-Basic signal, 21-hours, 5 min on/10 min off) can influence the evolution of the phenotypic differentiation at the middle term (6 additional days after exposure). As described in the methodology, the cells were exposed to RF-EMF at day 2 postplating. After the 21-hour exposure, the cells were grown for 6 additional days in the absence of the GSM stimulus. At the end of this period, the cells were immunostained with O1 for mature oligodendrocyte identification, GFAP for astrocytes and ß-tubulin III for neurons. All experiments and analysis were conducted following blind protocols. The data (N= 5 experimental replicates) indicate that the GSM-Basic signal promotes marked morphological changes in differentiating oligodendrocytes and astrocytes derived from NSC (Figure 98).

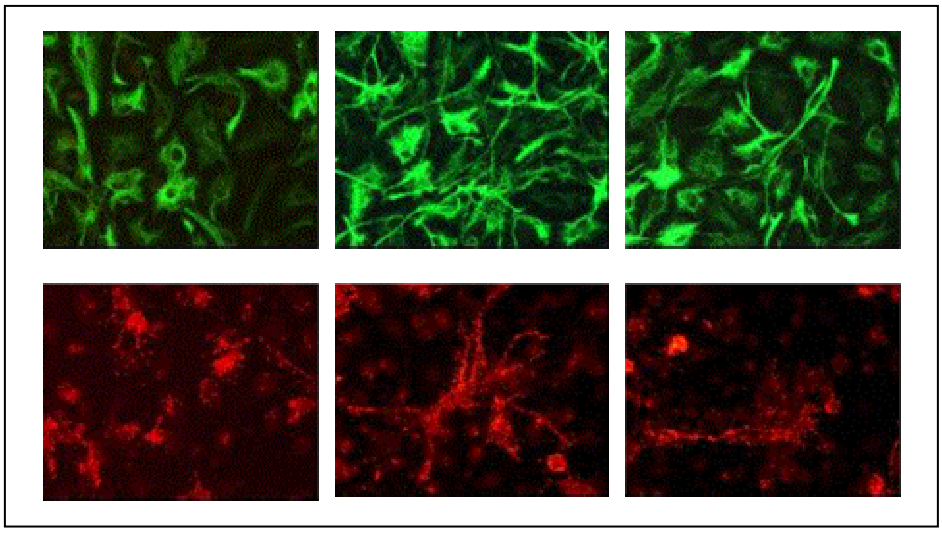

Figure 98. Photomicrographs of neural stem cells progeny. Astrocytes labelled with GFAP (green) and oligodendrocytes labelled with O1 (red) immunostaining: A, Control; B, and C, exposed to the GSM-Basic signal. The exposure increases cell extension in astrocytes and oligodendrocytes.

Similar experiments have been carried out to evaluate the phenotypic differentiation of NB69 cells treated with the above GSM-signal and exposure conditions, in the presence or absence of RA. As described in the methodology, the cells were exposed to the field at day 3 postplating, during a 24-hour period, and then grown for 2 additional days in the absence of GSM exposure. After that, the cells were analysed for expression of mature neuronal cell marker ß-tubulin III, and for tyrosine hydroxylase (TH) marker. Exogenous, basic fibroblast growth factor was used as a positive control. The data show that the neuronal outgrowth of NB69 cells (Figure 99) and the percent of TH+ cells seem not to be altered by the exposure to the GSM-Basic signal. Only the treatment with bFGF promoted the neuronal microtubules network in these cells.

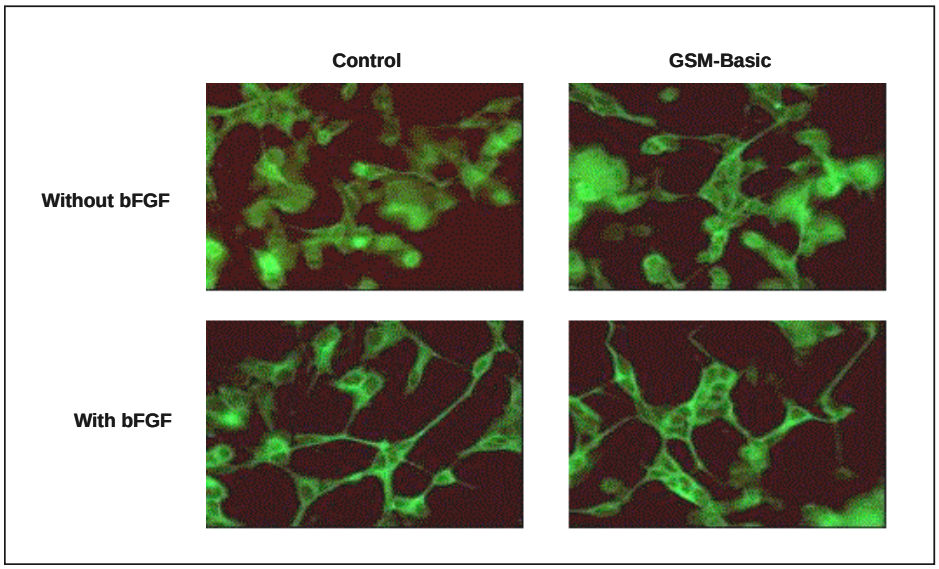

Figure 99. Photomicrographs of NB69 cells analysed 3 days after the exposure and/or incubation in the presence or absence of bFGF. Cells stained with anti-beta-tubulin antibody. The neuronal outgrowth of NB69 cells seems not to be altered by the exposure to the GSM-Basic signal. However, the treatment with bFGF promotes the neuronal microtubules network in these cells.

3.2.2.2 Human lymphocytes and thymocytes (Participant 8)

RF-EMF did not affect proliferation, cell cycle and activation of human lymphocytes.

The experiments with RF-EMF were performed at SAR 1,4-2,0 W/kg using different RF modulations or time exposure. Studies on cell proliferation were performed discriminating CD4+CD28+/- and CD8+CD28+/-lymphocytes subpopulation. Cells were exposed to Talk modulated RF-EMF (2 W/kg) and two intermittent types of exposure were applied: 1) 10 min on/20 min off for 44 hours; 2) 2 hours on/22 hours off for 72 hours. We performed experiments with cells from 6 donors using the former approach, from 11 donors using the latter approach. All cells were acquired and analysed after 72 hours and 120 hours of culture. A small increase (3%) of proliferating CD8+CD28+ T lymphocytes was observed in exposed cells both at 72 hours and 120 hours of culture. Since the differences observed are similar to the calculated standard error, we considered this effects not relevant. In Tables 22 and 23 data related to proliferating and not proliferating cells subsets after 72 hours and 120 hours of culture, respectively, are reported.

Table 22. T lymphocytes subsets exposed to talk modulated RF-EMF 2 hours on/22hours off for 72 hours. Data are reported as mean (% ± s.e.) of all experiments performed

Lymphocyte subsets	Sham % ± se	RF % ± se	p
P CD4+CD28+	30.7 ± 2	28.2 ± 2	ns
P CD4+CD28-	0.9 ± 0.4	0.7 ± 0.3	ns
NP CD4+CD28+	13.0 ± 2	12.4 ± 2	ns
NP CD4+CD28-	1.8 ± 0.9	0.8 ± 0.3	ns
P CD8+CD28+	19 ± 2	21 ± 2	0.042
P CD8+CD28-	7.9 ± 3	7.7 ± 3	ns
NP CD8+CD28+	8.0 ± 1	9.3 ±1	ns
NP CD8+CD28-	1.1 ± 0.2	1.0 ± 0.4	ns

P = proliferating; NP = non proliferating; ns = not significant

Table 23. T lymphocytes subsets exposed to Talk modulated RF-EMF 2 hours on/22 hours off for 72 hours and analysed at 120 hours of culture. Data are reported as mean (% ± s.e.) of all experiments performed

Lymphocyte subsets	Sham % ± se	RF % ± se	p
P CD4+CD28+	61.0 ± 2	62.1 ± 2	ns
P CD4+CD28-	0.60 ± 0.07	0.80 ± 0.11	ns
NP CD4+CD28+	9.3 ± 0.2	8.7 ± 0.2	ns
NP CD4+CD28-	1.4 ± 0.1	1.72 ± 0.11	ns
P CD8+CD28+	32 ± 4	35 ± 4	0.048
P CD8+CD28-	5.4 ± 3	4.3 ± 2	ns
NP CD8+CD28+	5.4 ± 0.7	4.7 ± 0.9	ns
NP CD8+CD28-	0.9 ± 0.3	0.8 ± 0.3	ns

P = proliferating; NP = non proliferating; ns = not significant

Cell cycle analysis was performed in PBMCs exposed at three RF-EMF modulations and in the case of Talk signal also PBMCs from old donors were analysed. In all the cases observed no differences were found between exposure and control cells. Some slight differences (1-2%, sometimes increase and sometimes decrease) were observed when analysis of activation markers on CD4+ and CD8+ T lymphocytes were performed on both young and old donors. Since the effects were really small, we

performed from 5 up to 8 replications of T lymphocyte phenotypical analysis, using cells from the same donor.

Results obtained from replications did not confirm the data previously obtained, thus suggesting that such small significant effects must be considered at the noise level of the statistical analysis. Moreover, we performed a more sophisticated analysis on fluorescence intensity in order to verify if the number of molecular markers could be changed in RF exposed cells in comparison with sham exposed cells. We found that in T helper lymphocytes from elderly, but not from young donors, and exposed to Talk modulated RF-EMF, CD95 molecules shifted significantly their fluorescence from bright to dim, as reported in Figure 96. This effect means that in the exposed cells the number of molecular markers on membrane surface was slightly decreased (around 9%).

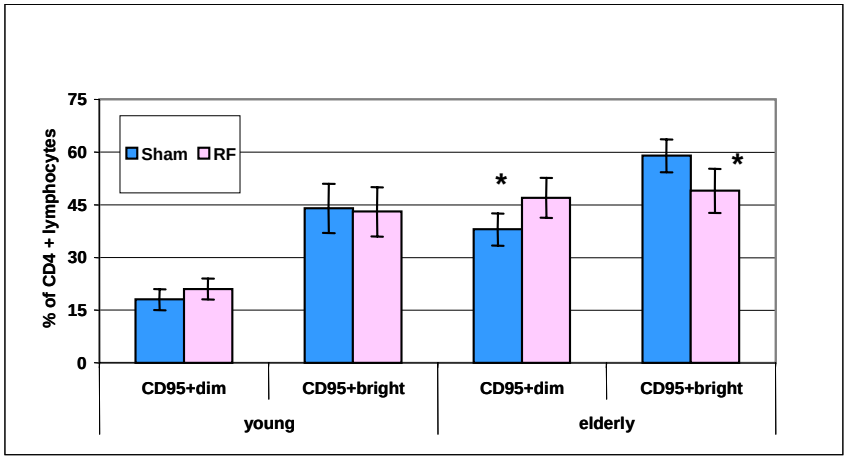

Figure 100. Analysis of fluorescence brightness of proliferating CD4+CD95+ from 10 young and 8 elderly donors, after sham and talk modulated RF-EMF exposure (2W/kg). * = $p < 0.05$. Data are represented as mean ± s.e.

RF-EMF (DTX) may inhibit the production of IL-1beta in human lymphocytes, but did not affect the production of IL 6.

The results obtained showed no significant differences between cells sham-exposed or differently modulated RF-EMF exposed, except in the case of IL-1beta. Indeed, we found a decrease of IL-1beta production (around 13%) in CD3-stimulated PBMCs exposed to DTX modulated RF-EMF in comparison with sham-exposed cells. As demonstrated in Figure 101, the decrease observed was statistically significant on 6 experiments performed. This result was not found when PBMCs were exposed to Talk modulated RF-EMF or using the other stimulus.

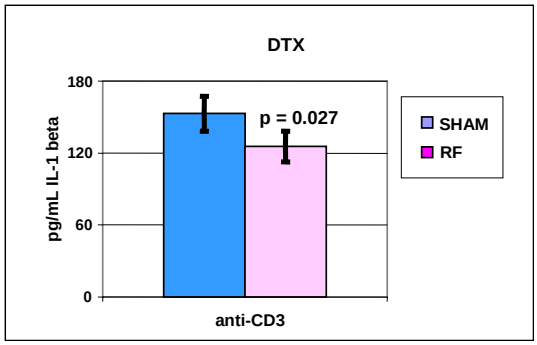

Figure 101. Effect of DTX modulated RF (SAR 1.4 W/kg) on IL-1 beta production in CD3-stimulated PBMCs.

RF-EMF did not affect thymocyte differentiation.

HTOC were performed in order to assess *in vitro* phenotypical differentiation and apoptotic phenomena due to negative selection, which usually occurs in vivo inside the thymus. Thus, different subsets of thymocytes were analysed such as CD71+CD4-CD8-, CD3-/+CD4+CD8+, abTCR-/+CD4+CD8+, gdTCR-/+CD4-CD8-, CD3+CD4+CD8-, CD3+CD4CD8+, abTCR+CD4+CD8-, abTCR+ CD4-CD8+ cells. Each population represents a different phase of development, which was monitored before the exposure and at the end of culture, in presence or absence of RF-EMF. Thymocyte apoptosis was assessed with two different methods, in the same conditions, but the data obtained from 6 human thymus on thymocyte differentiation and apoptosis did not suggest positive results on both the endpoints. Actually, a small increase (4%) of double positive thymocytes (CD4+CD8+) was found in RF-EMF-exposed cultures in comparison with sham-exposed tissue fragments. Also in this case the effect is of the order of the standard error thus we consider these results irrelevant.

3.2.2.3 Human promyelocytic cell line HL-60 (Participant 2)

RF-EMF did not affect the cell cycle of HL-60 cells as shown by flow cytometric analysis.

See 3.2.1.1

RF-EMF did not affect the growth behaviour of HL-60 cells with respect to growth velocity and DNA synthesis.

See 3.2.1.1

Indicators for HL-60 cell growth were the proliferation rate, reflected by the cellular doubling time, and the synthesis of the enzyme thymidine kinase (TK). The enzyme thymidine kinase plays an important role in DNA synthesis. It has been well established that the cellular activity of thymidine kinase is correlated with the growth rate of cells (Johnson et al. 1982). Its relation to the cell cycle has been shown in previous studies (Chang 1990; Kit 1976; Pelka-Fleischer et al. 1987; Piper et al. 1980).

Cellular doubling time

Cellular growth behaviour with respect to growth velocity was assessed by determination of the cellular doubling time. Cellular doubling time of HL-60 cells following RF-field exposure (1800 MHz, 24h) for different SARs (continuous wave, 0.2, 1.0, 1.3, 1.6, 2.0 and 3.0 W/kg) and different signal modulations (continuous wave, C.W., 5 min on/10 min off, GSM-217Hz, GSM-Talk) was compared to controls and sham-exposure. No alteration of the cellular doubling time was observed for any of the different SARs or signal modulations tested (Figures 101, 102). The value of the doubling time for the control was 20.8 ± 2.8 h. Calculation of the average HL-60 doubling time after exposure to all SAR levels tested revealed a value of 22.0 ± 3.8 h (n=21) versus that for all sham-exposed cells: 21.6 ± 4.5 hours (n=21). On the other hand the calculation of the average HL-60 doubling time after exposure to all signal modulations tested at SAR = 1.3 W/kg revealed a value of 21.3 ± 4.2 h (n=14) versus that for all sham-exposed cells: 21.7 ± 4.5 h (n=14).

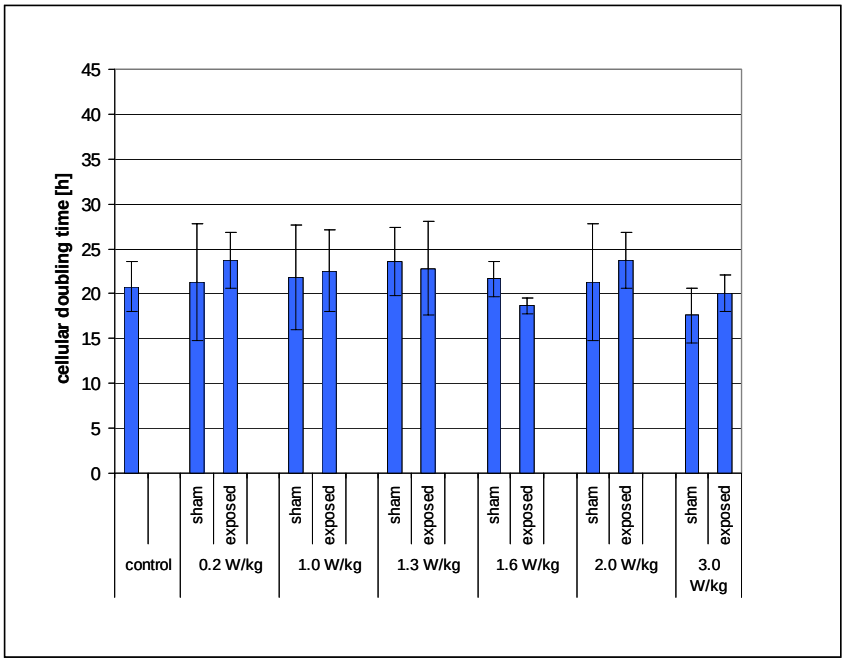

Figure 102. Effect of RF-field exposure (1800 MHz, continuous wave, SAR 0.2, 1.0, 1.3, 1.6, 2.0 and 3.0 W/kg, 24h) on HL-60 cell growth with respect to growth velocity compared to control and sham-exposure, determined by the cellular doubling time. Each bar represents the mean ± SD of results obtained in at least three independent experiments, except for control (n=6) and SAR 1.3 W/kg (n=6).

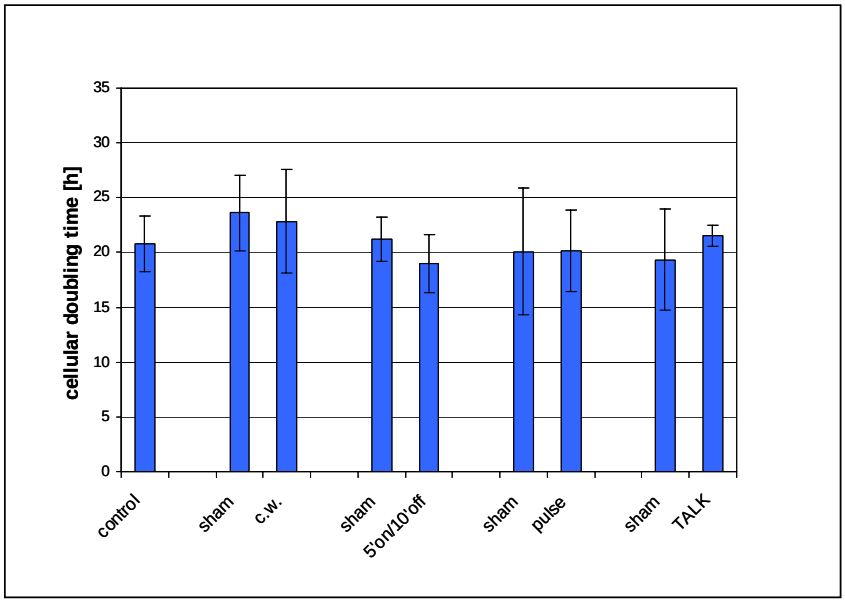

Figure 103. Effect of RF-field exposure (1800 MHz, different signal modulations, SAR 1.3 W/kg, 24h) on HL-60 cell growth with respect to growth velocity compared to control and sham-exposure, determined by the cellular doubling time. Each bar represents the mean ± SD of results obtained in at least three independent experiments, except for control (n=6), continuous wave (n=6) and GSM-Talk (n=2).

Thymidine kinase (TK) activity

Intracellular thymidine kinase (TK) activities were determined by radioenzyme assay with ^{125}I-deoxyuridine monophosphate as substrate (Prolifigen® TK-REA, AB Sangtec Medical, Bromma, Sweden). The level of radioactivity is directly proportional to the enzyme activity, the TK value is calculated from the standard curve and expressed as U/l.

TK activities of HL-60 cells following RF-field exposure (1800 MHz, continuous wave, 1.3 W/kg, 24 h) was compared to control and sham-exposure. Table 24 represent levels of thymidine kinase activities for two independent experiments. No changes in intracellular TK activities were found in HL-60 cells following RF-field exposure compared to control and sham-exposure. In summary, the growth behaviour of HL-60 cells with respect to growth velocity and DNA synthesis are not altered by RF-EMF exposure compared to control and sham-exposure using the assays described above.

Table 24. Thymidine kinase (TK) activity in HL-60 cells after exposure to RF-field (1800 MHz, continuous wave, 1.3 W/kg, 24h), compared to control and sham-exposed cells

Group	thymidine kinase activity [U/l]	
	exp. 1	exp. 2
control	121.4	126.8
sham	151.1	116.3
RF-field	121.9	118.4

3.2.2.4 Mouse embryonic stem cells (Participant 4)

RF-EMF did not induce cardiac differentiation of R1 ES cells and cardiac differentiation and proliferation of P19 EC cells, but may affect the bcl-2 mediated apoptotic pathway in ES-cell derived neural progenitors and neuronal differentiation by inhibiting nurr-1 and TH transcription.

See 3.2.4.1

3.2.2.5 Summary (Participant 1)

Our data did not reveal a significant effect of RF-EMF on proliferation and differentiation of various cell systems such as neuroblastoma cells (NB69) (see 3.2.2.1), R1-embryonic stem cells and embryonic cancer cells (P19) (3.2.2.4 and 3.2.4.1), human lymphocytes and human thymocytes (3.2.2.2) and HL-60 cells (3.2.2.3), though some effects on the differentiation process in neural stem cells were observed (see 3.2.2.1). These effects may be of indirect nature possibly through modulation of the expression of various genes and proteins. With respect to neural stem cells, RF-EMF may affect proliferation and differentiation via up-regulation of bcl-2 which mediates the apoptotic pathway and via inhibiting nurr-1 and TH transcription (see 3.2.2.4 and 3.2.4.1)

3.2.3 Apoptosis

3.2.3.1 Brain cells of different origin and human monocytes (Participant 9)

RF-EMF did not affect apoptosis in neuronal cells.

Spontaneous apoptosis was found higher in sensitive primary nerve cells than in the human neuroblastoma cell line SH-SY5Y) (around 20% versus 10% using the $DiOC_6$ dye). A high percentage of spontaneous apoptosis in granule cells was found using Annexin V staining compared to $DiOC_6$ staining. This observed difference seems to be cell type-dependent and it appeared difficult, in this case, to

correlate information given by these two dyes. Besides this technical consideration, exposure of primary granule cells to GSM-900 at 2.0 W/kg for one hour did not induce apoptosis as shown by the time-kinetics up to 24 hours after exposure (Figure 104). The same observation was made with the SH-SY5Y cell line. To test longer time exposure, we decided to expose granule cells and SH-SY5Y to GSM-900 during 24 hours and to quantify apoptosis at the end of exposure. In these exposure conditions, no significant difference was observed between sham and exposed cells in both cases (Figure 105).

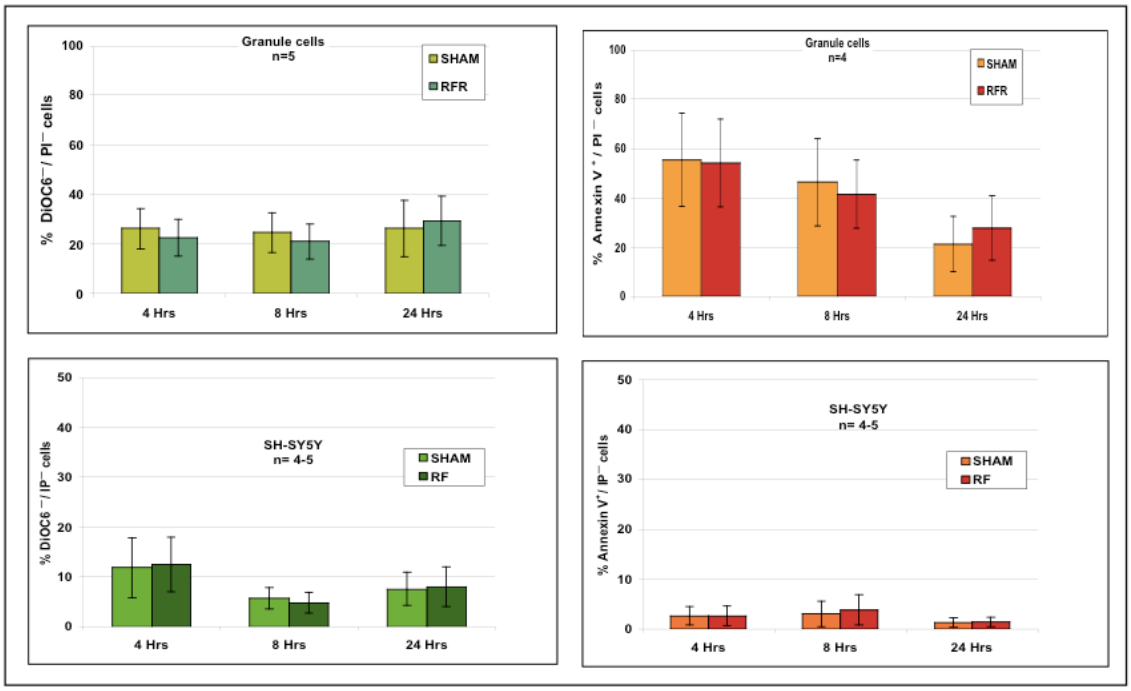

Figure 104. Effect of a one-hour exposure to GSM-900 on apoptosis in nerve cells. Results are expressed as the percentage of cells with depolarised mitochondrial transmembrane potential ($DIOC6^-/PI^-$, left panel) and apoptotic cells (ANX^+/PI^-, right panel) after exposure of primary granule cells (upper panels) and human neuronal cells (lower panels) to frame GSM-900 signal at 2.0 W/kg for 1 hour. Apoptosis was measured 4, 8 and 24 hours after the exposure began. Data are presented as the mean ± SEM of 4 to 5 independent and blind experiments.

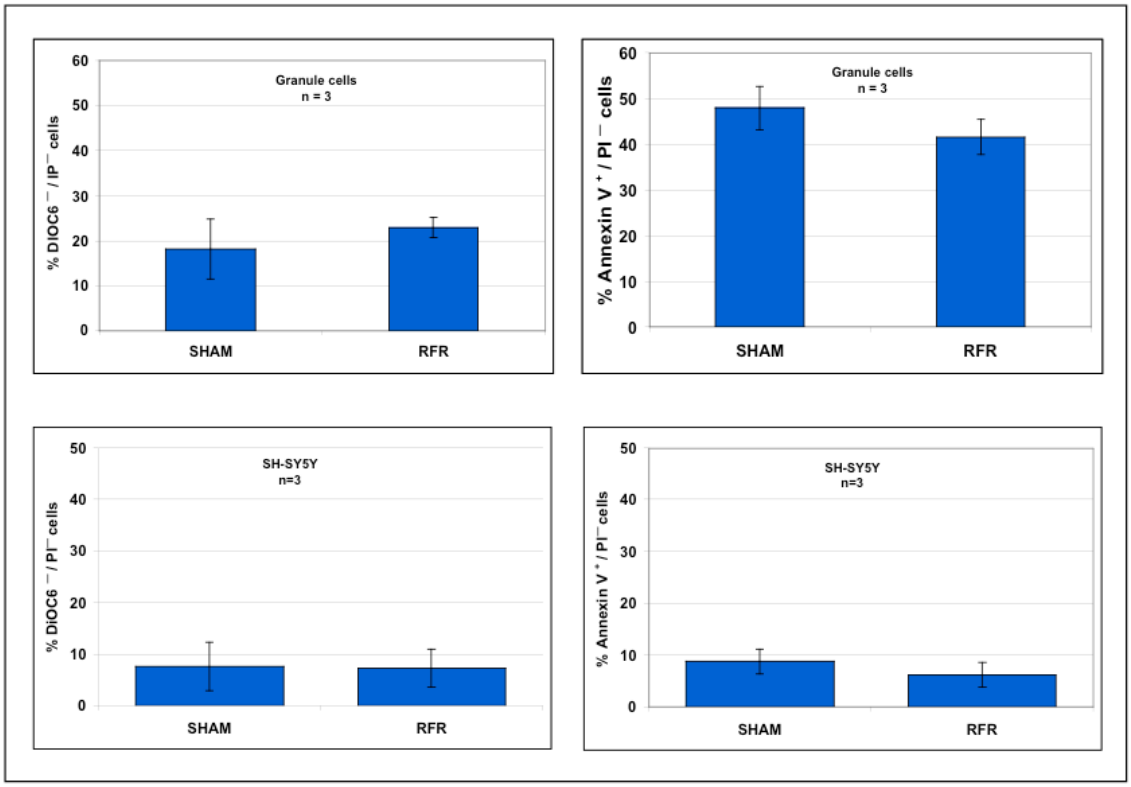

Figure 105. Effect of a 24-hour exposure to GSM-900 on apoptosis in nerve cells. Results are expressed as the percentage of cells with depolarised mitochondrial transmembrane potential ($DIOC6^-/PI^-$, left panel) and apoptotic cells (ANX^+/PI^{--}, right panel) after exposure of rat primary neurons (upper panels) and human SH-SY5Y neuroblastoma cells (lower panels) to frame GSM-900 signal at 2.0 W/kg for 24 hours. Apoptosis was measured immediately after exposure. Mean ± SEM of 3 independent, blinded experiments are presented.

We conclude from our results that granule cells and SH-SY5Y cells are not sensitive to GSM-900 exposure for up to 24 hours.

RF-EMF did not affect apoptosis in astrocytic cells.

Primary cultures of astrocytes and human U87 glioblastoma cells were sham-exposed or exposed to GSM-900 for one hour at 2.0 W/kg and apoptosis was followed up during 24 hours in the conditions described previously. Figure 105 shows the data obtained using the primary culture and the U87 cell line. In the two cell types, no difference in the number of cells with depolarised mitochondrial potential or in AnnexinV-positive cells could be evidenced after exposure to GSM-900. An increase in apoptotic astrocytic cell population measured with $DiOC_6$ was noticed, correlated to the time spent in culture. Nevertheless, no significant difference was observed between sham- and GSM-900 exposed cells. In the exposure conditions tested, no demonstration of a significant effect of GSM-900 signal on primary astrocytes or glioblastoma U87 cells could be made.

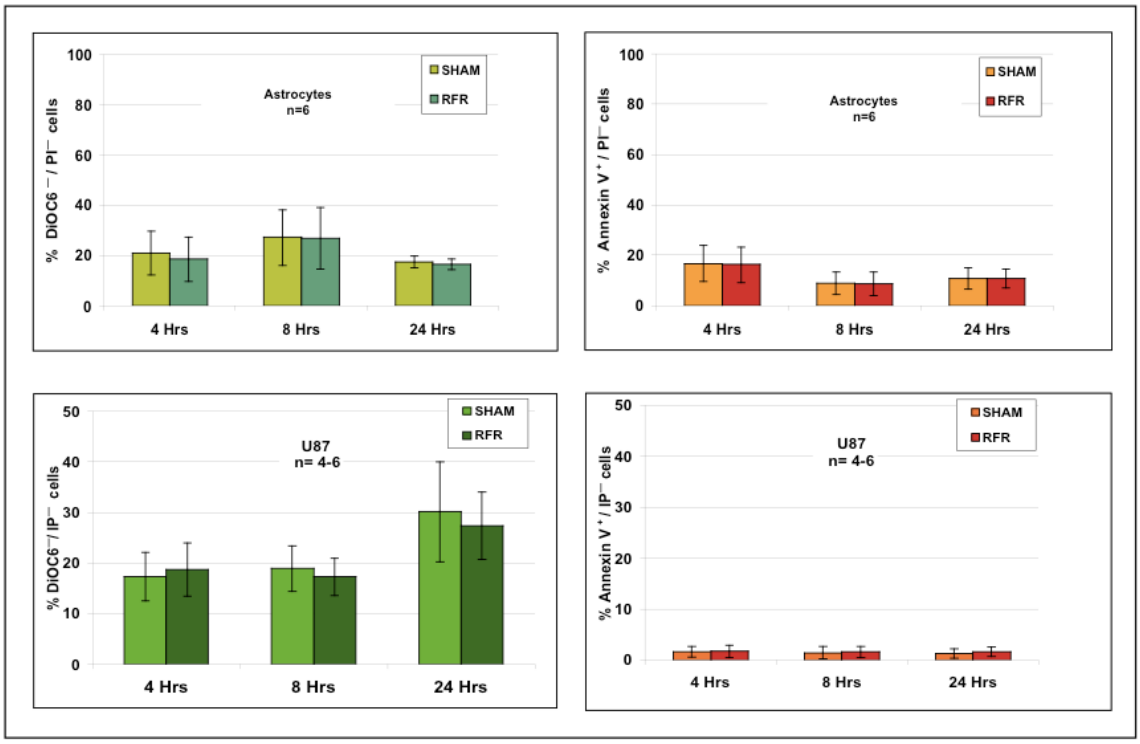

Figure 106. Effect of a 1-hour exposure to GSM-900 on apoptosis in astrocytic cells. Results are expressed as the percentage of cells with depolarised mitochondrial transmembrane potential ($DIOC6^-/PI^-$, left panel) and apoptotic cells (ANX^+/PI^-, right panel) after exposure of primary astrocytes (upper panels) and human astrocytic cells (lower panels) to GSM-900 signal at 2.0 W/kg for 1 hour. Apoptosis was measured 4, 8 and 24 hours after the exposure began. Data from 4 to 6 independent experiments are presented as the Mean ± SEM.

In summary, an immediate or delayed effect of RF-EMF on apoptosis in rat primary cells and human cell lines could not be demonstrated.

RF-EMF did not influence apoptosis in immune cells.

The ability of the human U937 promyeloma cells to undergo apoptosis was tested by using camptothecin as a positive control (Figure 107). We show a significant 4- to 8-fold increase ($p<0.01$), depending of the marker of apoptosis used, in U937 cells treated for 4 hours with CPT (4 µg/ml).

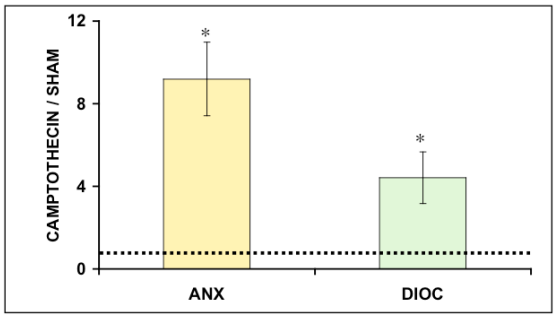

Figure 107. Effect of camptothecin treatment on apoptosis in human U937 cells. The results are expressed as the ratio of apoptotic cells (ANX^+/PI^-, left panel) and cells with depolarised mitochondrial transmembrane potential ($DIOC^-/PI^-$, right panel) in camptothecin-treated versus sham-exposed U937 promyeloma cells. U937 cells were sham-exposed for 1 hour and then treated for 4-hours with camptothecin (4 µg/ml). Data are presented as the mean ± SEM of 5 independent experiments. *=$p<0.01$

Sham-sham experiments (n=3-4) showed that inter-incubator (incubator used for RFR exposure versus incubator used for sham-exposure) variation of U937 apoptotic cells was around 1.1 ± 0.5 after one hour and 1.2 ± 0.6 when the cells were placed back in a control incubator for 4 hours after the one hour spent in the dedicated incubators (Figure 108). The effect of CPT treatment was very similar when the samples were put for one hour in either dedicated incubator. We therefore concluded that both dedicated incubators were equivalent within a range of 50% of ratio variation and that an at least two-fold increase in apoptosis in RFR-exposed cells could be considered as significant.

No statistically significant influence of GSM-900 could be evidenced on spontaneous apoptosis of U937 cells (Figure 109), when they were exposed for one hour at a SAR of 0.7 W/kg and even at the highest SAR tested (2.0 W/kg). No difference could be detected either immediately after exposure or after a 4-hour resting period in a control incubator. Hence, no delayed effect of GSM-900 on apoptosis could be evidenced. A longer exposure duration, i.e. 48 hours, to GSM-900 at the lowest SAR tested (0.7 W/kg) was also not able to alter spontaneous apoptosis in the human cell line.

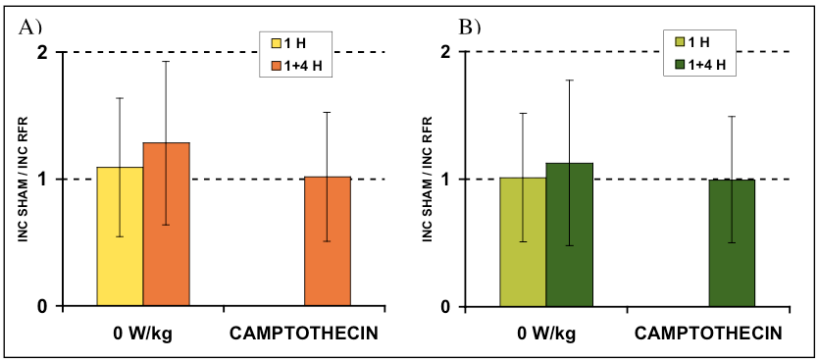

Figure 108. Comparison of occurrence of apoptosis in U937 cells in both dedicated incubators. Results are expressed as the ratio between apoptotic U937 cells in the incubator used for RFR exposure and apoptotic U937 cells in incubator used for sham-exposure. Sham-sham exposure lasted 1 hour and cells were harvested either immediately (1 H) or after an additional 4-hour resting period or campthotecin treatment (1+4 H). A) apoptotic U937 cells (ANX^+/PI^-) and B) U937 cells with depolarised mitochondrial transmembrane potential ($DIOC6^-/PI^-$). Data are presented as the mean ± SEM of 3 to 4 independent experiments.

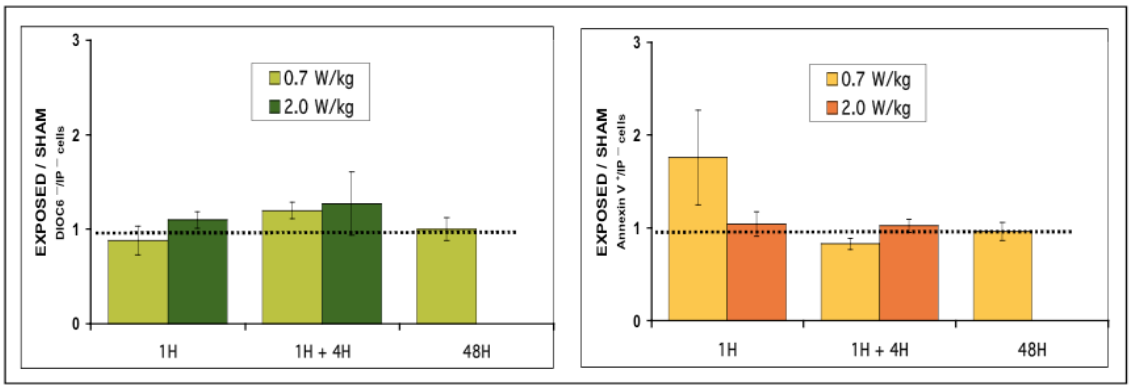

Figure 109. Effect of GSM-900 exposure on apoptosis in human U937 cells. Results are expressed as the ratio of cells with depolarised mitochondrial transmembrane potential ($DIOC6^-/PI^-$, left panel) and apoptotic cells (ANX^+/PI^-, right panel) in GSM-900- versus Sham-exposed U937 cells. U937 cells were exposed to GSM-900 at 0.7 W/kg (n=7) and 2.0 W/kg (n=6) for 1 hour, for 1 hour followed by a 4-hour resting period or for 48 hours. Data are presented as the mean ± SEM.

RF-EMF did not influence chemically-induced apoptosis in immune cells.

When possible interaction between RFR and camptothecin was tested, we show that a one-hour treatment with GSM-900 at either 0 .7 or 2.0 W/kg was not able to influence camptothecin-induced apoptosis (Figure 110).

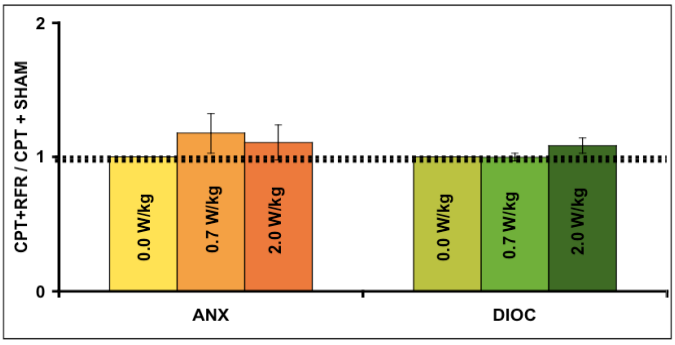

Figure 110. Effect of GSM-900 exposure on camptothecin (CPT)-induced apoptosis. The results are expressed as the ratio of apoptotic cells (ANX $^{+}$/PI $^{-}$, left panel) and cells with depolarised mitochondrial transmembrane potential (DIOC6 $^{-}$/PI $^{-}$, right panel) in GSM-900 plus camptothecin-treated versus GSM-exposed U937 promyeloma cells. U937 cells were sham-exposed or exposure to GSM-900 for 1 hour and then treated for 4-hour with camptothecin (4 µg/ml). The SAR level was 0.7 W/kg (n=7) or 2.0 W/kg (n=6). Data are presented as the mean ± SEM.

In summary, we showed no evidence for an immediate, cumulative or delayed effect of RF-EMF on apoptosis in a human monocytic cell line. We conclude from our results that U937 cells are not sensitive to GSM-900 exposure for up to 48 hours. Taken together, our results strongly suggest that the apoptotic process is not a major biological target for GSM mobile telephony-related signals.

3.2.3.2 Human lymphocytes (Participant 8)

RF-EMF did not affect apoptosis in human lymphocytes.

Negative results were obtained studying spontaneous or dRib-induced apoptosis, when PBMCs were exposed at all the three signal modulations. Moreover, PBMCs from old donors were exposed to Talk modulated RF, but also in this case no effects on spontaneous or oxidative stress-induced apoptosis were found. These results were also confirmed by mitochondrial membrane polarisation, since no differences were noticed in dependence of the exposure and age of donor.

RF-EMF did not increase the Hsp70 level in human lymphocytes after induction of apoptosis.

dRib induces an increase of hsp70 in treated cells in comparison with untreated cells already detectable after 3h of treatment (unpublished data) up to 44 hours of treatment. When we studied RF-EMF effects (1800 MHz, GSM talk signal, 2 W/kg), we did not found any alteration of hsp70 gene product, after 44 hours of intermittent exposure, in PBMCs from 7 young donors, as showed in Figure 111. In this figure it is possible to notice the significant difference between the level of hsp70 in untreated cells versus the dRib-treated cells. Additional analysis were performed in separated lymphocytes and monocytes, but no differences were found between RF-exposed and sham-exposed cell populations.

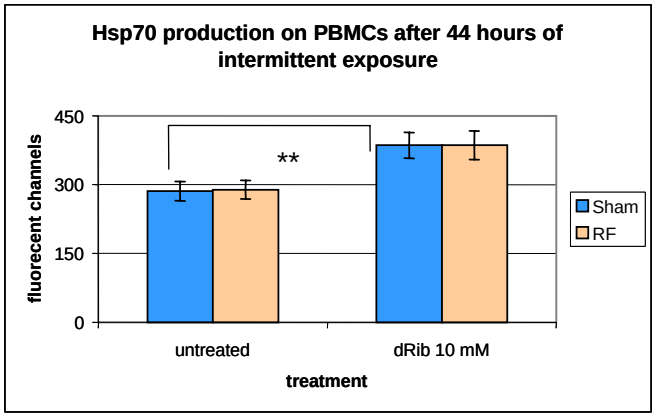

Figure 111. Hsp70 production in untreated and dRib treated PBMCs after 44hours of intermittent exposure. PBMCs were obtained from 7 donors and data are represented as mean of fluorescent channels ± s.e. ** = p< 0.01, untreated PBMCs versus dRib treated PBMCs.

RF-EMF did not affect apoptosis in thymocytes.

Thymocyte apoptosis was assessed with two different methods, in the same conditions, but the data obtained from 6 human thymus on thymocyte apoptosis did not suggest positive results on both the endpoints. Actually, a small increase (4%) of double positive thymocytes (CD4+CD8+) was found in RF-EMF-exposed cultures in comparison with sham-exposed tissue fragments. Also in this case the effect is of the order of the standard error thus we consider these results irrelevant.

3.2.3.3 Human promyelocytic cell line HL-60 (Participant 2)

RF-EMF did not affect apoptosis in HL-60 cells as shown by flow cytometric analysis and the Annexin V and TUNEL assay.

See 3.2.1.1

3.2.3.4 Embryonic stem cells of mice (Participant 4)

RF-EMF exposure may influence the bcl-2 mediated apoptotic pathway in ES-cell derived neural progenitors.

See 3.2.4.1

3.2.3.5 Human endothelian cell lines (Participant 6)

The RF-EMF-induced enhancement of hsp27 phosphorylation as well as the concomitantly RF-EMF-induced down-regulation of proteins of Fas/TNFα suggest that the anti-apoptotic pathway in RF-EMF exposed cell systems may be modified.

See 3.2.4.6

3.2.3.6 Summary (Participant 1)

Our data did not reveal a significant effect of RF-EMF on apoptosis in various cell systems such as brain cells and human monocytes (see 3.2.3.1), human lymphocytes and thymocytes (see 3.2.3.2), human endothelial cells (3.2.4.6) and HL-60 cells (see 3.2.3.3). On the other hand, an indirect effect on apoptosis through modulating the expression of various genes and proteins cannot be excluded at present. Up-

regulation of bcl-2 in differentiating embryonic stem cells (see 3.2.3.4 and 3.2.4.1) and of hsp27 in endothelial cells (see 3.2.4.6) both of which may affect the apoptotic process support such an assumption.

3.2.4 Gene and protein expression

3.2.4.1 Mouse embryonic stem cells (Participant 4)

Loss of p53 function rendered pluripotent ES cells sensitive to RF-EMF after prolonged exposure.

Exposure of undifferentiated cells to GSM-217 signals for 6 hours (Table 25) did not evoke any short-term modification of gene expression patterns neither in wt nor in p53-/- ES cells (Figure 112A). On the other hand, long-term (48 hours) GSM-217 exposure of p53-/- cells during EB development resulted in the up-regulation of transcript levels of 4 out of 6 analysed genes. Whereas c-jun, p21 and c-myc mRNA levels were only transiently up-regulated at early stages (days 2, 5 and 5+2 of EB differentiation, Figure 112B, a prominent induction of hsp70 levels in p53-/- cells was observed throughout the differentiation period. The same experimental protocol was applied to analyse the influence of GSM signals simulating talking and listening phases during a typical conversation (GSM-Talk). However, no changes of gene expression patterns in both wt and p53-/- cells were observed upon the exposure to GSM-Talk signals regardless of the protocol used. These observations indicate that the genetic constitution of cells determined by the p53 function affected cellular responsiveness to GSM-modulated EMF, whereas low frequency components characteristic for GSM-Talk modulation were not responsible for these effects.

Table 25. Conditions of the exposure of p53-proficient and deficient pluripotent embryonic stem cells to RF-EMF and summary of the effects on transcript levels of regulatory genes.

GSM-Basic	
1.5 W/kg (5min on/30 min OFF)	
$p53^{+/+}$ ES cells	**$p53^{-/-}$ ES cells**
6h, (5min ON/30 min OFF) (n=3) no EMF effect	6h, (5min on/30 min OFF) (n=3) no EMF effect
48h, (5min on/30 min OFF) (n=3) no EMF effect	48h, (5min on/30 min OFF) upregulation of hsp70, (n=3) c-jun,c-myc and p21

GSM-Talk (33% GSM-Basic, 66% DTX)	
0.4 W/kg (5min on/30 min OFF)	
$p53^{+/+}$	**$p53^{-/-}$**
6h, (5min on/30 min OFF) (n=3) no EMF effect	6h – (5min on/30 min OFF) (n=3) no EMF effect
48h,(5min on/30 min OFF) (n=3) no EMF effect	48h (5min on/30 min OFF) (n=3) no EMF effect

GSM – DTX (100% DTX)	
0.11W/kg	
$p53^{+/+}$	**$p53^{-/-}$**
6h, (5min on/30 min OFF) (n=3) no EMF effect	6h, (5min on/30 min OFF) (n=3) no EMF effect

n- number of experiments

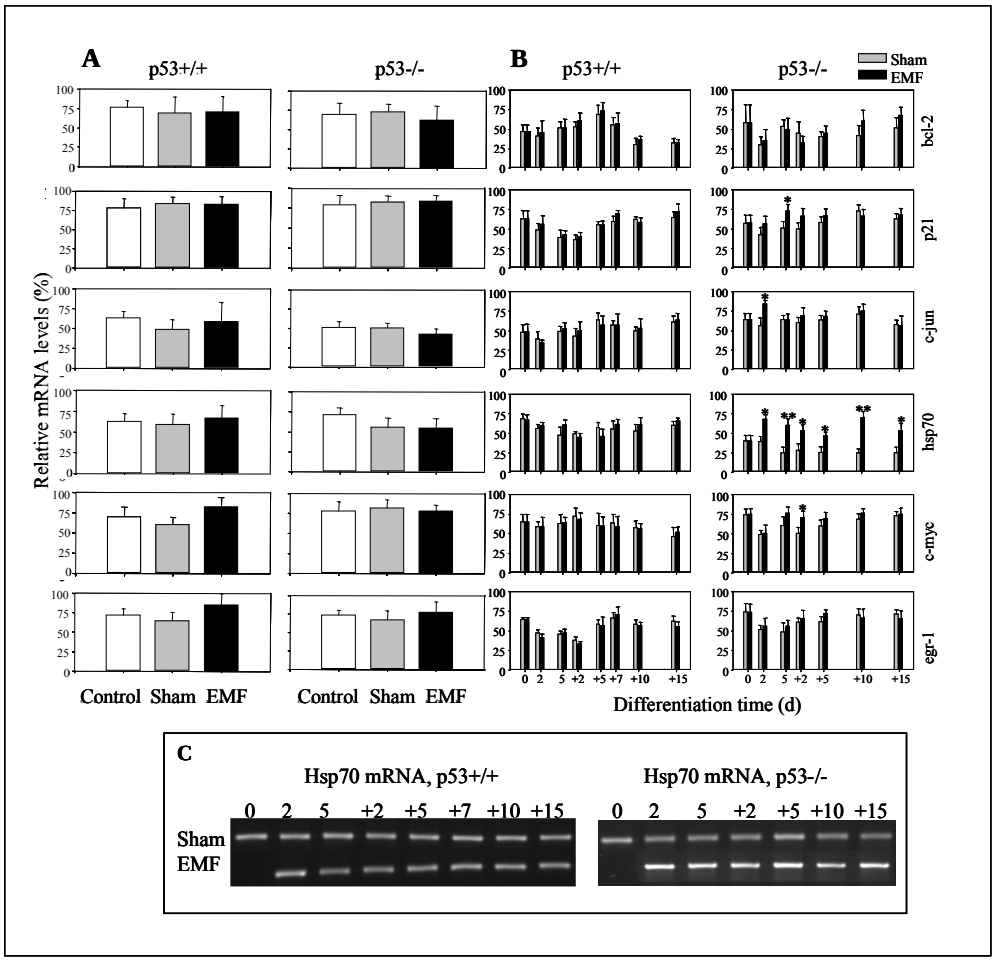

Figure 112. Relative mRNA levels of genes encoding bcl-2, p21, c-jun, hsp70, c-myc and egr-1 in p53-deficient ($p53^{-/-}$) and wild-type ($p53^{+/+}$) D3 ES cell-derived EBs after 6 (A) and 48 (B) hours GSM-217 Hz exposure. GSM-217 exposure resulted in a significant and long-lasting upregulation of hp70 transcripts (C) paralleled by a temporary upregulation of c-myc, c-jun and p21 levels in differentiating $p^{-/-}$ ES cells after 48h exposure (B), but not after 6h (A) exposure. Error bars represent standard deviations. Statistical significance was tested by the Student's t-test for significance levels of 1 and 5% (**, $p<0.01$, *,<0.05)

RF-EMF did not influence cardiac differentiation and gene expression levels in R1 ES cells.

For the evaluation of embryotoxic effects of chemical compounds in vitro, the mouse embryonic stem cell test, EST (Spielmann 1997), studying cardiac differentiation of ES cells as endpoint has been established. Therefore, we further analysed effects of EMF on cardiac differentiation in R1 ES and P19 EC cells. R1-derived EBs were exposed to EMF for 5 days and the cells were analysed after further differentiation. Similarly to D3 wt cells, no effect of GSM-217 signals on the expression of the regulatory genes including p53 was observed in R1 wt cells. Moreover, no significant differences in cardiac differentiation were found between sham- and EMF-exposed variants during EB differentiation. The results of morphological investigations were confirmed by RT-PCR analyses, where no differences in cardiac α-MHC mRNA levels between sham- and EMF-exposed variants were observed.

RF-EMF did not induce cardiac differentiation and gene expression and the proliferation of P19 EC cells.

Contrary to ES cells, which spontaneously differentiate into the cardiac lineage, differentiation of P19 cells has to be stimulated by external differentiation factors, i.e. DMSO or retinoic acid. To elucidate, whether EMF signals interfere with DMSO-induced cardiac differentiation, undifferentiated P19 EC cells were exposed to GSM-217 signals for 22 and 40h, respectively, and differentiated in the absence or

presence of 1% DMSO. The mRNA levels of regulatory genes were not affected by EMF exposition, and no significant differences were found between EMF-, sham-exposed and control variants of undifferentiated P19 cells, respectively.

Without DMSO induction, only low levels (5-10%) of spontaneous cardiac differentiation were found. By differentiation induction with DMSO during the first 48 hours of EB development, the differentiation of spontaneously beating cardiac cells was increased to a maximum level of 90% in both variants. Exposure of P19 cells to GSM-217 signals for 22 and 40 hours did not result in significant changes of cardiac differentiation suggesting that EMF had no effects on spontaneous or DMSO-induced cardiogenesis. Furthermore, undifferentiated EC cells were EMF- (GSM-217) and sham-exposed at a SAR value of 2.0 W/kg for 22 or 40 hours, and the lengths of cell cycle phases were analysed by flow cytometry. In both cases, no differences in the distribution of cells in G1, S or G2/M phases were observed between sham- and EMF-exposed variants.

RF-EMF exposure may affect the bcl-2 mediated apoptotic pathway in ES-cell derived neural progenitors and neuronal differentiation by inhibiting nurr-1 and TH transcription.

We used an experimental protocol that has been shown to be efficient for differentiation induction of ES cells into the neural lineage (Figure 6) for our experiments aimed at defining the influence of RF-EMF (1.71 GHz, 1.5 W/kg, 5 min on/30 min off) as shown in Table 26. Neural progenitors were analysed at stage 4+4d to 4+6d, where nestin-positive cells were detected in ca. 60-80% of the cells. The exposure conditions applied for 6 or 48 hours are shown in Table 23. The analysis of hsp70, bax and p21 mRNA levels after RF-EMF exposure of neural progenitor cells did not provide evidence of gene expression changes. Bcl-2 was significantly up-regulated after the RF-EMF exposure at the terminal stage 4+23d (Figure 109, $p<0.01$). In addition, we investigated the effect of RF-EMF exposure on GADD45 transcript levels and found that GADD45 mRNA levels were significantly up-regulated at the same stage of differentiation at 4+23d (Figure 113, $p<0.05$). The data on the influence of RF signals on gene expression pattern in differentiating neuronal cells revealed statistically significant down-regulation of nurr-1 at stage 4d+11 and TH at terminal stage 4d+23d, but no clear shifts in transcript levels of the tissue specific genes GFAP, Nestin and En-1 (Figure 113). Quantitative RT-PCR with specific primers and TaqMan probe confirmed the up-regulation of GADD45 at 4+23d stage, but not for bcl-2. According to the Q-RT-PCR data nurr-1 was down-regulated both at stage 4+7d and 4+11d, but the decrease in mRNA levels was statistically significant for stage 4+7d (Figure 114).

Table 26. Conditions of the exposure of neuronal progenitor cells to PL-MF or RF-EMF.

Intermittent exposure (5min on/30 min off)			
48h, GSM 217 Hz (1.71 GHz)		**6h, GSM 217 Hz (1.71 GHz**	
1.5 W/kg	Alterations of GADD45 transcript levels Down-regulation of nurr-1. No effect on DNA break induction (n=7)	1.5 W/kg	Low, but statistically significant induction of double-strand DNA breaks (n=7)

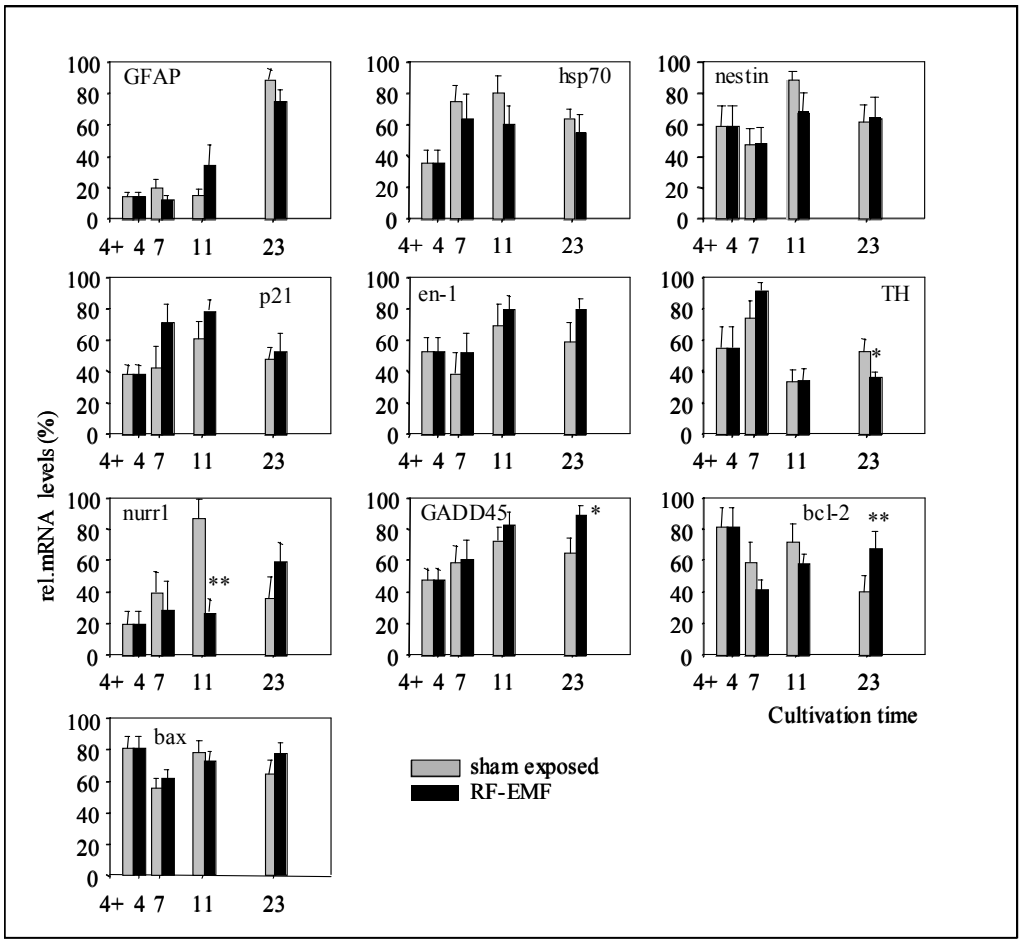

Figure 113. Relative mRNA levels analysed by semi-quantitative RT-PCR of genes encoding bcl-2, p21, c-jun, hsp70, c-myc and egr-1 in p53-deficient (p53-/-) and wild-type (p53+/+) D3 ES cell-derived EBs and EB outgrowths after 6 (A) and 48 hours (B) exposure to GSM-Talk. No effects of GSM-Talk on gene expression levels in ES cells were observed.

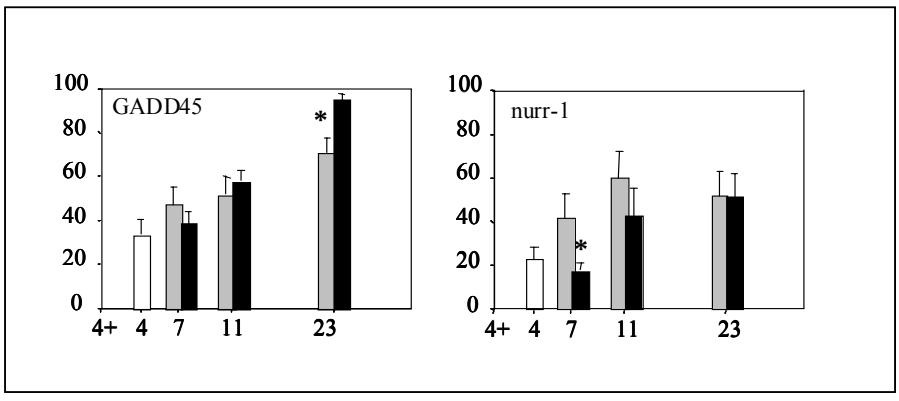

Figure 114. Quantitative RT-PCR with specific primers and Taqman probe for estimation of relative mRNA levels of the growth arrest and DNA damage inducible gene GADD45 and the nurr-1 gene involved in neuronal differentiation in ES-derived neural progenitors after 48 hours RF - EMF (GSM signal 217-Hz) exposure (1.5 W/kg, 1.71 GHz, intermittency 5 min ON/30 min OFF), at stage 4+4d - 4+6d. EMF exposure resulted in a significant transcript down-regulation, followed by up-regulation of GADD45 and down-regulation of nurr-1 at stage 4+7d. Error bars represent standard deviations. Statistical significance was tested by the Student's two-tailed paired t-test for a significance level of 5% (*, $p < 0.05$).

3.2.4.2 Human neuroblastoma cell line NB69 and neural stem cells (NSC) (Participant 5)

RF-EMF (GSM-CW and GSM-Basic) interfered with the expression of FGF receptors in NB69 human neuroblastoma cells.

In a first experiment the cellular response to a chemical promoter of differentiation was characterised. Immunocytochemical staining using antibodies against phenotype-specific antigens revealed that NB69 cells contain the neuroblast-specific protein ßIII-tubulin, but not the neuroepithelial marker nestin, which is present in immature progenitors and in some neuroblastoma cells (Kashima et al. 1995). Untreated NB69 cells remain in an undifferentiated state. Immunocytochemistry for FGFR1-3 revealed the three types of receptors in the human neuroblastoma cell line. On day 3 after plating approximately 70% of cells expressed R1, whereas FGFR3 and FGFR2 were present in a smaller proportion of cells, 30% and 20%, respectively (Figure 115, grey colour). Basic fibroblast growth factor (bFGF), which induces morphological changes including neurite extension at a 20-ng/ml concentration, was used as a positive control for the subsequent EM treatments. This growth factor reduced the number of NB69 cells expressing FGF receptors R1, R2 and R3. Such an effect was accompanied with changes in the cellular morphology associated to differentiate phenotypes. These changes included increased neural outgrowth, neural microtubule network and cell surface. As shown in this Figure 115, the 24-hour treatment with bFGF induced a consistent reduction in the percent of FGFR positive cells for the 3 receptors tested ($p<0.0001$; ANOVA).

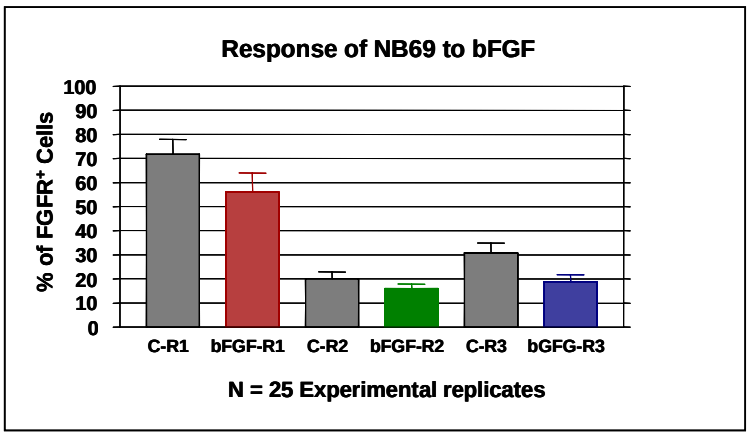

Figure 115. Expression of FGF Receptors 1, 2 and 3 in NB69 cells after a 24-hours treatment with 20-ng/ml bFGF. See text for details.

In the following experimental series, the cellular responsiveness to a differentiation-promoter was confirmed through treatment with bFGF, which induced a reduction of the percent of cells expressing FGF receptors R1, R2 and R3. Such an effect was associated with cell enlargement and neurite arborisation. In contrast, the treatment with GSM-Talk (SAR of 2 W/kg) signal alone (N= 4 experimental replicates), does not modify significantly the normal expression of the FGF protein receptors R1, R2 and R3 in NB69 cells (Figure 116). However, the results of the combined treatment bFGF + GSM-Talk signal show that the EMF seems to antagonize the significant reduction of FGFR-2 expression induced by bFGF. This indicates that the GSM-Talk signal might interfere with some of the cellular responses to bFGF.

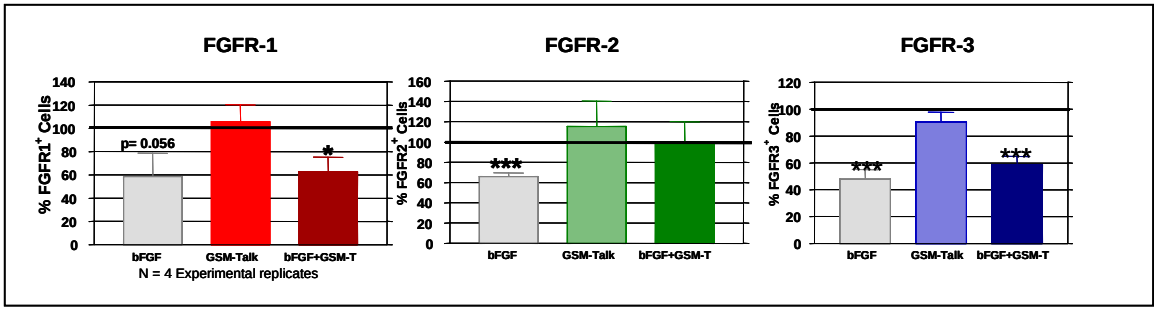

Figure 116. Response of NB69 cells to GSM-Talk signal. Percent of cells expressing FGF Receptors R1, R2 and R3. The treatment with bFGF induced significant reductions in the percent of cells expressing the receptors. Data normalised over the respective controls. (*, p<0.05; **, p<0.01; ANOVA followed by Student's T test).

When administered alone, the exposure to GSM 1800-Basic signal at a 2 W/kg SAR was found to induce a decrease in the number of cells expressing the FGFR-1 (15% reduction vs. controls, Figure 117) and photomicrographs of NB69 cell cultures) without affecting significantly the number of cells expressing receptors R2 and R3. The magnitude of the effect on R1 was equivalent to that induced by bFGF at a 20 ng/ml concentration. However, unlike bFGF, the exposure to GSM-Basic alone did not provoke changes in the cellular morphology. Provided that, as described previously, the GSM-Basic treatment does not induces significant changes in the total cell number or the cell viability, the present results indicate that the GSM-Basic-induced effect on FGFR-1 is not due to a reduction in the number of cells, but to a loss of expression of this receptor.

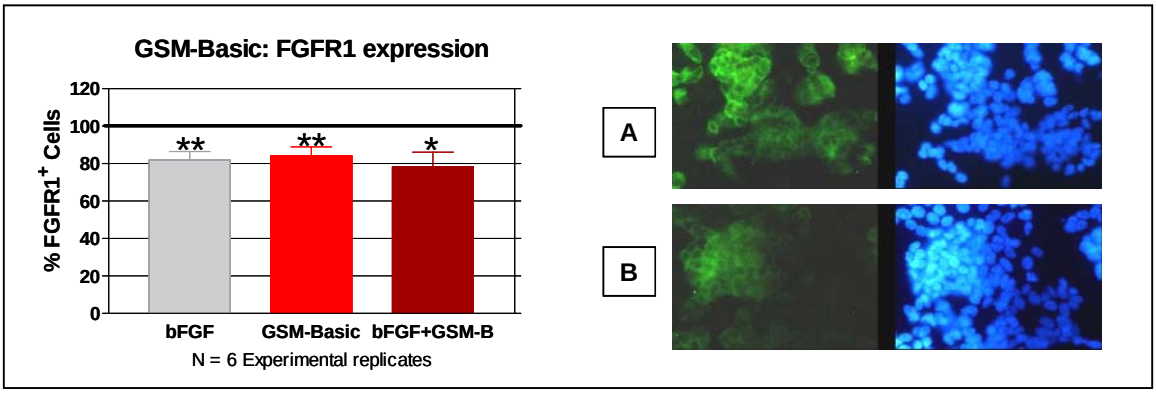

Figure 117. Photomicrographs of NB69 cell cultures: A, control; B, exposed to GSM-Basic signal. Immunocytochemistry for FGFR1. The image analysis showed a statistically significant reduction in the protein expression in the exposed cells (left). The matched fields (right) show the total cells stained with Hoechst.

The treatment with RF-CW signal (SAR 2 W/kg) induced effects on the expression of FGFR-1 equivalent to those induced by the GSM-Basic signal (Figure 118A), whereas the exposure to GSM-DTX signal at a lower SAR (1 W/kg) did not modify significantly the normal expression of the FGF protein receptors R1 in NB69 cells (Figure 118B).

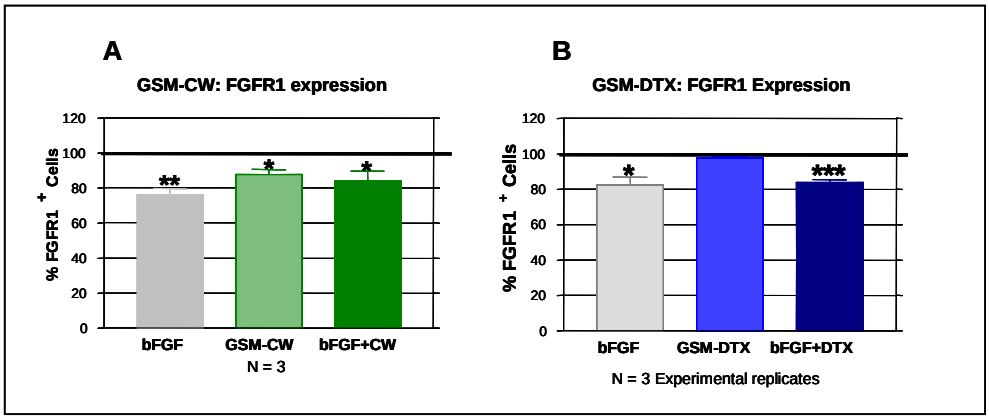

Figure 118. FGFR1 expression in NB69 cells after exposure to: (A) RF-CW signal, 2 W/kg and (B) GSM-DTX signal, 1 W/kg. Only RF-CW induced a significant response. *, $p<0.05$; **, $p<0.01$, ***, $p<0.001$ (ANOVA followed by Student's T test for unpaired data).

Taken together, the results on the expression of FGFRs in NB69 cells exposed to GSM-1800 MHz signals and RF-CW signals suggest that (1) these cells are sensitive to low-SAR signals, (2) the cellular response does not seem to be dependent on the tested low-frequency modulation and (3) the observed response on FGFR1 could be indicative of a EMF-induced promotion of cell differentiation. However, additional studies on the expression of differentiation markers have to be done to confirm this hypothesis. (4) The GSM signal does not seem to interfere significantly with the cellular response to bFGF.

RF-EMF affected the expression of FGF receptors in neural stem cells (NSC).

In order to enhance expansion of NS precursor cells, neurospheres were seeded onto adherent substrate and treated with the mitogen epidermal growth factor (EGF) during the first 3 days in culture. After this period the EGF was withdrawn, and cells grew in a defined medium, which promoted differentiation processes to neurons, astrocytes and oligodendrocytes. Between 2 h and 3 days cultures comprised mainly nestin-positive, undifferentiated precursors. At later stages, the total number of cells dropped, paralleling to a gradual loss of nestin content, and an enhancement in the differentiation processes of neurons, oligodendrocytes and astrocytes.

Immunocytochemistry for FGFR1-3 identified the three types of receptors in the progeny of EGF-expanded NSCs. During the first day after plating, approximately 70% and 50% of the precursors expressed FGFR1 and FGFR2, respectively, whereas FGFR3 was restricted to a less abundant population. At 3 days and thereafter the number of cells exhibiting FGFR1 and FGFR2 decreased gradually, so that at 3 days the percent of FGFR-1 was 35% and at 9 days postplating only approximately 15% of the cell population was immmunopositive for this receptor. FGFR1 immunostaining was preferentially localised in the cytoplasmic compartment, FGFR-3 was found in the cytoplasmic and/or nuclear compartments, and FGFR2 was frequently confined to the nucleus. In situ hybridisation studies on the third day postplating showed high levels of FGFR1 mRNAs in NSC.

On the basis of our previous data showing that the GSM-Basic signal induces a reduction in the percent of cells expressing FGF-R1 in human neuroblastoma cells, we tested firstly this signal (2 W/kg) on NSC. Like in NB69 cells, a significant decrease in FGFR1-positive NS cells was also observed after exposure to the GSM-Basic signal (50% reduction with respect to controls, Figure 119). Western blot analysis for FGFR1 confirmed this effect (data not shown). The study also indicates that the response of the neural stem cells seems to be dependent on the age of the culture (Figure 120).

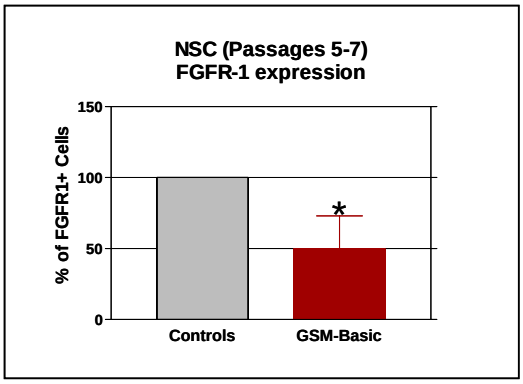

Figure 119. Percent of FGFR-1 positive labelling vs. total cell number normalised over their controls, quantification by the program for image analysis (IPWIN-3). Data represent the mean ± SEM of 3 independent experiments, done in duplicate (two coverslips), for the different treatment conditions. Student T-test *p< 0.05.

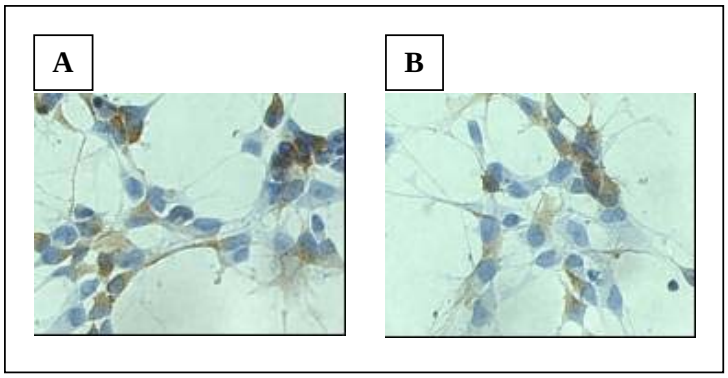

Photomicrographs of Neural Stem Cells, A, control and B exposed to GSM-Basic signal. Inmunocytochemistry for FGFR1-positive cells (brown).

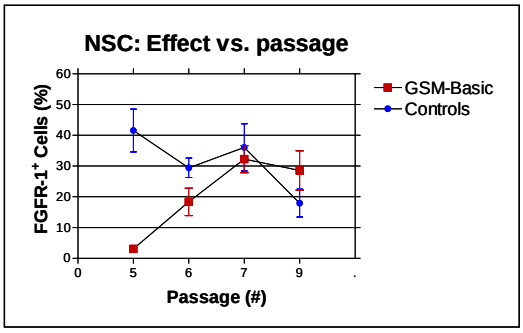

Figure 120. NSC exposed to GSM-Basic signal. The percent of FGFR-1 positive cells seems to be dependent on the passage number.

RF-EMF did not affect gene expression of FGF Receptor-1 in NB69 neuroblastoma cells and in neural stem cells (NSC)

In situ hybridisation studies were conducted on neural stem cells and in NB69 cells exposed for 21 hours (5 min on/10 min off) to the GSM-Basic signal. The objective is to evaluate potential EMF effects on gene expression of FGFR1. All experiments were conducted following blind protocols. The results on both cell types showed no differences in FGFR1 mRNA-expression between controls and exposed samples. An image-analysis study confirmed this result in NSC (Figure 121). Taken together, the

described effects on NB69 and NSC (FGFR1 protein-expression and FGFR1 mRNA-expression), suggest that the GSM-Basic signal can modulate FGFR1 protein translation without affecting protein transcription.

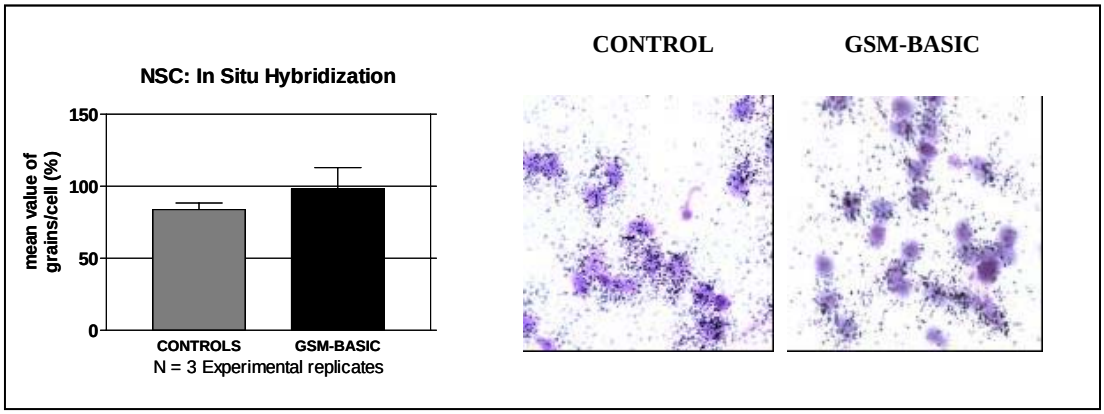

Figure 121. Quantification of in situ hybridisation staining by image-analysis technique (IPWIN 3.0) of the number of grains/cell. The photomicrographs show the developmental pattern of FGFR1 in NSC processed with Radiolabelled Probe Specific for Transcript of FGFR1.

3.2.4.3 Human promyelocytic cell line HL-60 (Participant 2)

RF-EMF exposure reproducibly up- and down-regulated protein expression in HL-60 cells (41 proteins showed to be up-, 1 protein to be down-regulated and 14 proteins appeared to be de-novo expressed).

The proteome screening approach included analysis of the entire HL-60 protein expression pattern by means of 2-D polyacrylamide gel electrophoresis (2D-PAGE). After having established the technique for HL-60 cells, cells were exposed to RF-fields at selected conditions in repeated independent experiments in order to obtain reproducible information on changes in the cellular protein pattern, correlated with RF-EMF-exposure.

HL-60 cells were exposed at 1800 MHz, continuous wave, SAR 1.3 W/kg, 24h, or were sham exposed in repeated independent experiments. Additionally, incubator controls were run and analysed for their protein expression pattern by 2D-PAGE. Cell samples were partly analysed as described above, partly stored at -80 °C for further analyses. Comparison of protein pattern after 2D-PAGE showed that optimal reproducibility is achieved when the 2-D separation step is performed in one series with identical reagent batches. In order to be able to perform statistics, appropriate numbers of comparable 2D-gels are required, also to have enough material for protein identification.

Figures 122, 123, and 124 show representative high-resolution 2-dimensional polyacrylamide gels (23 x 30 cm) for each of the conditions described above (incubator control, sham-exposure and RF-field exposure).

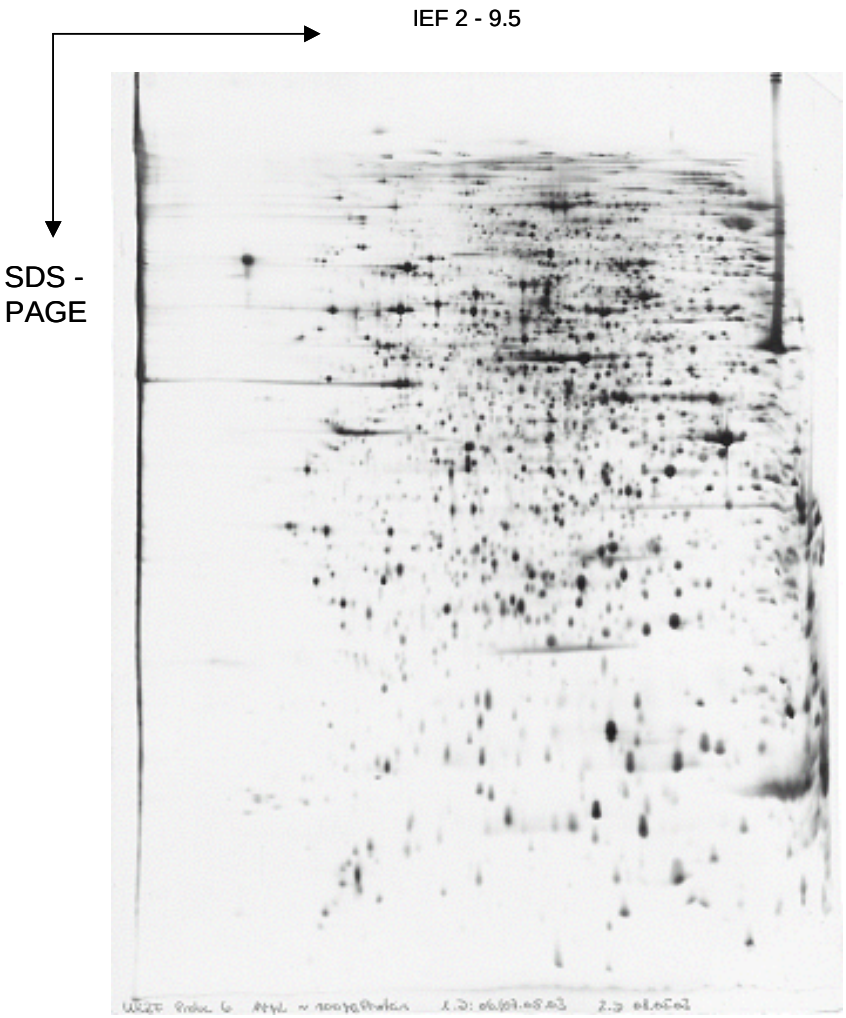

Figure 122. Two-dimensional polyacrylamide gel electrophoresis (2-D PAGE) profile of incubator control HL-60 cells (whole cell lysate). Incubation time: 24h. First dimension (isoelectric focussing): pH-gradient 2-9.5. Second dimension: 12.5% polyacrylamide gel, silver stain.

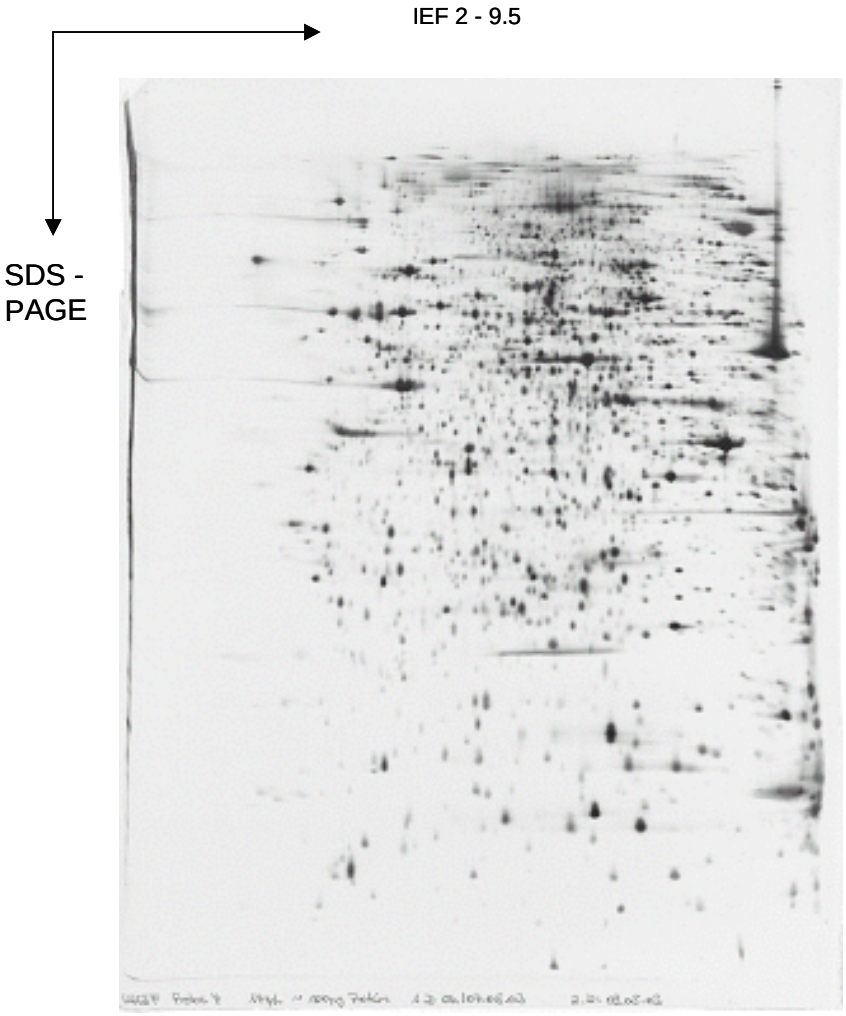

Figure 123. Two-dimensional polyacrylamide gel electrophoresis (2-D PAGE) profile of sham-exposed HL-60 cells (whole cell lysate). Exposure time: 24h. First dimension (isoelectric focussing): pH-gradient 2-9.5. Second dimension: 12.5% polyacrylamide gel, silver stain.

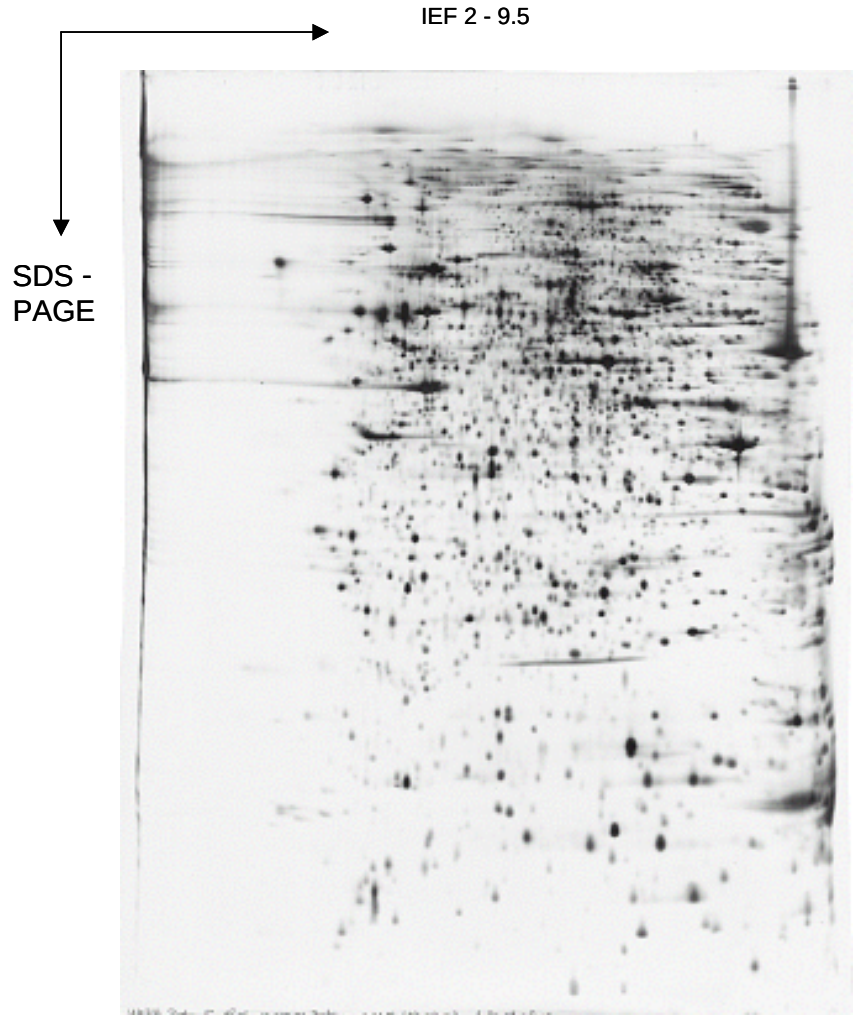

Figure 124. Two-dimensional polyacrylamide gel electrophoresis (2-D PAGE) profile of RF-exposed HL-60 cells (whole cell lysate). Exposure characteristics: 1800 MHz, continuous wave, 1.3 W/kg, 24h. First dimension (isoelectric focussing): pH-gradient 2-9.5. Second dimension: 12.5% polyacrylamide gel, silver stain.

Following digitalisation, in a second analysis step the qualitative and quantitative comparison of protein expression was performed by use of Proteom Weaver image analysis program. Figure 125 shows a representative comparative 2D-gel, in which expression differences between RF-field exposed and sham-exposed HL-60 cells are marked. Expression differences were quantified. In Table 27 (a-c) proteins up-or down-regulated and those that have disappeared after RF-field exposure are listed.

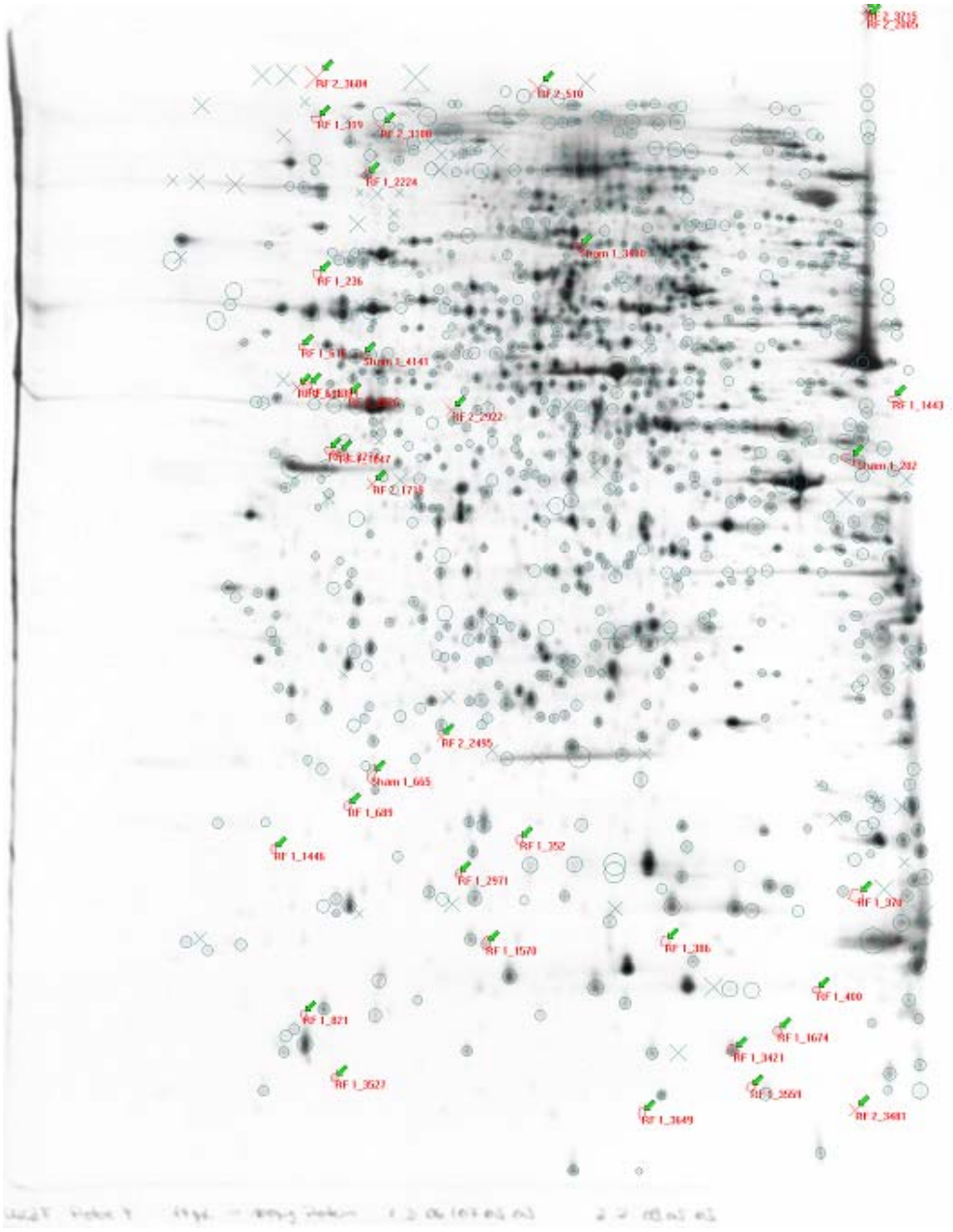

Figure 125. Representative qualitative and quantitative comparison of two-dimensional polyacrylamide gel electrophoresis (2-D PAGE) profiles of sham-exposed and RF-exposed HL-60 cells (whole cell lysate).

Exposure conditions: see above. Green arrows mark different proteins of sham-exposed cells compared to RF-field exposed cells (green arrows and red circles: up-regulated proteins; green arrows and red crosses: newly expressed or disappeared proteins).

Table 27. List of proteins in 2-DE patterns of HL-60 cells, differing between RF-field exposed and sham exposed cells. Exposure conditions: see above

a: List of proteins up-regulated in RF-field exposed HL-60 cells (average intensity see arrow) as compared to sham-exposed cells (average intensity see arrow).

				sham				⇩	RF-field				⇩
ID	ID	Name	Freq	X	Y	I	/	Avg	X	Y	I	/	Avg
1	1_3559	RF 1_3559	2	1163	1684	0,039	N.R.	0,039	1183	1726	0,278	7,1924	0,278
2	1_1443	RF 1_1443	2	1384	614	0,058	N.R.	0,058	1399	628	0,389	6,649	0,389
3	1_400	RF 1_400	2	1266	1533	0,055	N.R.	0,055	1278	1562	0,354	6,3801	0,354
4	1_689	RF 1_689	2	536	1247	0,048	N.R.	0,048	574	1271	0,267	5,5816	0,267
12	1_616	RF 1_616	2	464	533	0,031	N.R.	0,031	512	546	0,137	4,404	0,137
15	1_386	RF 1_386	2	1030	1458	0,057	N.R.	0,057	1056	1491	0,247	4,3329	0,247
16	1_1446	RF 1_1446	2	421	1315	0,046	N.R.	0,046	464	1345	0,193	4,2311	0,193
17	1_236	RF 1_236	2	489	421	0,047	N.R.	0,047	538	431	0,198	4,227	0,198
22	1_1391	RF 1_1391	2	474	594	0,094	N.R.	0,094	522	607	0,354	3,7725	0,354
24	1_821	RF 1_821	2	467	1570	0,042	N.R.	0,042	507	1611	0,157	3,7049	0,157
27	1_3274	RF 1_3274	2	506	694	0,067	N.R.	0,067	549	708	0,229	3,4382	0,229
28	1_1674	RF 1_1674	2	1205	1597	0,117	N.R.	0,117	1220	1631	0,394	3,3527	0,394
35	1_3649	RF 1_3649	2	994	1725	0,048	N.R.	0,048	1017	1778	0,15	3,102	0,15
36	1_370	RF 1_370	2	1329	1387	0,084	N.R.	0,084	1338	1406	0,261	3,0949	0,261
37	1_352	RF 1_352	2	804	1299	0,043	N.R.	0,043	834	1330	0,132	3,0908	0,132
41	1_1647	RF 1_1647	2	523	698	0,199	N.R.	0,199	565	712	0,59	2,9714	0,59
43	1_2971	RF 1_2971	2	708	1353	0,075	N.R.	0,075	743	1385	0,221	2,9515	0,221
45	1_2224	RF 1_2224	2	565	267	0,345	N.R.	0,345	607	275	1,016	2,9415	1,016
48	1_319	RF 1_319	2	489	178	0,058	N.R.	0,058	536	186	0,168	2,9054	0,168
49	1_3421	RF 1_3421	2	1136	1628	0,597	N.R.	0,597	1159	1669	1,728	2,8956	1,728
54	1_1570	RF 1_1570	2	751	1462	0,231	N.R.	0,231	784	1499	0,63	2,7259	0,63
61	1_3527	RF 1_3527	2	516	1670	0,075	N.R.	0,075	552	1717	0,187	2,5069	0,187

b: List of proteins down-regulated in RF-field exposed HL-60 cells (average intensity see arrow) as compared to sham-exposed cells (average intensity see arrow).

				sham				⇩	RF-field				⇩
ID	ID	Name	Freq	X	Y	I	/	Avg	X	Y	I	/	Avg
13	1_3400	Sham 1_3400	2	897	378	0,345	N.R.	0,345	927	389	0,12	0,3489	0,12

c: List of newly expressed or disappeared proteins in RF-field exposed HL-60 cells (average intensity see arrow) as compared to sham-exposed cells (average intensity see arrow) .

				sham				⇩	RF-field				⇩
ID	ID	Name	Freq	X	Y	I	/	Avg	X	Y	I	/	Avg
1	1_202	Sham 1_202	1	1317	708	0,417	N.R.	0,417	1326	716	X	N.A.	N.A.
2	2_2005	RF 2_2005	1	1343	21	X	N.R.	N.A.	1358	29	0,546	N.A.	0,546
3	2_1719	RF 2_1719	1	574	746	X	N.R.	N.A.	614	761	0,198	N.A.	0,198
4	2_3100	RF 2_3100	1	586	191	X	N.R.	N.A.	628	196	0,424	N.A.	0,424
5	2_688	RF 2_688	1	458	595	X	N.R.	N.A.	506	609	0,133	N.A.	0,133
6	2_2495	RF 2_2495	1	682	1138	X	N.R.	N.A.	718	1160	0,142	N.A.	0,142
7	1_4141	Sham 1_4141	2	560	546	0,158	N.R.	0,158	600	558	0,468	2,9721	0,468
8	2_2922	RF 2_2922	1	697	631	X	N.R.	N.A.	735	643	0,222	N.A.	0,222
9	2_3481	RF 2_3481	1	1325	1718	X	N.R.	N.A.	1337	1750	0,101	N.A.	0,101
10	2_510	RF 2_510	1	832	129	X	N.R.	N.A.	868	135	1,007	N.A.	1,007
11	2_3684	RF 2_3684	1	487	114	X	N.R.	N.A.	533	117	1,457	N.A.	1,457
12	2_2826	RF 2_2826	1	537	609	X	N.R.	N.A.	582	622	0,146	N.A.	0,146
13	2_3715	RF 2_3715	1	1343	8	X	N.R.	N.A.	1358	16	0,199	N.A.	0,199
14	1_665	Sham 1_665	2	572	1199	0,124	N.R.	0,124	609	1227	0,13	1,0504	0,13

Overall, 56 polypeptides of HL-60 cells are influenced in their expression under RF-EMF. Reproducibly, 41 proteins showed to be up- and 1 protein to be down-regulated following RF-field exposure. 14 proteins appeared to be de-novo expressed after RF-field exposure of HL-60 cells.

By use of these lists identification strategies are further performed. They will include in gel-cleavage, identification of selected proteins by mass spectrometry (MALDI-TOF) and mass spectrometric sequencing (ESI-MS/MS). Further identification of selected proteins will include immunoblotting and functional protein assays.

3.2.4.4 Human lymphocytes (Participant 8)

RF-EMF did not affect gene expression in human lymphocytes.

T lymphocyte gene expression analysis was performed in collaboration with Participant 12 and Dr. Daniel Remondini in Bologna. The results suggest that no differences in gene expression are found between

quiescent T lymphocytes exposed to RF-EMF (DTX only) in comparison with sham-exposed cells. This finding did not suggest any significant interaction of RF-EMF with gene profile expression.

3.2.4.5 Brain cells of different origin (Participant 9)

RF-EMF exposure did not affect expression and activity of the inducible nitric oxide synthase (iNOS or NOS2) in nerve cells.

A basal level of NOS_2, probably due to the SVF deprivation, was detected in C6 cells, although inter-experiment's variation could be seen. A 48-hour treatment with LPS plus CK increased the expression of the enzyme by a factor 5 (Figure 126)

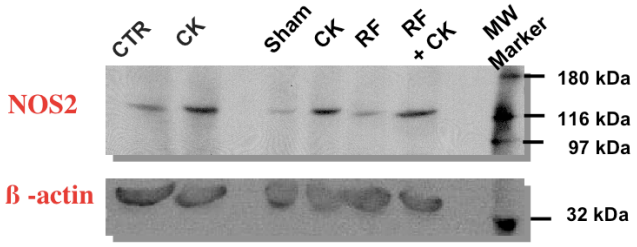

Figure 126. Representative blot for the detection of NOS_2 (upper blot) and ß-actin (lower blot) proteins.

Sham/sham experiments showed that a 15-20% inter-incubator variation had to be expected, so that a more than a 30% difference between sham- and RF-exposed data would be considered as a significant biological effect for both NOS_2 expression and nitrite accumulation (Figure 127).

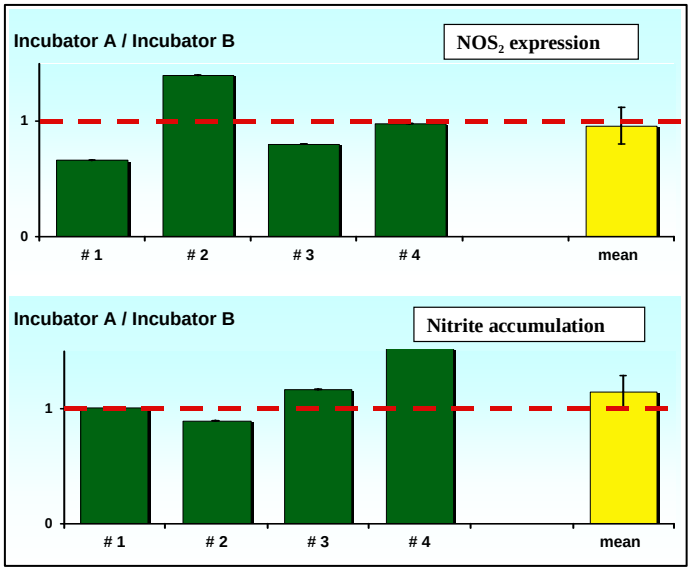

Figure 127. Expression of NOS_2 protein and nitrite accumulation (culture medium) in C6 cells in four sham/sham experiments (#1 to #4). Data are given as the ratio ± SEM between the levels found in the incubator A used for RF exposure and incubator B used for sham-exposure.

Exposure to GSM-900 at 0.2 W/kg and 2 W/kg for 48 hours was shown to not alter the expression of NOS_2 compared to sham exposure. Co-exposure to GSM and LPS plus cytokine was ineffective in modifying the effect of LPS plus cytokine treatment on NOS_2 expression (Figure 128).

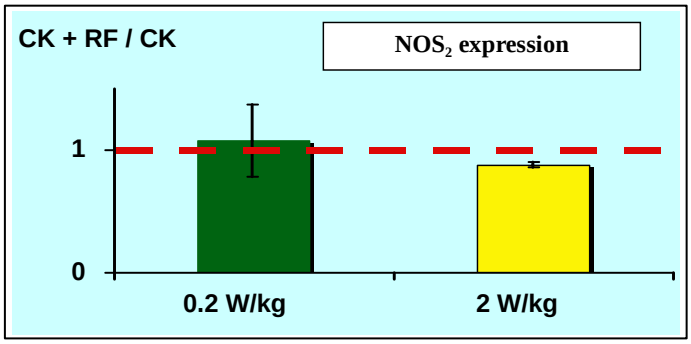

Figure 128. Expression of NOS_2 protein in C6 cells exposed to frame-GSM-900 at 0.2 and 2 W/kg for 48 hours. Data are given as the ratio ± SEM between the levels found in samples treated with CK+LPS (CK) and exposed to RF and those treated with CK alone.

Nitrite accumulation in culture medium was used as a marker of NOS_2 activation. No nitrite accumulation was shown in sham-exposed samples. Although inter-experiment variability, treatment with the cocktail of LPS plus CK led to a significant nitrite accumulation ($p<0.001$). As shown in Figure 129, a mean 20-fold increase in nitrite accumulation was measured after 48 hours of LPS plus CK treatment.

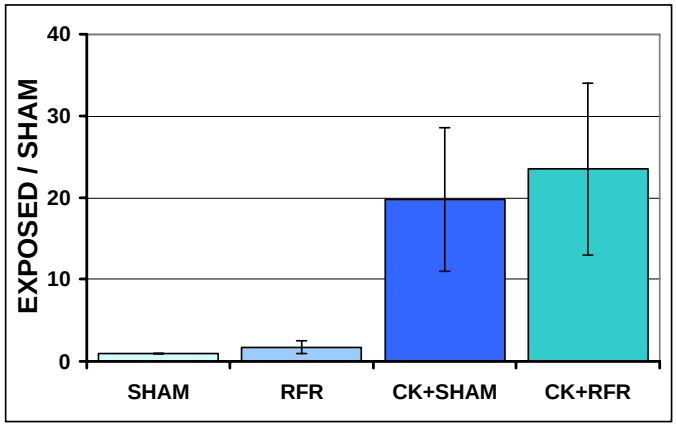

Figure 129. Nitrite accumulation in culture medium of C6 cells sham-exposed or exposed to GSM-900 at 0.2 W/kg and /or treated with CK+LPS (CK). In all cases, treatment duration was 48 hours. Data are given as the ratio ± SEM between the levels found in treated- versus sham-exposed samples.

No significant effect of GSM-900 exposure was detected on nitrite accumulation. When co-exposures to GSM-900 and LPS + CK treatment were performed, no modulation of chemically-induced NOS_2 expression. Overall, exposure to GSM-900 did not modulate CK+LPS-induced nitrite accumulation (Figure 130).

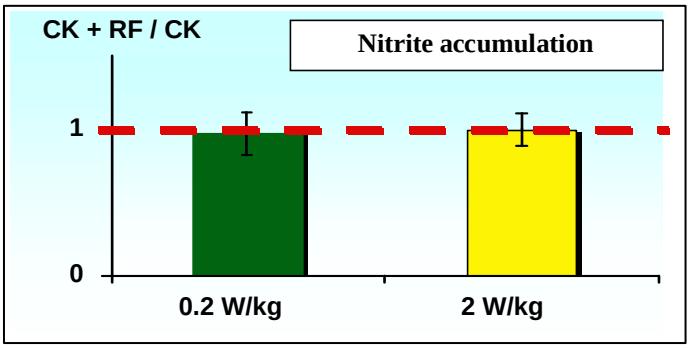

Figure 130. Nitrite accumulation (culture medium) in C6 cells exposed to frame-GSM-900 at 0.2 W/kg and 2 W/kg for 48 hours. Data are given as the ratio ± SEM between the levels found in samples treated with CK+LPS (CK) and exposed to RF and those treated with CK alone.

No evidence of an effect of RF-EMF (GSM-900) exposure on spontaneous expression and activity in C6 cells was obtained from our experiments. However, one can note that only strong treatments (serum deprivation plus long duration of chemical treatment) are shown to increase NOS_2 expression in C6 cells. It is noteworthy that most papers in the literature looked at the mRNA but not at the *protein* level as we did in the present work. Two SAR levels of GSM-900 were tested. Even at the highest SAR level of 2 W/kg corresponding to the public exposure limit recommended by the EU Commission, GSM-900 exposure was not shown able to influence NOS_2 expression or activity in activated C6 cells. Taken together, RF-EMF at a low SAR level were not identified as a stimulus for C6 cells activation.

RF-EMF (GSM-900 signals) did not affect heat shock protein expression in nerve cells.

When used as a positive control, heat shock (43°C for 20 min) increased expression of hsp70 in all nerve cell cultures, i.e. human U87 astrocytoma cells, rat C6 glioma cells and human SH-SY5Y neuroblastoma cell lines. However, when exposed to GSM-900 for 24 hours, none of the cell line showed a significant change in expression of hsp70 (Figures 131, 132). Altogether, our data show that exposure to ELF-EMF does not seem to be able to induce Hsp70 expression in rat and human nerve cells.

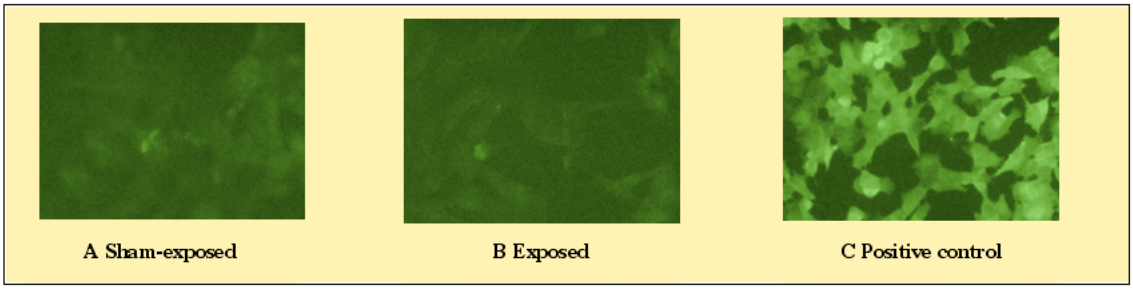

Figure 131. Fluorescent Hsp70 immunolabelling after sham-exposure or exposure of human SH-SY5Y neuroblastoma cells to frame GSM-900 signal at 2 W/kg for 24 hours (A and B) or to heat shock (43°C, 20 min) (C).

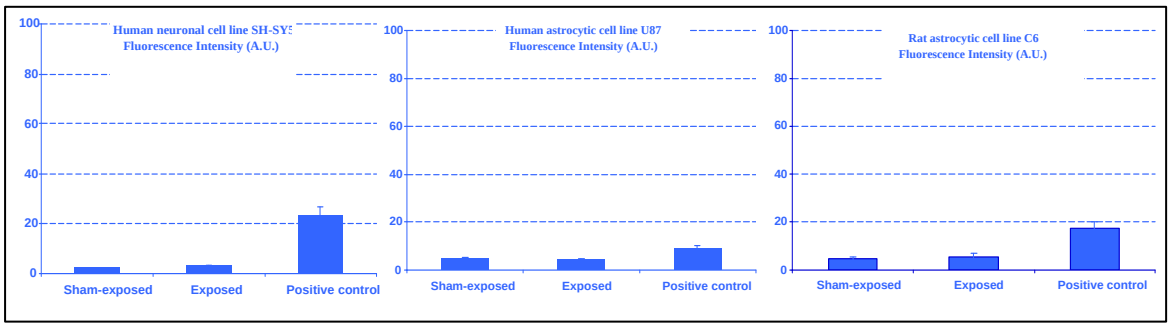

Figure 132. Effect of GSM-exposure (2 W/kg, 24h) or Heat Shock exposure (43°C, 20 min) (Positive control) on hsp70 expression in three different cell lines. Results are expressed in Fluorescence Intensity (A.U). Data from 3 independent experiments are presented as the Mean ± SEM

GSM-900 microwave exposure did not affect hsp27 expression in human endothelial cell line EA.hy926.

The hsp27 expression was measured using the immunofluorescence technique. Qualitative analysis did not allow for detecting any difference in fluorescence intensity in RFR exposed cells versus sham cells. Our quantitative results obtained after fluorescence image analysis of hsp27 expression in EA-hy926 revealed that no significant difference was observed between sham-or exposed cells in both cell lines (Figures 133, 134)

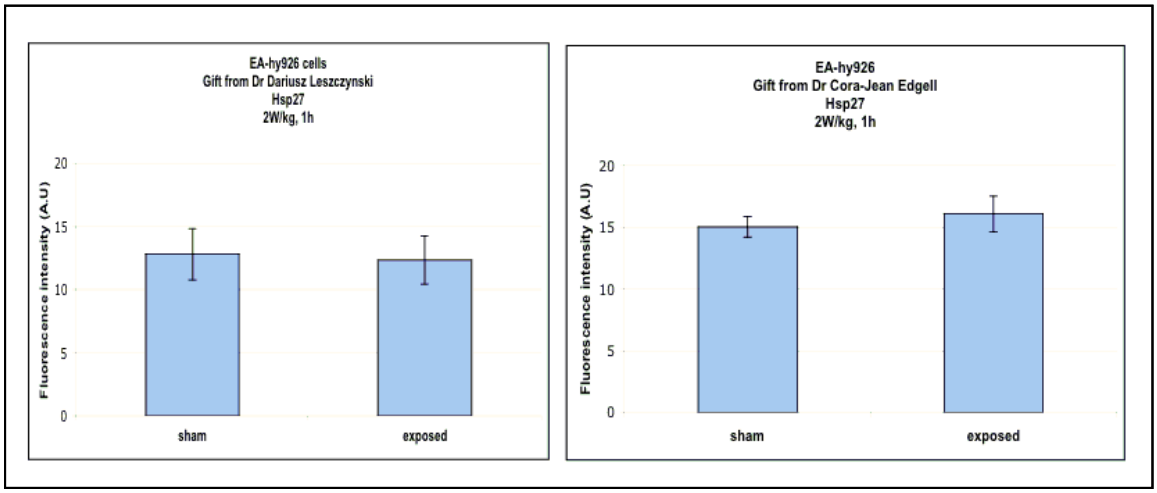

Figure 133. Effect of GSM-exposure (2 W/kg, 1 hour) on hsp27 in EA-hy926 cell lines given by Participant 6 and Dr Cora-Jean Edgell. Results are expressed as the fluorescence Intensity (A.U). Data from 5 independent experiments are presented as the Mean ± SEM.

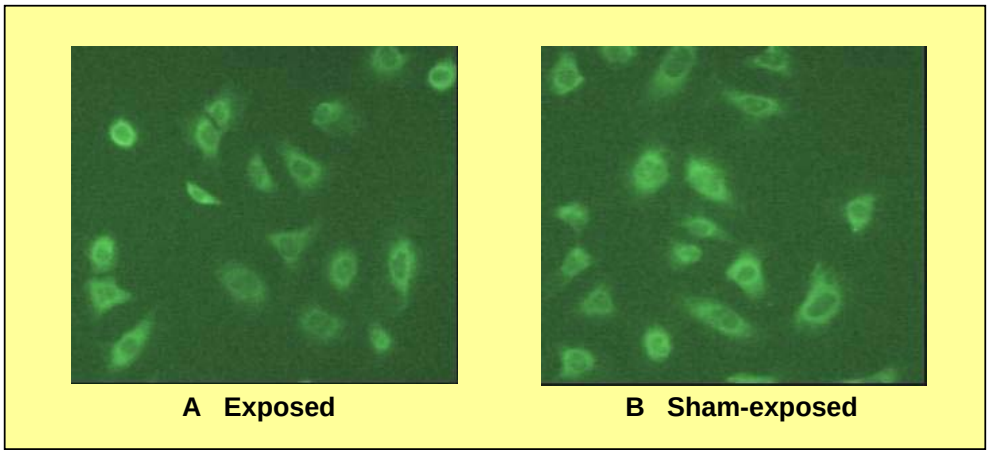

Figure 134. Fluorescent hsp27 immunolabelling after exposure(A) or sham-exposure(B) of EA-hy926 cell lines given by Participant 6 to GSM-900 signal at 2 W/kg for 1 hour.

A third method using Elisa test will allow us to quantify precisely if RFR are able to induce changes in hsp27 expression. However, with our method we were unable to confirm previous data on hsp27 expression in endothelial cell lines (Leszczynski et al., 2002). Therefore, we can not conclude that RFR induce stress response.

No conclusive data was obtained on the effect of RF-EMF exposure on Hsp27 expression in rat brain.

Table 28 shows results obtained on hsp27 expression in rat brains in the pilot experiment.

Results obtained on samples treated without perfusion show non-specific labelling disturbing the analysis. Results obtained on perfused brains show acceptable background noise. Image analysis obtained on perfused brains reveal conflicting and opposite results within groups preventing to draw conclusions.

Table 28. Hsp27 expression in rat brains

Experimental procedure	Background noise	Hsp27 labelling	Exposure conditions
Perfusion	-	+	Control
Perfusion	+	-	Control
Perfusion	-	-	Sham-exposed
Perfusion	-	+	Sham-exposed
Perfusion	-	-	Exposed
Perfusion	+	+/-	Exposed
Without perfusion	+	+	Control
Without perfusion	+	+	Control
Without perfusion	+	+/-	Sham-exposed
Without perfusion	+	++	Sham-exposed
Without perfusion	+	+	Exposed
Without perfusion	+	+/-	Exposed

– : negative labelling; + : positive labelling; +/- : negative or positive labelling depending of the area; +/+ : clear positive labelling

This pilot study did not allow us to draw conclusion on results obtained *in vitro* on hsp27 expression but it gave information on technical methodologies and on the number of animals to use.

RF-EMF (GSM-900) exposure weakly affected gene expression in immune cells.

This investigation was carried out in cooperation with Participant 12. Criteria for the selection of significantly altered gene expression was an exposed over sham ratio less than 0.5 for a significant decrease and more than 2.0 for a significant increase. Using these criteria, over 15588 human genes were detected, changes in expression of about 50 genes were significant corresponding to 0.3% of total number of detectable genes. Genes shown to be altered after RF-EMF exposure (increase or decrease) are known to be involved in signal transduction, ion electron transport, metabolism of energy and proteins, cell proliferation, apoptosis or differentiation, immune answer, inflammation, stress answer, extracellular matrix, cytoskeleton, adhesion and DNA repair. The largest modification in RNA expression corresponded to genes related to signal transduction (linked with GTP or calcium) and energy metabolism. Only a few genes involved in apoptosis or stress response were detected and show no significant sensitivity to RFR exposure. Concerning our purpose to investigate modification of genes involved in inflammatory response and processes, one gene corresponding to a component of major histocompatibilty complex class II and another acting as plasminogen activator were altered by RF-EMF. Finally, the largest increase of expression (30 fold increase), after mobile phone exposure, concerned genes described to participate in amine oxidase (copper containing) activity. This enzyme is involved in cell growth and proliferation but also in immune regulation.

3.2.4.6 Human endothelial cell lines EA.hy926 and EA.hy926v1 (Participant 6)

It has been suggested that high-throughput screening techniques (HTST) of transcriptomics and proteomics could be used to rapidly identify broad variety of potential molecular targets of RF-EMF and generate variety of biological end-points for further analyses (Leszczynski 2001). Combination of data generated by transcriptomics and proteomics in search for biological effects is called the “discovery science”. This term has been coined-in by Aebersold and co-workers (Aebersold et al. 2000) to define the new approach that will help in revealing biological mechanisms, some of which might be unpredictable using the presently available knowledge. This approach seems to be particularly suited for elucidation RF-EMF health hazard issue because it might reveal effects that are not possible to predict based on the present knowledge about the biological effects of RF-EMF. However, before committing large funds that are needed for HTST studies it is necessary to determine whether indeed this approach will be successful in unravelling physiologically significant biological events induced by RF-EMF. Due to their high sensitivity HTST are able to pick-up very small changes in protein or gene expression which changes might be of insufficient magnitude to alter cell physiology. Thus, although using HTST it might be possible to find biological effects induced by RF-EMF these effects might be of limited or no significance at all, from the physiological stand point. Therefore, to determine the usefulness of HTST approach to the issue of bio-effects induced by RF-EMF, we have performed a 5-step feasibility study and have shown that HTST might indeed help to identify experimental targets for physiological studies of RF-EMF-induced biological responses (Figure 135).

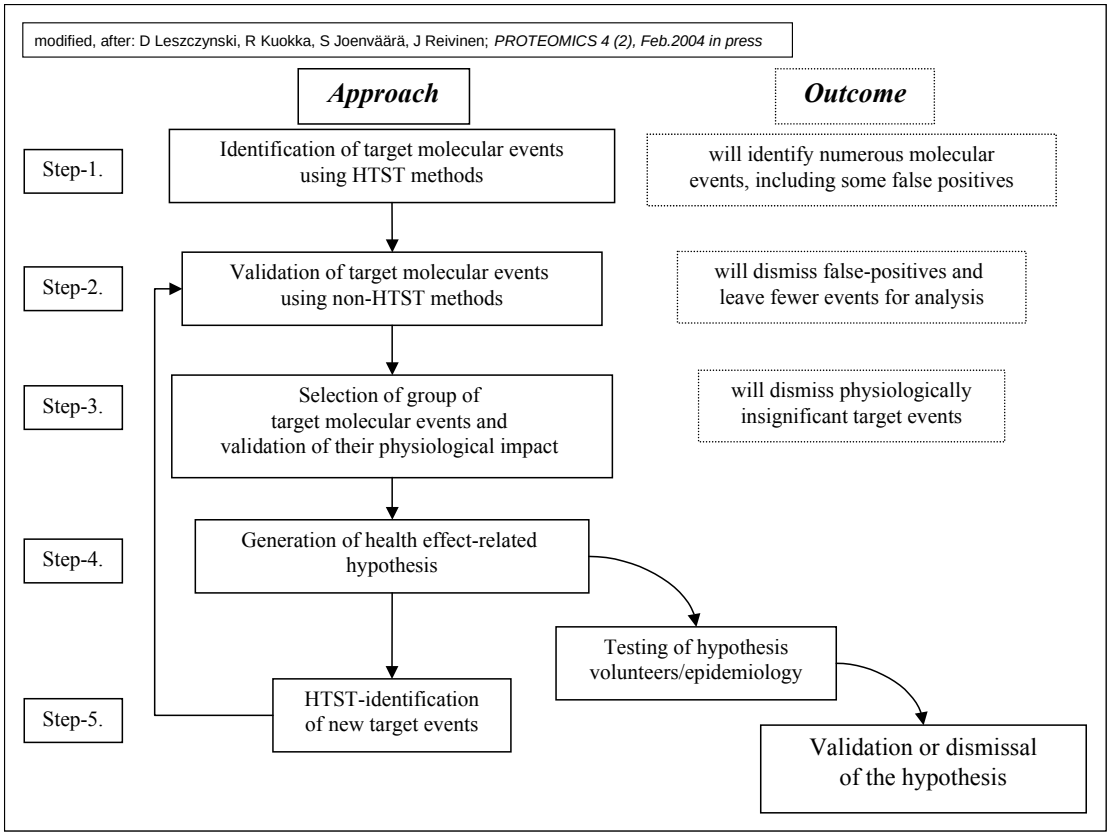

Figure 135. Scheme of experimental procedure which execution will elucidate new RF-EMF induced molecular events that might affect cell physiology. Events of magnitude sufficient to alter cell physiology could be then examined for their potential impact on the organ/whole body physiology in attempt to predict the extent of eventual health hazard.

A. The 5-step feasibility study

Step-1: HTST-identification of target molecular event

Firstly, we have determined the extent of cell response to RF-EMF (Leszczynski et al. 2002). This has been done by analysing global changes in the pattern of protein phosphorylation. As an experimental model we have used cultures of human endothelial cell line EA.hy926 (Edgell et al. 1983). Cells were exposed for 1 hour to 900MHz GSM mobile phone simulating signal at an average specific absorption rate (SAR) of 2.4 W/kg (Deli et al. 1995) that is slightly above the European safety limit (SAR=2.0 W/kg). In order to be able to determine changes in protein phosphorylation, the ^{32}P-labelled orthophosphate was present in the cell cultures during the 1 hour RF-EMF exposure period. Immediately after the end of exposure cells were harvested; proteins extracted and separated using standard two-dimensional electrophoresis (2-DE). Using PDQuest software (Bio-Rad, UK), some 1266 different protein spots were identified in silver-stained 2-DE gels (Figure 136A). Using autoradiography it was possible to determine that among the 1266 proteins spots, in non-irradiated control exposed cells, were detected some 110 phosphoproteins (Figure 136B), whereas in exposed cells were detected some 372 phosphoproteins (Figure 136C). The observed broad change in the pattern of global protein phosphorylation has suggested that cells respond to RF-EMF and that possibly any of the hundreds of phosphoproteins that have altered their phosphorylation status could, at least potentially, affect cell physiology. By using western blot or mass spectrometry, to identify the phosphoproteins present in the 2DE spots, it might be possible to find variety of protein targets that could be used in examining effects of mobile phone radiation on cell physiology. With this approach, the selection of molecular targets for further studies would not be based only on deduction of potentially affected events but on the knowledge of the identities of proteins that indeed respond to RF-EMF. Thus, in the continuation of Step-1, using

simple western blot screening with antibodies directed against various stress response proteins, we have identified hsp27 as one of the phosphoproteins responding to RF-EMF. Hsp27 is continuously expressed in endothelial cells (Edgell et al. 1983). In 2DE-western blots it appeared as two spots of 27kDa molecular weight but with different isoelectric points (pI=5.7 and pI=6.1) (Figure 136D). Only the $hsp27_{pI=5.7}$ isoform was phosphorylated and, following exposure to RF-EMF, the size of $hsp27_{pI=5.7}$-spot has increased (Leszczynski et al. 2002).

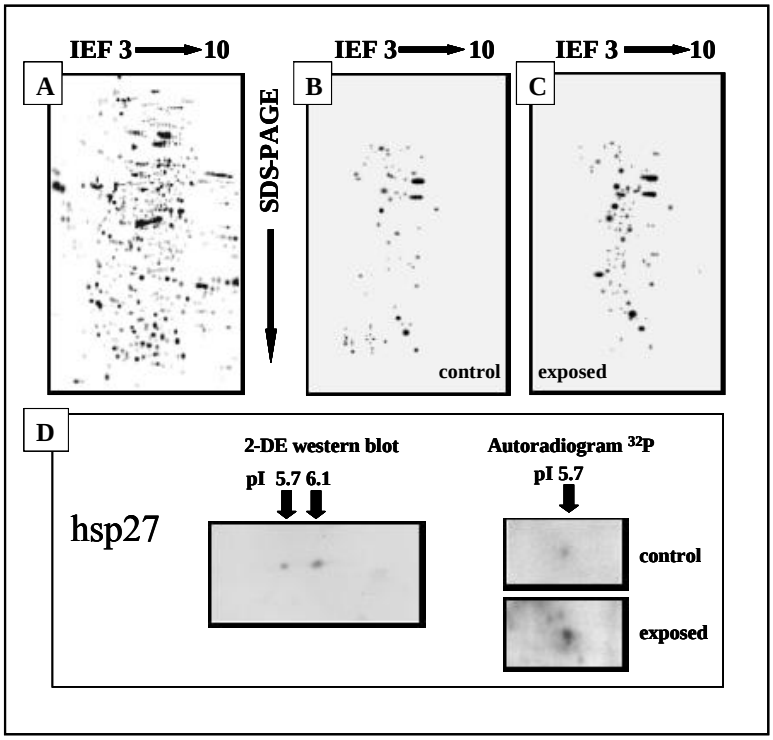

Figure 136. Identification of target molecular event for further studies – Step-1. Pattern of protein expression in EA.hy926 human endothelial cell line as determined by 2DE (panel A). Pattern of expression of ^{32}P-labeled phosphoproteins in control (panel B) and in exposed (panel C) cells. Hsp27 protein was identified, using 2DE western blot, as existing in EA.hy926 cells in two isoforms with different pI values (panel D-left). The pI 5.7 form was phosphorylated and its phosphorylation level has increased after RF-EMF exposure (panel D-right). For experimental details see Material and Methods section in Leszczynski et al. 2002.

Step-2: Validation of target molecular event

The change in phosphorylation status of hsp27 was confirmed in several ways to assure the validity of this observation (Leszczynski et al., 2002):

- immunoprecipitation of phosphorylated hsp27 (Figure 137A),
- immunoprecipitation of p38MAPK (Figure 137B), an up-stream kinase indirectly involved in phosphorylation of hsp27,
- inhibition of hsp27 phosphorylation by introduction to cell cultures of inhibitor of hsp27-up-stream kinase p38MAPK (SB203580) and determining hsp27 phosphorylation status by immunoprecipitation (Figure 137C).

Thus, in the Step-2 was confirmed that hsp27 is the valid molecular target event of the RF-EMF and that it is justified to further examine impact of this change on cell physiology.

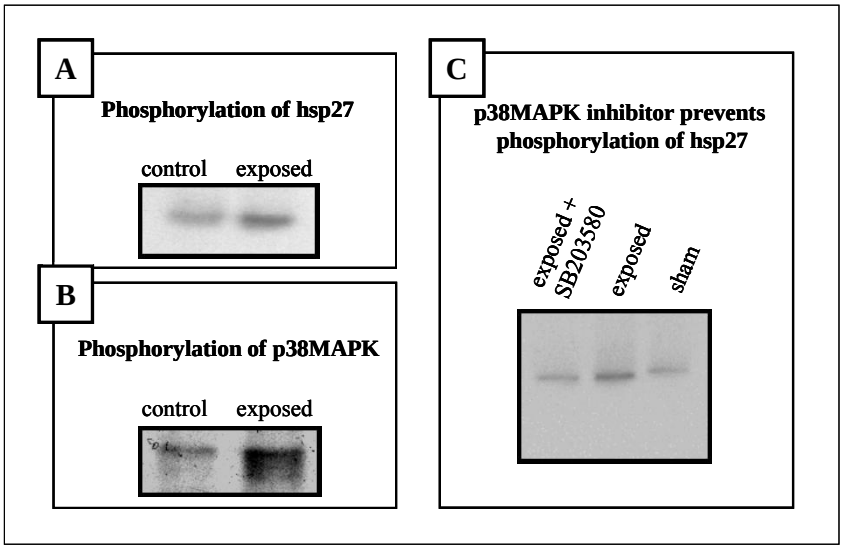

Figure 137. Validation of the target molecular event – Step-2. Increase in phosphorylation of hsp27 was confirmed by immunoprecipitation (panel A). Effect of p38MAP kinase on the RF-EMF-induced hsp27 phosphorylation was confirmed by determining, by immunoprecipitation, that p38MAPK is also activated by the RF-EMF exposure (panel B). As expected, presence of p38MAPK inhibitor, SB203580, in the culture medium during the exposure to RF-EMF, has prevented phosphorylation of hsp27 (panel C). For experimental details see Material and Methods section in Leszczynski et al. 2002.

Step-3: Cellular response – validation of the physiological event

Observed by us phosphorylation and increase in expression of hsp27 (Leszczynski et al. 2002) is a well-established mechanism of cell response to a broad variety of stress stimuli (Rogalla et al. 1999). Therefore, the observed by us doubling of Hsp27 expression and 2- to 7-fold increase in amount of phosphorylated hsp27 in cells (Leszczynski et al. 2002) have suggested that EA.hy926 cells have recognised RF-EMF as an external stress factor and that they have launched an hsp27-dependent counter response. Phosphorylation of hsp27 has been shown to regulate polymerisation of F-actin and stability of made of this protein - stress fibers (Landry and Huot 1995). Thus, we have examined status of the stress fibers in exposed cells by staining F-actin with AlexaFluor-labelled phalloidin. As shown in Figure 136A, RF-EMF exposure has caused increase in cellular staining with phalloidin what indicates increase in stability of F-actin stress fibers. The stability of stress fibers, as determined by the pattern of staining with phalloidin-AlexaFluor, increased after 1 hour irradiation and did not decline during the 1 hour of post-irradiation incubation. Induction of the stability of stress fibers caused cells to shrink and visible cell shrinking was observed among the cells brightly stained with AlexaFluor-phalloidin (Figure 138A; middle and right panels). The increase in the stability of stress fibers was prevented in the presence of p38MAPK inhibitor SB203580 (Figure 138B). Also it was possible to observe that in cells expressing high levels of hsp27 (Figure 138C), the cell edges were brightly stained with phalloidin-AlexaFluor, what indicates re-localisation of F-actin stress fibers to cell ruffles whereas in cells expressing low levels of hsp27, network of stress fibers was seen throughout the whole cytoplasm but not in the ruffles. Such behaviour of hsp27 and stress fibers in cells exposed to RF-EMF is in agreement with the general pattern of cellular response to stimuli that activate hsp27-dependent stress response (Landry and Huot 1995).

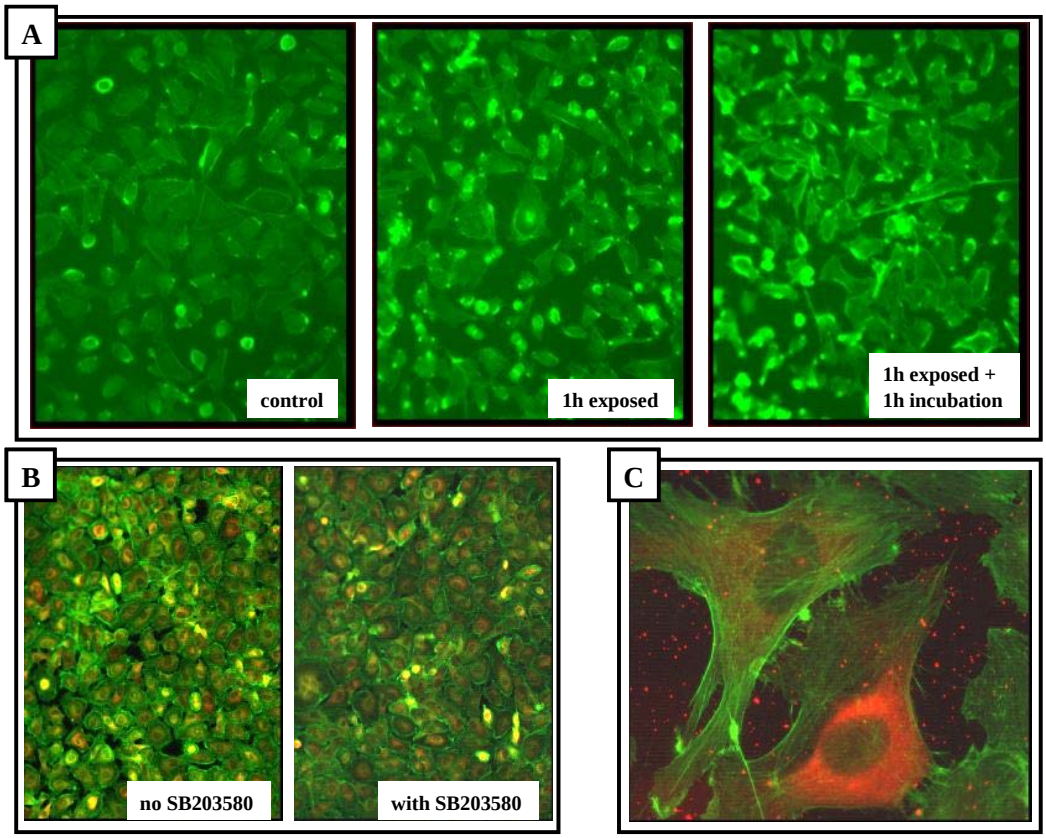

Figure 138. Cellular response to RF-EMF – validation of physiological event – Step-3.Exposure of cells to RF-EMF has caused increase in cell staining with AlexaFluor-labelled phalloidin (panel A). This suggests the increase in the expression/stability of F-actin, protein that forms cellular stress fibers. Rounding up is visible among the cells expressing highest F-actin content (the brightest staining with AlexaFluor-phalloidin). This effect persisted during the 1-hour post-exposure incubation of cells in control conditions. Presence of p38MAPK inhibitor, SB203580, in cell culture medium has prevented increase in AlexaFluor-phalloidin staining (panel B). Large magnification of cells shown in panel C demonstrates difference in distribution of AlexaFluor-phalloidin stained stress fibers (green colour) in cells with high (cell on the right) and low (cell on the left) content of hsp27 protein (indirect immunohistochemical staining; red fluorescence).

Step-4: Generation of hypothesis based on molecular and physiological events

The above results (Leszczynski et al. 2002) have formed basis and support for our working hypothesis (Figure 132, Step-4). Stabilisation of stress fibers and caused by it cell shrinking, when occurring in endothelial cells lining brain's capillary blood vessels, might be of importance for the functioning of blood-brain barrier. Stabilisation of stress fibers and cytoplasmic distribution of F-actin was previously shown to cause: (i) cell shrinkage (Landry and Huot 1995; Piotrowicz and Levin 1997a), that might lead to opening of spaces between cells, (ii) increase in the permeability and pinocytosis of endothelial monolayer (Deli et al. 1995; Lavoie et al. 1993), (iii) increase in formation of the so called "apoptosis-unrelated" blebs on the surface of endothelial cells (Becker and Ambrosio 1987), which eventually might obstruct blood flow through capillary blood vessels, (iv) stronger responsiveness of endothelial cells to estrogen and, when stimulated by this hormone, to secrete larger than normally amounts of basic fibroblast growth factor (bFGF) (Piotrowicz et al. 1997b) which might, in endocrine manner, stimulate de-differentiation and proliferation of endothelial cells and possibly led to the associated with cell's proliferative state - cell shrinkage and unveiling of basal membrane. Also, the activated (phosphorylated) hsp27 has been shown to inhibit apoptosis by forming complex with the apoptosome (complex of Apaf-1 protein, pro-caspase-9 and cytochrome *c*), or some of its components, and preventing proteolytic activation of pro-caspase-9 into active form of caspase-9 (Pandey et al. 2000; Concannon et al. 2001). This, in turn, prevents activation of pro-caspase-3 which is activated by caspase-9. Thus, induction of the

increased expression and phosphorylation of hsp27 by the RF-EMF exposure might lead to inhibition of the apoptotic pathway that involves apoptosome and caspase-3. This event, when occurring in RF-EMF exposed brain cells that underwent either spontaneous or external factor-induced transformation/damage, could support survival of the transformed/damaged cells. Therefore, based on the known cellular role of over-expressed/phosphorylated hsp27 we have proposed a hypothesis (Leszczynski et al. 2002) that: the activation (phosphorylation) of hsp27 by mobile phone radiation might be the molecular mechanism (i) regulating increase in blood-brain barrier permeability, which would explain, observed in some animal experiments, increase in blood-brain barrier permeability, and (ii) regulating apoptosis through interference with the cytochrome c/caspase-9/caspase-3 pathway (Figure 139). Thus, it is possible that the RF-EMF might have effect on cytoskeleton-related and on the apoptosis-related cell functions. This notion supports and justifies further examination of cytoskeleton and apoptosis related properties of RF-EMF exposed endothelial cells.

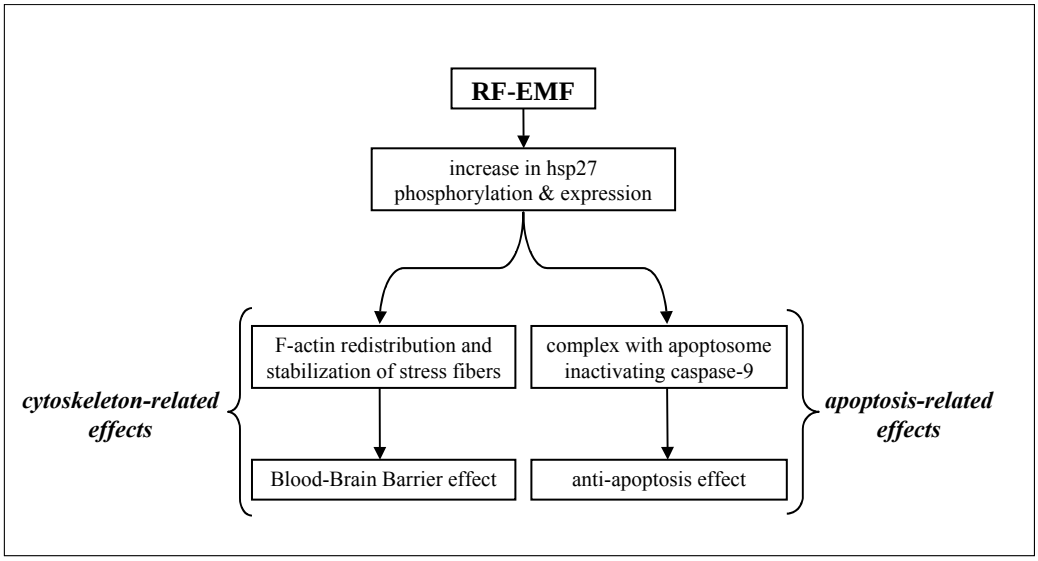

Figure 139. Hypothesis based on the molecular and physiological events – Step-4. Based on the known functions of hsp27 we have proposed that RF-EMF induced hsp27 phosphorylation might affect cell cytoskeleton and cell apoptosis. For full scheme and description of hypothesis see reference Leszczynski et al. 2002.

Step-5: HTST-identification of new target events, with support of hypothesis

Further experiments using HTST have revealed additional information pertinent to the cytoskeleton and apoptosis related properties of RF-EMF exposed endothelial cells.

The suggested changes in the cytoskeletal proteins were detected using 2-DE separated proteins. Approximately 1300 protein spots were detected 2-DE. Comparison of the control and exposed samples revealed some 49 protein spots which were statistically significantly (student T-test, $p<0.05$, $n=10$) affected by the exposure (increased or declined expression). Few of the spots were selected for the mass spectrometry identification using the following criteria: spots needed to be (i) enough separate from the adjacent spots, (ii) sufficiently large and (iii) well focused in all dimensions. Cytoskeletal proteins vimentins (Figure 140) and tubulin (not shown) were identified by mass spectrometry among the proteins that responded to RF-EMF. The suggested interference with apoptosis was further examined using cDNA Expression Arrays (Clontech) and screening expression of 3600 different genes. Among the genes that were down-regulated in cells exposed to RF-EMF were numerous genes encoding proteins of Fas/TNFα-apoptotic pathway (Figure 141). This pathway was suggested as target for the RF-EMF induced phosphorylated hsp27. Therefore, concomitantly observed increase in hsp27 phosphorylation, that is anti-apoptotic event, and down-regulation of proteins of Fas/TNFα apoptotic pathway suggest that further studies aiming at elucidation of RF-EMF effect on cell apoptosis are justified.

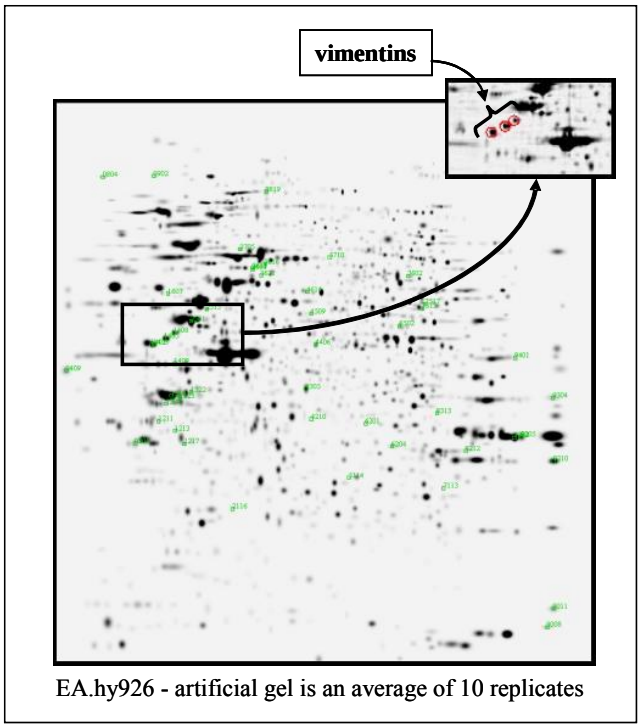

Figure 140. HTST-identification of new target events – cytoskeleton-related – Step-5. Using larger 2-DE gels (20x20 cm) and 10 replicates of each run we have identified some 49 proteins that, in statistically significant fashion, have altered their expression following RF-EMF exposure. Among the mass spectrometry identified spots were cytoskeletal proteins vimentins (inset) and tubulin (not shown).

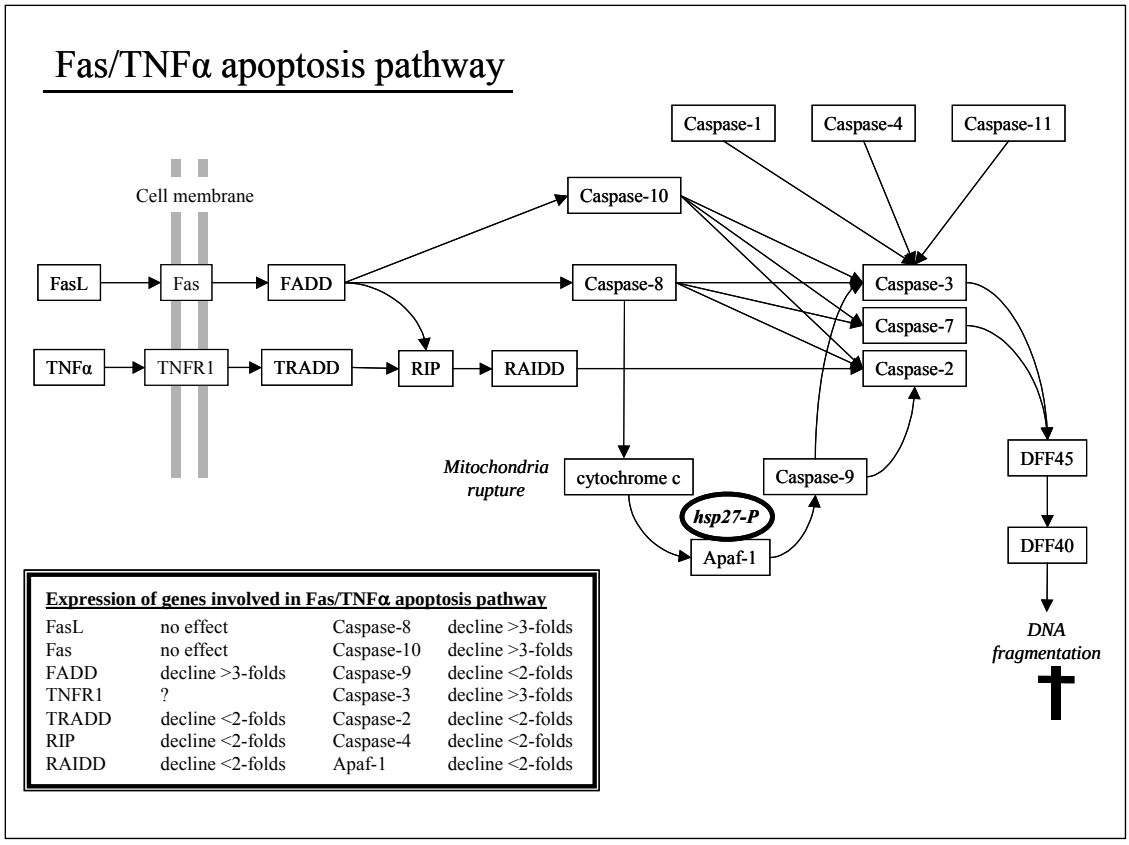

Figure 141. HTST-identification of new target events – apoptosis-related – Step-5. Analysis of RF-EMF-induced expression changes, using cDNA Expression Array for 3600 tumour-related genes, has revealed that the majority of genes that encode proteins forming Fas/TNFα apoptotic pathway are down-regulated (Table inset).

B. Genotype-dependent cell response to 900 MHz GSM radiation

We have compared response to mobile phone radiation of two human endothelial cell lines: fast proliferating EA.hy926 (Edgell et al., 1983) and its slow proliferating variant EA.hy926v1 (derived by sub-cloning from the EA.hy926 cell line).

Proteomics approach

Using 2-DE and MALDI-MS proteomics approach we have determined what proteins respond to the mobile phone radiation. Using PDQuest 6.2 software (Bio-Rad, UK) the 2-DE artificial gels (Figure 135) were generated from 10 independent protein samples from ten independent replicates of controls and irradiated cell cultures. The protein expression pattern in ten replicate control samples was then compared with the protein pattern in ten replicate irradiated samples. The normalised spot volumes of the proteins from control and exposed sample gels were statistically analysed using student t-test at the confidence level of 95%. The most striking observation was that the comparison in-between the two cell lines showed that their protein expression patterns are very different in spite of the closely related origin of both cell lines (Figures 142A, 142B). Only approximately half of all of the protein spots could be matched confidently between the cell lines. This difference in protein expression pattern might explain the observed differences in the growth rate between the cell lines. Because of the observed differences in the protein expression and proliferation between the cell lines, it was not a surprise that the response to the mobile phone radiation also varied between EA.hy926 and EA.hy926v1 cell lines. The comparison of the exposed and control samples has shown several tens of protein spots with radiation-induced statistically significant change in expression levels (t-test $p<0.05$). In EA.hy926 cell line there were 38 of protein spots which expression was altered by the radiation exposure (Figure 142A) whereas in EA.hy926v1 cell line there were 45 differentially expressed protein spots (Figure 142B). The identity of

the all radiation-responding protein spots is being determined by MALDI-MS and will be reported in due time.

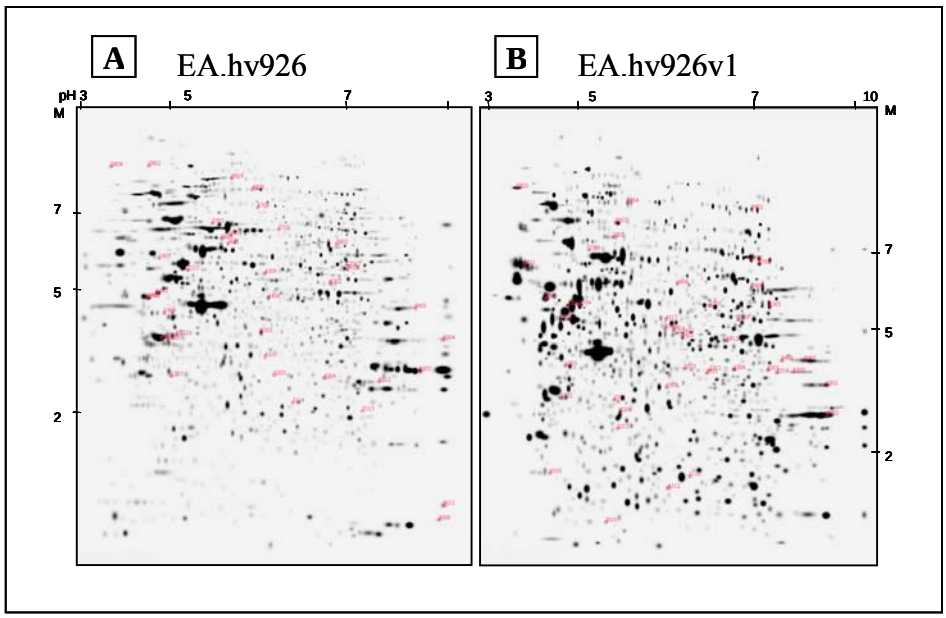

Figure 142. 2-DE gels of proteins extracted from human endothelial cell lines; EA.hy926 (A) and EA.hy926v1 (B). The 1st dimension IEF using pH gradient 3-10 NL, 2nd dimension 8% SDS-PAGE. Statistically significantly (t-test $p<0.05$) differing spots in the cell lines are numbered using PDQuest SSP numbers.

(A) EA.hy926 cell line - 38 statistically significantly differing spots. Four spots: vimentin (1402 and 1405), isocitrate dehydrogenase 3 (NAD+) alpha (4305), and heterogeneous nuclear ribonucleoprotein H1 (4406), were identified using mass spectrometry.

(B) EA.hy926v1 cell line; 45 statistically significantly differing spots.

Few of the protein spots, which expression was statistically significantly altered by the irradiation, were identified using MALDI-MS (Figure 143). In order to increase probability of a single protein present in the single spot, the protein spots that were selected for MALDI-MS analysis had to fulfil the following requirements: (i) spots were well separated from other spots in both 2-DE dimensions, (ii) spots were sufficiently large (Figure 143A). The MALDI-MS analysis service was purchased from the Protein Chemistry Laboratory of the Institute of Biotechnology at the Helsinki University, Finland. The selected spots were reduced with DTT and alkylated with iodoacetamide before overnight digestion with a sequence-grade modified trypsin (Roche, France). The peptide mixture was concentrated and desalted using Millipore ZipTip™ µ-C18 pipette tips. The peptide mass fingerprints were measured with Bruker Biflex™ MALDI-ToF mass spectrometer in a positive ion reflector mode using α-cyano-4-hydroxycinnamic acid as a matrix. The database searches were performed using ProFound and Mascot searches. The protein spots that were identified with MALDI-MS were as follows (Figure 143):

- Protein spot 4305 - isocitrate dehydrogenase 3 (NAD+) alpha (Kim et al. 1995) is a subunit of the mitochondrial enzyme, which catalyses the conversion of isocitrate to 2-oxoglutarate in the citric acid cycle. The expression level of this protein was moderately down-regulated in the exposed samples having a ratio exposed vs. control 0.72 with the p-value of 0.03. The down-regulation of this protein might affect cellular energy production.
- Protein spot 4406 - heterogeneous ribonucleoprotein H1 (Honore et al. 1995) is a component of the heterogeneous nuclear ribonucleoprotein (HNRNP) complexes which provide a substrate for the processing events which pre-mRNAs go through before becoming functional mRNAs in the cytoplasm. The expression level of this protein is slightly down-regulated in the exposed samples with a ratio exposed vs. control 0.61 with the p-value 0.03. The potential down-regulation of this protein might affect protein translation process.

- Protein spots 1402 and 1405 - vimentin (Ferrari et al. 1986) is a protein component of class III-intermediate filaments. In EA.hy926 cells it was found to be expressed in at least two different iso-forms differing in molecular weight and isoelectric point. Both vimentin iso-forms were up-regulated; spot 1402 (experimental MW/pI ca. 47 kDa/4.4) by 2.5-fold with p-value of 0.006 and spot 1405 (experimental MW/pI ca. 48kDa/4.8) by 2.2-fold with p-value of 0.02.

A

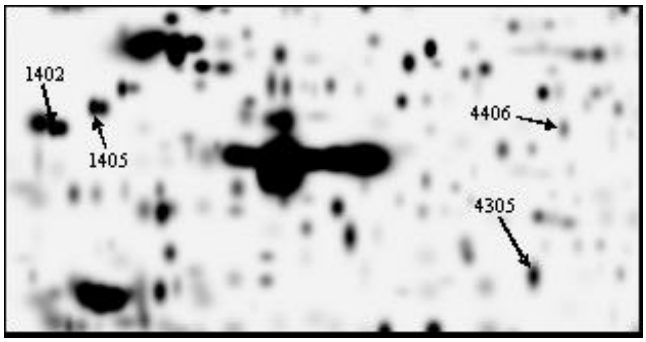

B

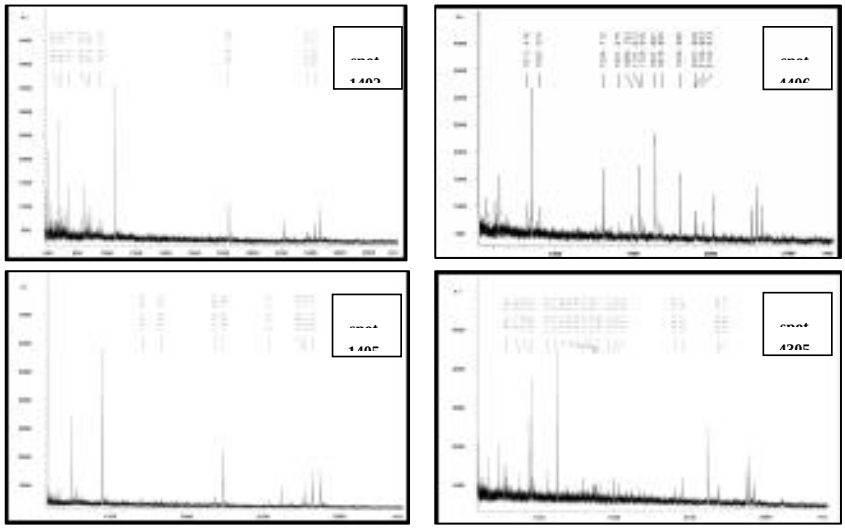

C

SSP	Protein name	Swiss-prot ID code	Sequence coverage	Swiss-prot annotations
4305	Isocitrate dehydrogenase 3 (NAD+) alpha	P50213	21%	component of enzyme complex catalysing conversion of isocitrate to 2-oxoglutarate
4406	Heterogeneous nuclear ribunocleoprote in H1	P31943	34%	component of HNRNP complex providing a substrate for pre-mRNA processing
1402	vimentin	P08670	19%	class III-intermediate filament
1405	vimentin	P08670	14%	class III-intermediate filament

Figure 143. (A) Fragment of the 2-DE gel of EA.hy926 cells with marked spots that were identified with MALDI-MS. (B) MALDI-MS spectra showing peptide finger prints of the four identified protein spots. (C) Table summarising the properties of the identified proteins**.**

Alterations in the vimentin expression suggest that some form of cytoskeletal response might be taking place in cells exposed to the mobile phone radiation. This notion agrees with our earlier observation of the effect of the mobile phone radiation on the stability of F-actin stress fibers (Leszczynski et al. 2002; Leszczynski et al. 2004). Changes in the vimentin expression observed in 2-DE were further confirmed by SDS-PAGE and western blotting and by cell staining using indirect immunofluorescence method. For SDS-PAGE/western blotting a standard protocol was used. Briefly, the cell lysates were separated using 7.5% SDS-PAGE, blotted to PVDF-membrane, blocked with 5% non-fat dry milk and exposed to the primary vimentin antibody (Zymed, USA) and the secondary antibody containing a HRP-conjugate (Dako, Denmark). The signal was detected using enhanced chemiluminescence (Pierce, UK). For immunocytochemistry cell were fixed in 3% paraformaldehyde, membranes were permeabilised in 0.5% Triton X-100 and as a primary antibody was used vimentin antibody (Zymed, USA) and the secondary antibody was TRICT-conjugated (Dako, Denmark). The images were captured using a Leitz fluorescence microscope and computerised image acquisition system (Metafer, Germany).

SDS-PAGE and western blot have confirmed that EA.hy926 cells express two iso-forms of vimentin. The higher molecular weight form (experimental MW ca. 57 kDa) was present both in control and in irradiated cells and its expression was not affected by the irradiation (Figure 144A). The lower molecular weight vimentin (experimental MW ca. 48 kDa) was not detectable in the non-irradiated cells but was expressed in the irradiated cells (Figure 144B). Indirect immunohistochemistry staining of vimentin has shown the change in the distribution pattern of the vimentin filaments after the exposure to the mobile phone radiation (Figure 143C, 143D). Together, the observed changes in the vimentin expression suggest that the mobile phone radiation might potentially alter cell physiology by affecting cellular cytoskeleton.

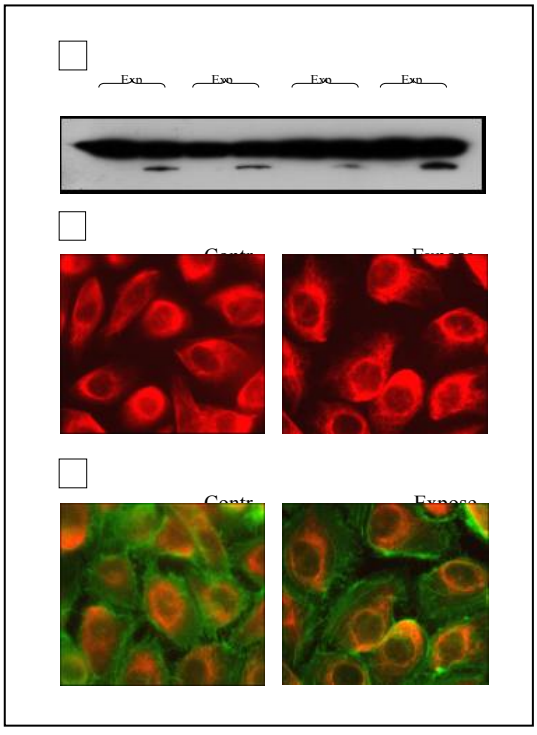

Figure 144. (A) Western blot-detected expression of vimentin in non-irradiated EA.hy926 cells (C-lanes) and in exposed cells (RF-lanes). MW ca. 57 kDa and ca. 48 kDa. Four separate experiments are shown. (B) Immunostaining of vimentin in non-exposed and in exposed EA.hy926; red colour – vimentin. Note diffuse-like staining for vimentin in non-exposed cells as compared with more filament-like expression in exposed cells.(C) Immunostaining of vimentin (red colour) and F-actin stress fibers (green colour) in non-exposed and in exposed EA.hy926. F-actin was detected with phalloidin-AlexaFluor. Note diffuse-like staining for both vimentin and F-actin in non-exposed cells as compared with more filament-like expression in exposed cells.

Transcriptomics approach

Using cDNA Expression arrays (Clontech, USA) we have determined that number of genes increased/declined expression in both cell lines following the exposure to mobile phone radiation (900 MHz GSM). Most strikingly, genes that were up regulated in one of the cell lines were down-regulated or not affected in the other cell line (Tables 29, 30, and 31). It suggests that the cell response might depend on the genotype.

Table 29. Genes which were up-regulated in EA.hy926 cell line following to the exposure to the 900 MHz GSM.

Gene name	**EA.hy926 (*fast proliferating*)**		**EA.hy926v1 (*slow proliferating*)**	
Increased expression in EA.hy926	**Ratio RF/sham**	**Difference RF-sham**	**Ratio RF/sham**	**Difference RF-sham**
proliferating cell nucleolar antigen P120; NOL1	**29,71**	**18734**	**0,38**	**-6343**
Homo sapiens mRNA for beta 2-microglobulin	**14,70**	**3895**	**0,50**	**-5312**
MCM7 DNA replication licensing factor; CDC47 homolog; p1.1-MCM3	**12,18**	**9029**	**0,98**	**-172**
zinc-finger protein (ZNFPT7) (fragment).	**8,43**	**15053**	**0,46**	**-2512**
chloride conductance regulatory protein ICLN; nucleotide-sensitive chloride channel 1A; chloride ion current inducer protein (CLCI); reticulocyte PICLN	**5,37**	**16944**	**0,79**	**-1686**
HHR23A; UV excision repair protein protein RAD23A	**4,42**	**20499**	**0,66**	**-7485**
ferritin heavy chain (FTH1); FTHL6	**4,30**	**6961**	**0,93**	**-2435**
CD166 antigen precursor (activated leukocyte-cell adhesion molecule) (ALCAM).	**4,09**	**3184**	**0,70**	**-2869**
nucleolar phosphoprotein B23; nucleophosmin (NPM); numatrin	**3,89**	**50540**	**0,97**	**-1699**
annexin IV (ANX4); lipocortin I; calpactin II; chromobindin 9; phospholipase A2 inhibitory protein	**3,68**	**7176**	**4,20**	**15254**
N4-(beta-N-acetylglucosaminyl)-L-asparaginase precursor (EC 3.5.1.26) (glycosylasparaginase) (aspartylglucosaminidase) (N4-(N-acetyl-beta-glucosaminyl)-L-asparagine amidase) (AGA).	**3,63**	**13266**	**0,55**	**-1060**
glial growth factor 2 precursor (GGFHPP2); neuregulin; heregulin-beta3 + neu differentiation factor + heregulin-alpha	**3,53**	**21908**	**0,70**	**-3070**
serine/threonine protein phosphatase PP1-alpha 1 catalytic subunit (PP-1A)	**3,31**	**7521**	**1,08**	**1402**
flavin reductase (EC 1.6.99.1) (FR) (NADPH-dependent diaphorase) (NADPH-flavin reductase) (FLR) (biliverdin reductase B) (EC 1.3.1.24) (BVR-B) (biliverdin-IX beta-reductase) (green heme binding protein) (GHBP)	**3,17**	**15395**	**0,77**	**-2827**
cytochrome c	**2,97**	**12337**	**0,82**	**-2047**
DNA-directed RNA polymerase II 19 kD polypeptide (EC 2.7.7.6) (RPB7).	**2,88**	**12043**	**0,88**	**-1360**

Table 30. Genes which were down-regulated in EA.hy926 cell line following to the exposure to 900 MHz GSM.

Gene name	EA.hy926 (*fast proliferating*)		EA.hy926v1 (*slow proliferating*)	
Decreased expression in EA.hy926	**Ratio RF/sham**	**Difference RF-sham**	**Ratio RF/sham**	**Difference RF-sham**
pyruvate kinase M2 isozyme (PKM2)	**0,33**	**-6273**	**0,90**	**-2490**
RAD51-interacting protein	**0,31**	**-3405**	**0,79**	**-510**
glutathione S-transferase mu1 (GSTM1; GST1); HB subunit 4; GTH4	**0,29**	**-3486**	**1,59**	**599**
glutathione S-transferase A1 (GTH1; GSTA1); HA subunit 1; GST-epsilon	**0,29**	**-4095**	**0,36**	**-2545**
early growth response protein 1 (hEGR1); transcription factor ETR103; KROX24; zinc finger protein 225; AT225	**0,28**	**-4223**	**0,54**	**-1932**
caspase-3 (CASP3); apopain precursor; cysteine protease CPP32; YAMA protein; SREBP cleavage activity 1; SCA-1	**0,27**	**-5844**	**1,04**	**79**
calpain 2 large (catalytic) subunit; M-type calcium-activated neutral proteinase (CANP)	**0,27**	**-3464**	**0,95**	**-1210**
ras-related C3 botulinum toxin substrate 1; p21-rac1; ras-like protein TC25	**0,26**	**-6905**	**1,10**	**730**
alpha-actinin 1 cytoskeletal isoform; F-actin cross linking protein	**0,25**	**-5276**	**0,82**	**-2597**
ras-related protein RAB-11B; YPT3	**0,24**	**-2870**	**0,79**	**-3643**
DNA ligase I; polydeoxyribonucleotide synthase (ATP) (DNL1) (LIG1)	**0,22**	**-2969**	**0,38**	**-2497**
ATP synthase lipid-binding protein P2 precursor (EC 3.6.1.34) (ATPase protein 9) (subunit C)	**0,19**	**-4520**	**0,80**	**-1486**
EDF-1 protein	**0,14**	**-6951**	**0,68**	**-2931**
coatomer delta subunit; delta-coat protein; delta-COP; archain (ARCN1)	**0,14**	**-4280**	**n/a**	**n/a**
nuclear transport factor 2 (NTF-2) (placental protein 15) (PP15).	**0,14**	**-2836**	**0,65**	**-2155**
fascin (actin bundling protein).	**0,14**	**-16072**	**0,54**	**-6852**
neurogranin (NRGN); RC3	**0,11**	**-18728**	**0,86**	**-2175**
MYLE	**0,11**	**-4959**	**0,81**	**-539**
sepiapterin reductase (EC 1.1.1.153) (SPR).	**0,10**	**-3467**	**0,63**	**-1123**
caspase-8 precursor (CASP8); ICE-like apoptotic protease 5 (ICE-LAP5); MORT1-associated CED-3 homolog (MACH); FADD-homologous ICE/CED-3-like protease (FADD-like ICE; FLICE); apoptotic cysteine protease MCH-5	**0,05**	**-3359**	**1,90**	**1080**

Table 31. Genes which were affected in EA.hy926v1 cell line following to the exposure to 900 MHz GSM.

Gene name	EA.hy926v1 *(slow proliferating)*		EA.hy926 *(fast proliferating)*	
Increased expression in EA.hy926v1	**Ratio RF/sham**	**Difference RF-sham**	**Ratio RF/sham**	**Difference RF-sham**
procollagen C-proteinase enhancer protein precursor.	**9,58**	**10373**	**1,09**	**5589**
HOMER-3.	**9,45**	**3027**	**0,98**	**-25**
T-lymphoma invasion and metastasis inducing TIAM1	**5,55**	**6554**	**0,01**	**-1335**
elafin precursor (elastase-specific inhibitor) (ESI) (skin-derived antileukoproteinase) (SKALP).	**5,33**	**10720**	**1,53**	**12919**
mitochondrial matrix protein P1 precursor; p60 lymphocyte protein; chaperonin homolog; HUCHA60; heat shock protein 60 (HSP-60); HSPD1	**4,43**	**8459**	**1,00**	**-89**
proteasome component C8; macropain subunit C8; multicatalytic endopeptidase complex subunit C8	**4,06**	**5029**	**1,10**	**5254**
special AT-rich sequence binding protein 1 (SATB1); MAR/SAR DNA-binding protein	**3,48**	**11151**	**0,99**	**-222**
HLA class I histocompatibility antigen C-4 alpha subunit (HLAC)	**3,12**	**2805**	**0,64**	**-1344**
ras-related protein RAP-1B; GTP-binding protein SMG p21B	**3,04**	**4820**	**63,80**	**2512**
phospholipase A2; tyrosine 3-monooxygenase/tryptophan 5-monooxygenase activation protein zeta polypeptide (YWHAZ); 14-3-3 protein zeta/delta; protein kinase C inhibitor protein 1 (KCIP1); factor activating exoenzyme S (FAS)	**2,93**	**4033**	**1,14**	**767**
Decreased expression in EA.hy926v1				
tuberin; tuberous sclerosis 2 protein (TSC2)	**0,33**	**-7082**	**0,42**	**-16846**
KIAA0115; dolichyl-diphosphooligosaccharide protein glycosyltransferase 48-kDa subunit precursor; oligosaccharyl transferase 48-kDa subunit; HA0643	**0,27**	**-3494**	**0,19**	**-1968**
sodium channel beta-1 subunit precursor (SCN1B)	**0,27**	**-2842**	**0,00**	**-1846**
embryonic growth/differentiation factor 1 (GDF1) + UOG-1	**0,21**	**-3542**	**0,00**	**-702**
SH3P18 SH3 domain-containing protein	**0,05**	**-3389**	**0,00**	**-949**

C. Comparison of the effect of CW and modulated RF-EMF on protein expression

Using cICAT method combined with liquid-phase chromatography and mass spectrometry we have compared protein expression changes in cells exposed either to continuous wave or to radiofrequency modulated ("talk" signal) RF-EMF (1800 MHz GSM). The cICAT reagent labelled samples were analysed using an automated mass spectrometric approach in which those proteins showing abundance differences between the two conditions being compared were selectively identified. In total, 58 unique proteins were identified and determined to show significant changes in abundance using this approach. These proteins were selected for identification by MS/MS analysis based upon the criteria that the measured abundance ratios ($C^{13}(0)/C^{13}(9)$) were either >1.7 or <0.60. The average abundance ratio for all detected cICAT reagent labelled peptide pairs (n=1476) was 1.26 +/-0.38, indicating that the vast majority of proteins within the two samples did not change in abundance. Peptides detected as singlets (i.e. having no corresponding $C^{13}(0)$ or $C^{13}(9)$ signal) were also selected for MS/MS analysis. The threshold abundance ratio values were selected based on the following criteria: 1) In relation to previously described errors of quantitative measurements using the ICAT reagent, these values represent conservative estimates of significant abundance changes; 2) These values are significant outliers relative to the average and median $C^{13}(0)/C^{13}(9)$ values for this dataset. The average $C^{13}(0)/C^{13}(9)$ value for all detected cICAT reagent labelled peptides (n = 1476) was 1.26 +/-0.38, and the median was 1.19. The threshold values for significant changes in abundance are therefore well outside the standard deviation for this dataset. Furthermore, the fact that the average and median values are close to one indicates the accuracy of the quantitative measurements used here, as it is expected that the majority of proteins will be constitutively represented, giving ratios close to one.

In conclusion it appears that the "talk" signal has caused increase in expression of a variety of proteins whereas CW did not (Table 32). It suggests that the modulation might have impact on cell response to RF-EMF.

Table 32. List of proteins induced by "talk" signal but not by the CW signal.

Protein name	Accession No.	$C^{13}(0)/C^{13}(9)$	Confidence score
serine-threonine protein kinase	NP_055212	1.9	0.996
GP:AF090929_1		1.8	0.912
RING finger protein 20	AAK58539	2.0	0.958
Homo sapiens cDNA FLJ20303	AK000310	2.4	0.957
hypothetical protein FLJ20420	NP_060282	2.0	0.984
fatty-acid synthase	PIR:G01880	2.2	0.993
hypothetical protein DKFZp434G171.1	T42678	1.9	0.855
hypothetical protein DKFZp564N1563.1 (2)	T46270	0.5	0.921
Serine/threonine protein phosphatase 2A	Q15173	1.8	0.950
Beta-adaptin 1	Q10567	2.0	0.813
Actin-like protein 2	O15142	2.0	0.993
Sarcoplasmic/endoplasmic reticulum calcium ATPase 2 (2)	P16615	1.9	0.944
CD59 glycoprotein precursor (6)	P13987	2.4	0.995
Chloride intracellular channel protein 1	O00299	2.7	0.997
Cellular nucleic acid binding protein (2)	P20694	2.2	0.980
Cofilin, non-muscle isoform	P23528	1.7	0.990
Coatomer alpha subunit	P53621	2.4	0.997
Coatomer beta subunit	P53618	2.0	0.993
Cleavage and polyadenylation specificity factor	Q9P2I0	1.9	0.994
Cyclophilin A (3)	P05092	2.2	0.975
Destrin (Actin-depolymerizing factor)	P18282	1.7	0.990
Aspartyl aminopeptidase	Q9ULA0	1.8	0.993
D-dopachrome tautomerase	P30046	1.7	0.952
Elongation factor 2	P13639	2.0	0.982
Alpha enolase	P06733	2.1	0.981
Fatty acid synthase (2)	P49327	2.1	0.975
Filamin A (2)	P21333	2.5	0.975
FL cytokine receptor precursor	P36888	1.9	0.970
Follistatin-related protein 1 precursor Q12841	Q12841	1.7	0.942
PROTEIN KINASE C SUBSTRATE	P14314	1.7	0.984
Transducin beta chain 1	P04901	1.9	0.993
Transducin beta chain 2	P11016	1.8	0.964
Guanine nucleotide-binding protein beta subunit-like protein (3)	P25388	2.9	0.998
Stress-induced-phosphoprotein 1	P31948	2.2	0.993
Pyruvate kinase, M1 isozyme	P14618	1.9	0.983
LAM2_HUMAN, partial CDS	AAC34573	0.6	0.994
Galectin-1 (3)	P09382	1.9	0.996
Myosin heavy chain, nonmuscle type A	P35579	0.6	0.996
Myoferlin (2)	Q9NZM1	2.9	0.940
NHP2-like protein 1 (3)	P55769	3.6	0.980
Nitric-oxide synthase, endothelial (2)	P29474	2.0	0.990
Purine nucleoside phosphorylase (2)	P00491	1.9	0.997
40S ribosomal protein S27a	P14798	3.0	0.974
Heterogeneous nuclear ribonucleoprotein D0	Q14103	3.0	0.984
Heterogeneous nuclear ribonucleoprotein K	Q07244	2.6	0.880
Heterogenous nuclear ribonucleoprotein U	Q00839	2.1	0.992
ribosomal protein S2 (2)	P15880	1.8	0.940
40S ribosomal protein S3a	P49241	2.1	0.991
Splicing factor, arginine/serine-rich 9	Q13242	2.0	0.986
Tubulin beta-2 chain	P05217	2.8	0.998
T-complex protein 1, theta subunit (2)	P50990	4.9	0.995
Transcription intermediary factor 1-beta	Q13263	2.3	0.995
Thioredoxin	P10599	2.1	0.935
Hypothetical UPF0123 protein BK223H9.2	Q9UH06	2.1	0.994
Splicing factor U2AF 35 kDa subunit (2)	Q01081	2.4	0.945
Ubiquitin-activating enzyme E1	P22314	1.8	0.963
Zinc finger protein 147	Q14258	3.7	0.995
Nuclear pore complex protein Nup133	Q8WUM0	2.3	0.914

3.2.4.7 Whole-genome analysis of various cell lines exposed to RF-EMF (Participant 12)

Altogether, 58 whole-genome analyses of 10 different cell lines (sham-exposed cells and control cells) were performed (Table 1). After primary data analysis, we only worked on genes which were reproducibly regulated in several experiments (see materials and methods) and which belonged to certain gene families (Table 33). We defined gene families which are potentially relevant for the cellular answer on EMF exposure: signal transduction, ion/electron transport, metabolism of energy/proteins, cell proliferation/apoptosis, immune answer/inflammation and extracellular matrix/cytoskeleton. Each gene family was sub-divided in subgroups again, e.g. GTP proteins in the signal transduction family (Tables 33, 11). In a first step, we did not go into single genes, but simply counted genes up- or down-regulated in the different gene families. The total number of regulated genes in a certain gene family is not very meaningful, because the sizes of the gene families are of course very different. Therefore, the total numbers of genes on the human array belonging to a gene family are shown in the first column of Tables 33 and 11. Although a single gene might appear in different categories (e.g. all small G proteins are GTP binding proteins), the tables give a good overview on what might happen in the cells after EMF exposure on the molecular level.

Although appearing regulated in all experiments, mitochondrial genes, ribosomal genes and cell cycle genes especially showed a high rate of regulation in the some RF-EMF experiments (U937 human monocytic cells and microglia cells, Participant 9; HL-60 human hematopoietic leukemia cells, Participant 2).

Moreover, the bio-statistical analysis of RF-EMF experiments (Participant 8, Dr. Remondini) allowed some interesting conclusions from the experiments with HL-60 cells (Participant 2), endothelial cells (Participant 6) and U937 cells (Participant 8, Table 34). Again, the regulation of mitochondrial and ribosomal genes was evident with this analysis. Most of the regulated genes in endothelial cells appear in the groups of ATP-associated genes (energy metabolism), transcription, and cytoskeleton. Remarkably, compared to ELF-EMF experiments, we find more up-regulated genes in RF-EMF experiments (Table 34, see also Table 12). However, the results do have to be interpreted in more detail, because down-regulation of a special gene does not mean that the respective process is down-regulated as well (for example, down-regulation of Bcl-2 might lead to up-regulation of apoptosis).

For T-lymphocytes (Participant 8) and microglia cells (Participant 9) the bio-statisitical analysis did not reveal significant data.

In detail, the following genes were extracted by bio-statistics so far:

Actin associated proteins (belong to cytoskeleton):
- Caldesmon (tropomysin binding, actin binding. Activation of ERK MAP kinases lead to phosphorylation of caldesmon. Regulatory protein of the contractile apparatus): down-regulated (endothelial cells, Participant 6).
- Gamma-actin: down-regulated ((endothelial cells, Participant 6, and U937 cells, Participant 8)
- “coactosin-like”: down-regulated (endothelial cells, Participant 6)
- “actin-binding”: down-regulated (endothelial cells, Participant 6)
- “procollagen-proline 2”: down-regulated (endothelial cells, Participant 6)
- “actin modulating activity”: up-regulated (endothelial cells, Participant 6)
- “actin-binding, calcium ion binding”: down-regulated (endothelial cells, Participant 6)
- CD2-associated protein, actin binding: down-regulated (endothelial cells, Participant 6)
- Tropomodulin 3: actin binding down-regulated (endothelial cells, Participant 6)

Calcium (Ca2+)-associated proteins:
- Ca: “hypothetical protein” (actin-binding): down-regulated (endothelial cells, Participant 6)
- “hypothetical protein”: down-regulated (endothelial cells, Participant 6)
- voltage-gated Ca channel: up-regulated (perhaps up-regulated, because Ca goes down? Endothelial cells, Participant 6)

Cytoskeleton (compare also actin and calcium-associated proteins):
- “hypothetical protein”: down-regulated (endothelial cells, Participant 6)
- “protein phosphatase 4, caldesmon): down-regulated (endothelial cells, Participant 6)
- “SH3 protein interacting with Nck”: down-regulated (endothelial cells, Participant 6)
- “in kinesin complex”: down-regulated (endothelial cells, Participant 6)

Table 33. Numbers of genes regulated within different gene families

Gene Family	total number of clones in Human Unigene RZPD-2	partner 8 U937 monocytes RF up-regulated genes	partner 8 microglia cells RF up-regulated genes	partner 8 U937 monocytes RF down-regulated genes	partner 8 microglia cells RF down-regulated genes	partner 6 endothelial cellsPr1 RF 900MHz up-regulated genes	partner 6 endothelial cells RF 1800 MHz Exp1 up-regulated genes	partner 6 endothelial cells RF 1800 MHz Exp2 up-regulated genes	partner 6 endothelial cellsPr1 RF 900MHz down-regulated genes	partner 6 endothelial cells RF 1800 MHz Exp2 down-regulated genes	partner 6 endothelial cells RF 1800 MHz Exp2 down-regulated genes	partner 2 HL-60 RF ON/OFF up-regulated genes	partner 2 HL-60 RF continuous waves Exp1 up-regulated genes	partner 2 HL-60 RF continuous waves Exp2 up-regulated genes	partner 2 HL-60 RF ON/OFF down-regulated genes	partner 2 HL-60 RF continuous waves Exp2 down-regulated genes	partner 2 HL-60 RF continuous waves Exp2 down-regulated genes	Gene "Superfamily"
Signal	2528	149	40	##	45	190	176	92	160	149	149	91	153	162	190	155	72	signal transduction
GTP	560	37	15	45	14	42	58	24	49	40	51	20	43	51	49	38	18	signal transduction
Small G	235	16	5	20	3	14	17	10	23	15	19	8	17	18	21	18	7	signal transduction
Jak	23	2	0	1	1	1	4	2	1	4	0	1	4	2	1	1	0	signal transduction
Rab	80	3	1	11	3	6	6	4	6	4	9	0	5	5	6	3	5	signal transduction
Ras	66	4	2	7	0	4	4	1	6	4	7	2	6	6	7	2	2	signal transduction
wnt	5	0	0	0	0	0	0	0	0	0	0	0	0	0	0	0	0	signal transduction
phosphatase	334	24	6	21	7	24	31	17	23	20	25	19	18	26	19	29	9	signal transduction
protein kinase	304	19	6	19	4	19	24	16	27	15	16	18	16	25	23	11	13	signal transduction
phospholipase	72	6	1	7	1	6	4	5	1	2	4	1	3	7	7	5	2	signal transduction
calcium	715	40	6	39	14	56	51	27	45	30	45	20	45	44	45	35	13	signal transduction
calmodulin	131	8	2	6	1	8	6	1	11	8	9	6	5	8	11	10	4	signal transduction
channel	348	12	1	18	7	12	12	8	16	12	11	12	28	11	16	13	6	ion/electron transport
voltage-gated	164	3	0	6	2	7	5	3	3	5	4	5	12	9	7	2	3	ion/electron transport
electron transport	423	25	11	29	6	35	44	20	37	17	34	25	19	36	26	18	15	ion/electron transport
ion transport	501	22	8	32	11	35	21	13	25	18	21	26	39	29	27	37	14	ion/electron transport
metaboli	1241	80	21	81	15	98	124	68	91	71	86	66	87	110	114	64	39	metabolism of energy/proteins
ATP	1234	81	27	92	24	75	116	49	111	77	83	86	102	104	111	82	47	metabolism of energy/proteins
mitochon	574	50	10	63	19	55	61	32	67	46	55	49	51	76	64	66	24	metabolism of energy/proteins
ribosom	254	39	14	39	19	32	35	15	30	25	32	33	31	23	26	37	13	metabolism of energy/proteins
translation	168	21	2	13	9	18	14	12	25	14	18	18	12	12	21	14	17	metabolism of energy/proteins
transcript	1991	116	39	##	41	172	142	78	144	120	129	122	143	138	138	130	75	metabolism of energy/proteins
cell cycle	478	34	11	39	14	42	46	28	46	37	39	44	49	42	46	22	23	cell proliferation/apoptosis/differentiation
apoptos	373	29	8	26	10	34	36	12	18	31	29	18	30	39	32	30	10	cell proliferation/apoptosis/differentiation
differentiat	177	17	2	20	1	14	11	8	5	6	13	6	7	9	12	7	4	cell proliferation/apoptosis/differentiation
immun	390	19	5	26	7	22	44	21	25	19	24	19	31	30	29	17	18	Immune answer/inflammation/stress answer
inflamma	184	8	1	6	3	15	15	8	13	13	9	10	11	6	12	14	2	immune answer/inflammation/stress answer
stress	118	5	6	7	2	8	16	5	8	5	13	5	8	12	10	11	4	immune answer/inflammation/stress answer
peroxidase	32	2	2	7	0	3	4	2	5	3	16	1	4	4	4	5	3	immune answer/inflammation/stress answer
heat shock	188	2	2	4	2	3	5	4	6	6	2	3	3	2	4	6	1	immune answer/inflammation/stress answer
DNA repair	154	10	3	17	4	11	15	6	13	16	15	7	13	12	17	7	8	immune answer/inflammation/stress answer
early	8	0	0	1	0	0	1	0	0	1	2	1	0	0	2	1	1	immune answer/inflammation/stress answer
adhesion	573	30	5	28	9	42	44	19	42	28	38	19	34	31	32	28	14	extracellular matrix/cytoskeleton/adhesion
extracellular matrix	226	14	4	7	5	12	12	7	7	8	8	5	11	10	11	10	8	extracellular matrix/cytoskeleton/adhesion
cytosk	529	33	9	36	21	39	41	19	33	37	43	24	30	46	48	32	21	extracellular matrix/cytoskeleton/adhesion
junction	129	0	3	11	5	3	10	2	9	3	10	5	5	7	4	8	2	extracellular matrix/cytoskeleton/adhesion
actin	494	35	7	35	19	42	39	24	38	41	40	28	30	34	44	40	21	extracellular matrix/cytoskeleton/adhesion

Table 34. Numbers regulated genes in different expression profiling experiments (bio-statistical analysis by Dr. Remondini/Participant 8)

GeneFamily	total number of clones in Human Unigene RZPD-2	partner 6 endothelial cells RF up-regulated genes	partner 6 endothelial cells RF down-regulated genes	partner 2 HL-60 cell RF up-regulated genes	partner 2 HL-60 cell RF down-regulated genes	partner 8 U937 cells RF up-regulated genes	partner 8 U937 cells RF down-regulated genes	Gene "Superfamily"
Signal	2528	4	9	1	0	1	1	signal transduction
GTP	560	1	2	1	0	0	0	signal transduction
Small G	235	0	1	0	0	0	0	signal transduction
Rab	80	0	1	0	0	0	0	signal transduction
Ras	66	0	0	0	0	0	0	signal transduction
phosphatase	334	0	1	0	0	1	0	signal transduction
protein kinase	304	0	2	0	0	0	0	signal transduction
calcium	715	1	2	0	0	0	0	signal transduction
calmodulin	131	0	1	0	0	0	0	signal transduction
channel	348	1	0	1	0	1	0	ion/electron transport
voltage-gated	164	1	0	0	0	0	0	ion/electron transport
ion transport	501	1	0	0	0	0	1	ion/electron transport
electron transport	423	1	1	0	0	1	0	ion/electron transport
metaboli	1241	3	0	0	0	2	0	metabolism of energy/proteins
ATP	1234	1	4	0	0	0	1	metabolism of energy/proteins
mitochon	574	2	1	0	0	0	0	metabolism of energy/proteins
ribosom	254	0	1	0	0	1	4	metabolism of energy/proteins
translation	168	0	0	0	0	0	0	metabolism of energy/proteins
transcript	1991	1	6	3	0	2	0	metabolism of energy/proteins
cell cycle	478	0	3	1	0	0	0	cell proliferation/apoptosis/differentiation
apoptos	373	1	0	0	0	0	0	cell proliferation/apoptosis/differentiation
differentiat	177	0	1	1	0	0	0	cell proliferation/apoptosis/differentiation
immun	390	0	0	0	0	0	0	immune answer/inflammation/stress answer
DNA repair	154	0	1	0	0	0	0	immune answer/inflammation/stress answer
inflamma	184	0	0	0	0	1	0	immune answer/inflammation/stress answer
adhesion	573	0	1	0	0	1	0	extracellular matrix/cytoskeleton/adhesion
extracellular matrix	226	1	0	0	0	1	0	extracellular matrix/cytoskeleton/adhesion
cytosk	529	0	5	0	0	1	1	extracellular matrix/cytoskeleton/adhesion
actin	494	0	4	0	0	1	1	extracellular matrix/cytoskeleton/adhesion
junction	129	0	1	0	0	1	0	extracellular matrix/cytoskeleton/adhesion

3.2.4.8 Summary (Participant 1)

Our data indicate an effect of RF-EMF on gene and protein expression in various cell systems. This conclusion is based on the following findings:

- RF-EMF exposure at a SAR value of 1.5 W/kg caused a transient up-regulation of p21 and c-myc genes and a long-term up-regulation of the stress response gene hsp70 in embryonic stem cells deficient of the p53 gene (3.2.4.1)
- RF-EMF exposure at a SAR value of 2 W/kg reduced the expression of the receptor FGFR1 of fibroblast growth factor (FGF) in human neuroblastoma cells (NB69) and in neural stem cells of rats (3.2.4.2).
- RF-EMF exposure at a SAR value of 1.3 W/kg up- or down-regulated the expression of various genes and proteins in HL-60 cells and in endothelial cells of human origin (3.2.4.3, 3.2.4.6, 3.2.4.7).
- RF-EMF exposure at a SAR value of 2.4 W/kg activated the p38MAPK/hsp27 stress response pathway in endothelial cells of human origin (3.2.4.6).
- RF-EMF exposure at a SAR value of 2.4 W/kg changed the global pattern of protein phosphorylation in endothelial cells of human origin with possible consequences for the signal transduction pathway (3.2.4.6).
- RF-EMF exposure at a SAR value at 2 W/kg did not significantly affect gene expression in human lymphocytes, although a few genes among several thousand tested with the micro-array system were found altered in two human immune cell lines (3.2.4.4, 3.2.4.5).
- RF-EMF exposure at a SAR value of 2 W/kg did not affect the expression and activity of the inducible nitric oxide synthase (iNOS) and the expression of hsp27 and hsp70 in nerve cells (3.2.4.5).
- The increased expression of hsp27 in endothelial cells (EA.hy926) after RF-EMF exposure as described in 3.2.4.6 could not be reproduced in another laboratory where slightly different methods were used (3.2.4.5).